FILE

Institute of
Oceanographic Sciences
Deacon Laboratory

A review of observational techniques and instruments for current measurement in the open sea

P G Collar

Report No 304 1993

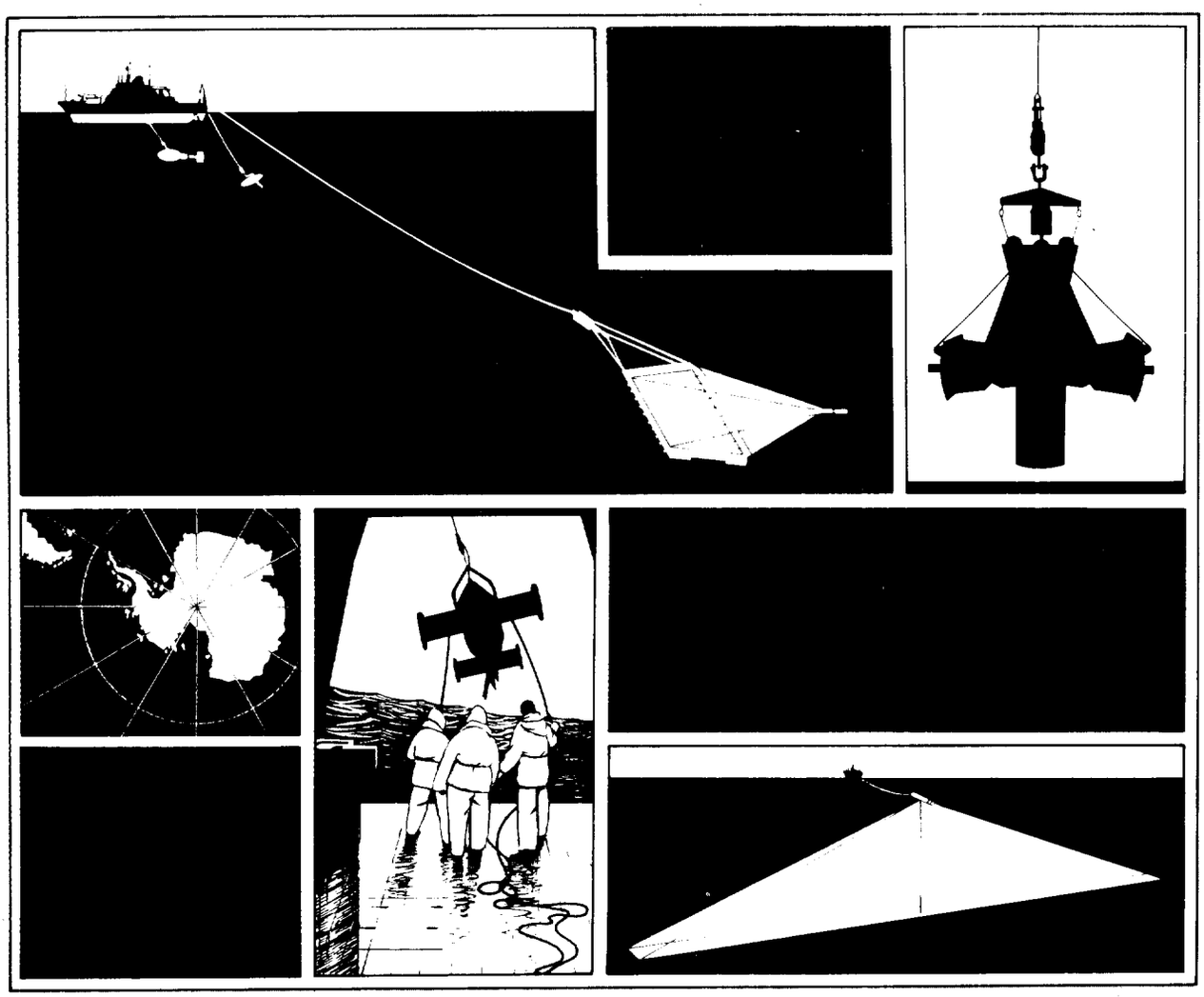

Natural Environment Research Council

INSTITUTE OF OCEANOGRAPHIC SCIENCES

DEACON LABORATORY

Wormley, Godalming,
Surrey, GU8 5UB, U.K.

Telephone: 0428 79 4141
Telex: 858833 OCEANS G
Telefax: 0428 79 3066

Director: Dr. C.P. Summerhayes

Natural Environment Research Council

INSTITUTE OF OCEANOGRAPHIC SCIENCES

DEACON LABORATORY

REPORT NO. 304

A review of observational techniques and instruments for current measurement in the open sea

P G Collar

1993

DOCUMENT DATA SHEET

AUTHOR	PUBLICATION DATE
COLLAR, P G	1993

TITLE

A review of observational techniques and instruments for current measurement in the open sea.

REFERENCE

Institute of Oceanographic Sciences Deacon Laboratory, Report, No. 304, 124pp.

ABSTRACT

The report describes techniques developed in the oceanographic community for the measurement of currents at all depths in the sea. Eulerian measurements using moored instruments are outlined, including principles of operation and relative advantages and disadvantages of some commonly used types of mechanical, electromagnetic and acoustic current meters. Mooring methods are briefly reviewed and the problems of measuring mean current in the surface wave zone are discussed.

In recent years much effort has been expended on the development and proving of acoustic doppler current profilers, both shipborne and moored. The performance of these instruments is examined and a list of some recent intercomparisons with moored instruments is presented. Techniques are also described which provide for measurement at larger scales, including acoustic tomography and electromagnetic measurements using the geomagnetic field, namely submarine cables, vertical profilers, towed electrodes.

The measurement of near surface currents is particularly challenging. High frequency (hf) and microwave radar backscatter have introduced powerful new tools, which can permit rapid wide area survey. The nature of this measurement in relation to point measurement is outlined.

Lagrangian drifters represented the earliest means of current measurement. A section is devoted to these techniques, examining various kinds of hull and drogue forms and including discussion of various methods of position location. The evolution of deep ocean transponding floats is traced, from early Swallow floats to long range SOFAR and RAFOS floats and the new ALACE system, which has a facility for periodic surfacing for satellite communication.

A short section examines the application of correlation methods to acoustic transmissions and to satellite remote sensing imagery. The discussion concludes with a brief forward look at likely future development avenues.

KEYWORDS

ACOUSTIC DOPPLER CURRENT PROFILERS
ACOUSTIC TOMOGRAPHY
ADCP
ALACE
CALIBRATION
CORRELATION METHODS
CURRENT MEASUREMENT
CURRENT METERS
CURRENT SENSOR
DRIFTERS
ELECTROMAGNETIC CURRENT METERS
EULERIAN CURRENT MEASUREMENT
FLOATS
INSTRUMENTS
INTERCOMPARISON
LAGRANGIAN CURRENT MEASUREMENT
MOORINGS
OBSERVATIONAL TECHNIQUES
RAFOS
REVIEW ARTICLE
SOFAR
SOUND BACKSCATTER
SUBMARINE CABLES
TOWED SENSORS
WAVE ZONE

ISSUING ORGANISATION

Institute of Oceanographic Sciences
Deacon Laboratory
Wormley, Godalming
Surrey GU8 5UB. UK.

Director: Colin Summerhayes DSc

Telephone Wormley (0428) 684141
Telex 858833 OCEANS G.
Facsimile (0428) 683066

Copies of this report are available from: ***The Library,*** *PRICE* *£30.00*

CONTENTS

1.0 INTRODUCTION

1.1 Background

Fluid motion in the sea results from a number of primary forcing mechanisms. These include the deterministic tide generating potentials associated with the gravitational attraction of sun and moon; Earth's rotation; solar heating; the vertical distribution of density within the water column and forcing due to surface wind stress. Other major influences include the existence of land boundaries and the proximity of the sea bed. The effect of these forces and perturbations is to produce a spectrum of fluid motions which spans at least nine orders of magnitude in both its temporal and spatial scales (Fig. 1.1). At one end of the spectrum turbulent motions are at millimetric scales with periodicities of less than 10^{-1} seconds. At the other extreme a global pattern of ocean circulation exists which involves inter-basin exchanges and large scale boundary currents. Here the representative distance scales lie between 10^3 and 10^4 km and perturbations may have associated timescales of months or longer. Between these extremes extends a variety of physical processes - summarized in Table I - which contribute in various circumstances to fluid motions in different bands within the frequency spectrum.

Most of these processes are of a stochastic or episodic nature and are associated with substantial temporal and spatial fluctuations and hence with wide variability in energy density. Some processes can be considerably more energetic than others which take place concurrently. An example is provided by the three dimensional oscillatory flows associated with surface gravity waves, which may on occasion exceed the horizontal flow averaged over a few minutes by two orders of magnitude. The measurement of horizontal near-surface currents is consequently difficult and indeed represents one of the most challenging areas of measurement in the open sea.

The complexity of fluid motion in the sea, and the need to observe at a wide range of scales, has led in the past thirty years or so to the emergence of a variety of observational methods. These cover such diverse techniques as measurement by discrete, moored instruments, deep drifting floats tracked over 1000 km ranges using the deep sound channel, and h.f. backscatter radar which can provide maps of surface currents in shelf seas over areas of several hundred km^2. After many years of investigation or application some methods can now be considered to be mature. This is probably true of mechanical current meters, for example, which offer more than thirty years of development and application at sea, are in some cases close to optimum hydrodynamic design and have sampling schemes which are reasonably well suited to measurement in complex near surface flow. Other techniques, notably the application of acoustic tomography and long path velocimetry to measurement over thousand kilometre scales, are as yet at an embryonic stage.

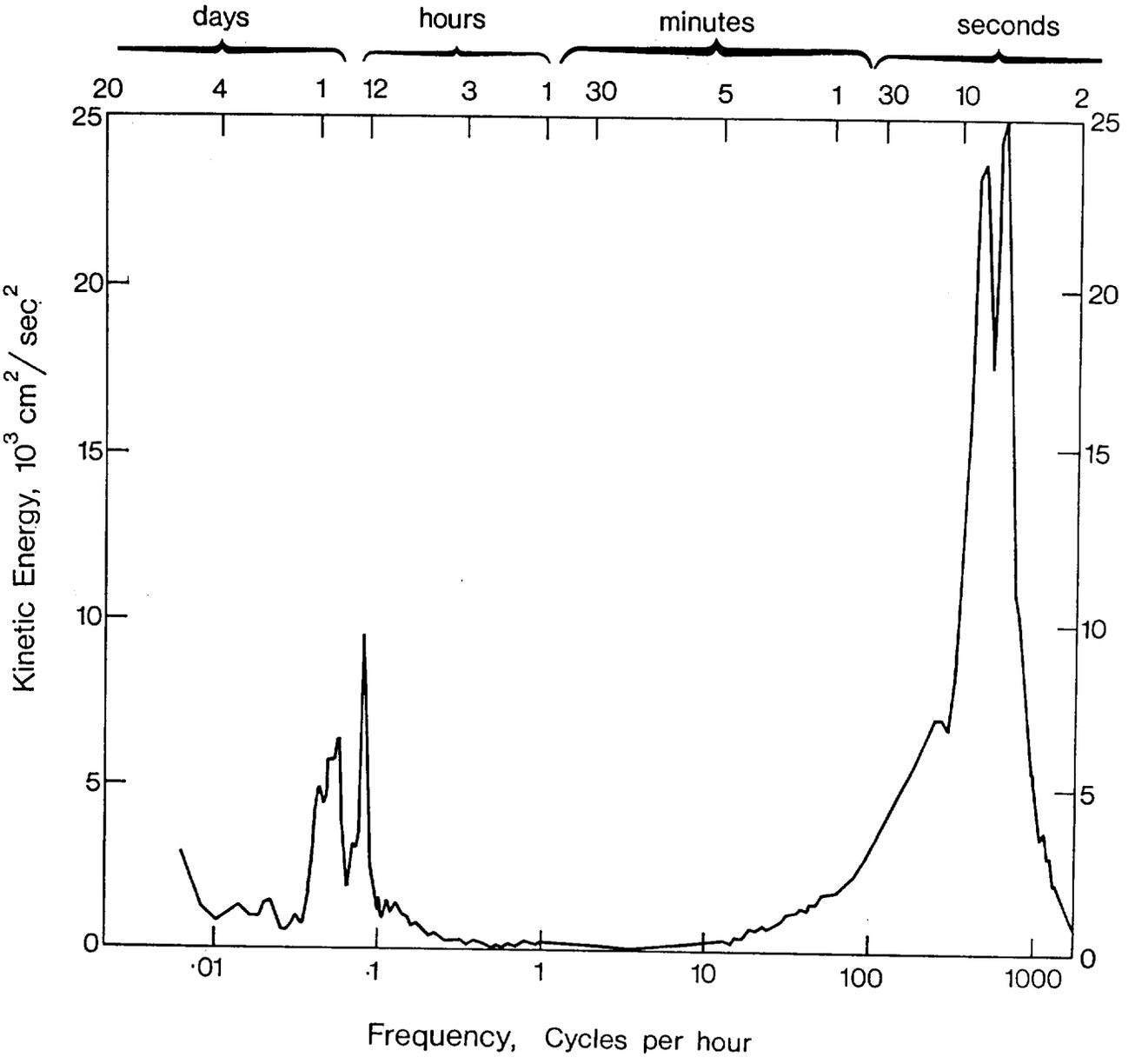

Fig. 1.1 Spectrum of fluid motions in the sea

Table 1 Characteristics of some principal current generating processes (Gould, 1977)

Motion	Period	Horizontal wavelength	Vertical wavelength	Typical amplitude cm/sec	Geographical area
Mean flow		Various	h (water depth)	0-10	Everywhere
Climatic change	10 yrs	Global	h	?	Everywhere
Seasonal variability	1 yr	Global	h	?	Everywhere
Mesoscale activity	30-100 days	400 km	h	5-100	All deep oceans
Meteorological disturbances	Aperiodic	Basin wide in shelf seas	h	100	Shelf seas and upper layer of ocean
Shelf and edge waves	2-10 days	10 km cross slope 500 km along slope	h	5-10	On topographic features e.g. seamounts, shelf edges etc.
Inertial oscillations	12 hrs Sin (latitude) 0.5-5 days	10s of km	100 m	5-50	All seas and oceans
Tidal oscillations	0.5-1 day	Basin width	h	10-20 deep sea 10-200 shelf seas	Everywhere
Internal waves	Inertial period to 10 minutes	1 km	100 m	5	Throughout the stratified ocean
Surface waves	1-20 secs	100 m	Limited to upper 30 m of water column	200	Everywhere
Small scale turbulence	100 Hz	cm	cm	cm/sec	Everywhere dependent on stability

This report reviews the broad range of techniques and instruments presently available for current measurement. We here define current in terms of the rate of displacement of a fluid element over a timescale significantly longer than surface gravity wave periods. The effects of waves on the measurement are discussed, but observational methods for resolving orbital velocities and smaller scale turbulent motions are not considered.

1.2 Eulerian and Lagrangian frames of reference

Before discussing measurement techniques it is important to distinguish between the two basic reference frames which might be used. In an idealized sense determination of current is considered to take place either in an Eulerian frame, which is fixed, or in the complementary Lagrangian frame, in which a conceptual particle of water is followed, and whose rate of displacement with time is observed. Clearly measurement should be carried out in whichever frame is most appropriate to the problem in hand. For example, Eulerian data are essential for the investigation of forces on offshore structures, which result from current action. On the other hand measurements concerned with dispersal, e.g. of pollution, fish larvae etc., are more appropriately Lagrangian. Whichever approach is adopted, the calculation of a quantity in one reference frame from observations made in the other can only be done if the data set is spatially and temporally complete. It is important to note that even limited data, if obtained in the frame of reference appropriate to the problem can permit conclusions to be drawn: but limited data obtained in the complementary reference frame will generally not suffice.

Discussion of the quantitative relationship between Eulerian and Lagrangian current measurement techniques lies outside the scope of this review - the reader is referred to Longuet-Higgins (1972) and to Davis (1982). There is, however, one important example in current measurement where the Eulerian-Lagrangian difference may impinge directly on the measurement process and thus merits closer consideration. This concerns the mass transport associated with irrotational surface gravity waves. Stokes (1847) showed that in the Lagrangian frame, water particles in waves experience a slightly higher forward velocity at the crest than in the trough. The result is that orbital motion is not closed: there exists a net forward transport - Stokes drift or wave drift. In a progressive deep water wave of small amplitude a, wavenumber k, travelling in the x direction, horizontal and vertical orbital velocity components at depth z (measured positively downwards) are given by

$$V_x = a\sigma e^{-kz} \sin (kx - \sigma t)$$

$$V_z = a\sigma e^{-kz} \cos (kx - \sigma t)$$

By considering a small expansion in x and z in these equations and integrating to obtain displacement the Stokes drift can be shown to be of order $a^2\sigma k e^{-2kz}$. An example is shown in Fig. 1.2. The drift evidently decays more rapidly with depth than does the wave motion itself, but it is nevertheless generated to depths well below the wave troughs.

In contrast, wave momentum in the Eulerian frame is distributed entirely between wave trough and wave crest. By integration of V_x it can be shown that the mean forward velocity is zero at a wave trough, increases to a maximum just above the mean water level and falls to zero at the crest. But at any fixed point (x_o, z_o) below the trough, the net forward velocity is

$$\bar{u} = a\sigma e^{-kz_o} \int_0^{2\pi/\sigma} \sin(kx_o - \sigma t).dt = 0$$

and so a fixed current meter, immersed beneath the wave trough, will record no mean drift.

An Eulerian and a Lagrangian measurement system will, in this case, produce completely different, though equally valid observations. The implications of this fact for current measurements in the wave zone are examined in later sections.

In discussing Eulerian and Lagrangian concepts, it should be borne in mind that in practice few of the wide variety of techniques that now exist for current measurement conform exactly to these ideals - and therein lie a number of the problems associated with the measurement of currents and with interpretation of the resulting data. Ship drift observations, for example, include both a Lagrangian and an Eulerian element, while the recently emergent h.f. radar backscatter technique for surface current measurement operates in a fixed frame, but nevertheless includes the Lagrangian wave drift component of the current.

1.3 Measurement in the wave zone

In whichever reference frame is chosen, particular difficulties are associated with current measurement close to the sea surface, where an understanding of the underlying physical processes is important for a variety of scientific and economic reasons - yet where a dearth of good observations still exists. Given that wave motion at a spectral wavelength λ decays with depth, z, as $\exp(-2\pi z/\lambda)$ we can reasonably, if arbitrarily, define the near-surface region as having depth of order one quarter of the wavelength at the wave spectral peak. In many circumstances this is of order 10 m or less, though it can attain nearly an order greater in oceanic storms. Difficulties in achieving accurate measurement within this region can arise from a number of interrelated causes:

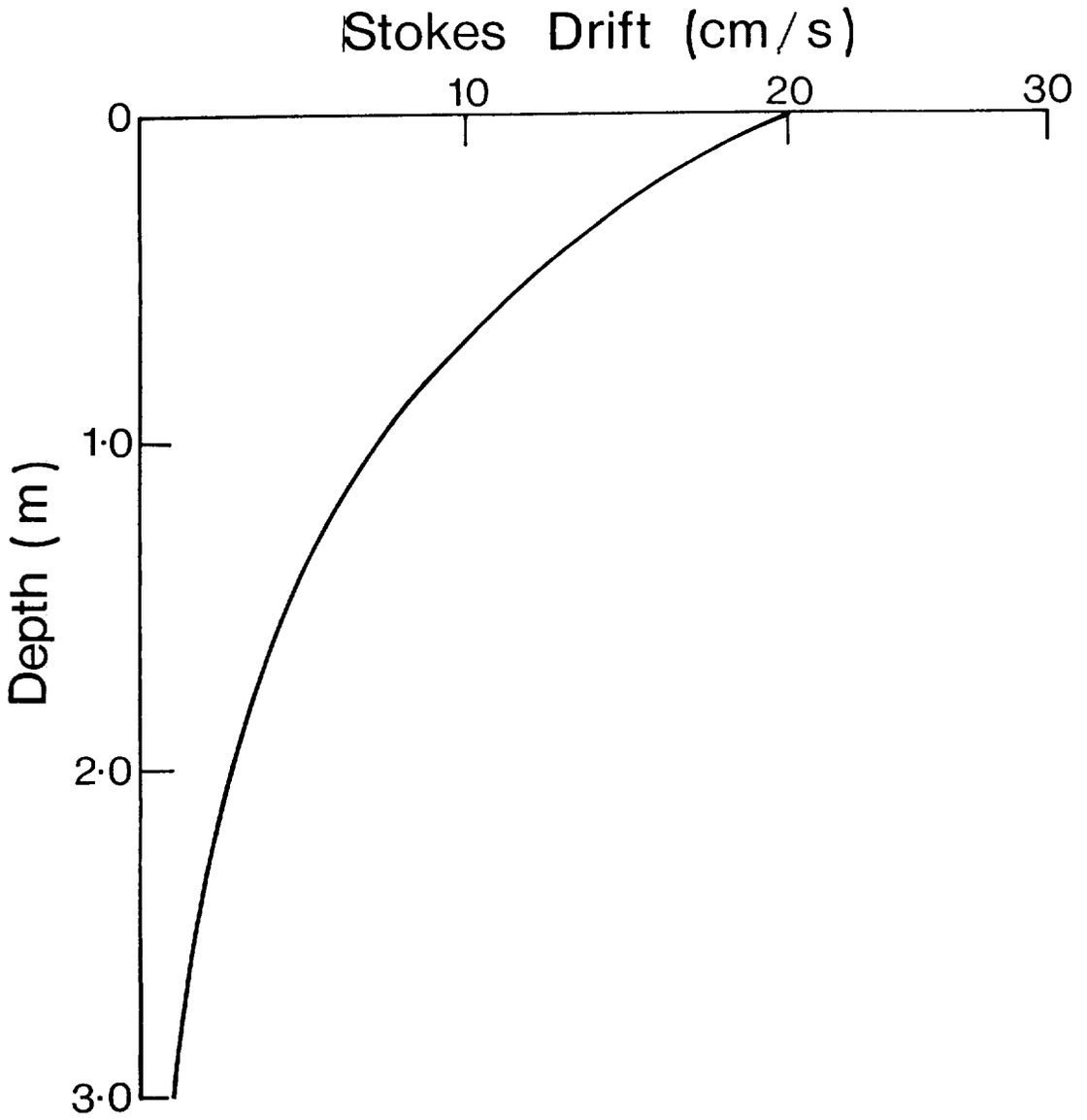

Fig. 1.2 Stokes Drift profile for regular waves of 0.5 m amplitude and 5 seconds period

- the coexistence of energetic, three dimensional, turbulent wave motions and a complex current structure, from which a relatively small mean current often has to be extracted;
- inadequacies in instrument or Lagrangian drifter characteristics;
- instrument motion and the consequences of departure from an ideal reference frame;
- unreliability of the measurement system overall in the harsh near-surface environment. This includes both Eulerian moorings and drogue tethers for Langrangian systems.

We now examine some implications of near-surface measurements for Eulerian sensor design and consider these further in the context of individual types of instrument: the effects of mooring motion on the measurement are discussed in Section 2.9. Lagrangian near surface measurements are discussed in Section 7.3.

2.0 CURRENT METERS

2.1 Current meter design criteria

In steady flows, commonly experienced at depth in the sea, relatively unsophisticated instruments often produce acceptable results. However, for measurement in the region subjected to wave influence - or wherever appreciable mooring motion is encountered - there are a number of attributes that a sensor and the associated sampling arrangements should possess. In a survey of near-surface measurement techniques McCullough (1980) defined the primary characteristics of an ideal sensor as follows. It should:

- measure orthogonal components of flow independently, the measurement along each axis being insensitive to the other off-axis components;
- have sufficient frequency response to follow, linearly, variations of interest, while limiting the bandwidth of input variations to the linear range of the sensor;
- average over clearly defined temporal and spatial scales without disturbing the flow;
- be sensitive, stable, rugged, small, inexpensive, easily calibrated, easily deployed and require little power, minimal maintenance.

If, as is usual, the sensor output is sampled in a discrete manner then the provisions of the Nyquist sampling theorem must also be adhered to, i.e. the sampling rate should be at least twice the highest frequency component of interest: $f_s > 2f_{max}$, while negligible spectral content should exist at frequencies $f > f_{max}$. In practice, the existence of significant wave energy and sensor motion down to periods of ~1 second means that sampling rates of at least 2 Hz are often used. At this frequency substantial amounts of data are generated and, unless the high frequency content is specifically of interest it is usual to average prior to storing or telemetering the data. If done correctly this involves the summation of orthogonal cartesian components individually prior to computation of the magnitude. Any other form of averaging, it should be noted, can produce wholly erroneous results.

In vector averaging, for instantaneously sampled flow V_i at angle θ_i relative to North, the instrument computes from direct polar measurements the geographical cartesian components

$$\bar{E} = \frac{1}{n}\sum_{i=1}^{n} V_i \sin\theta_i, \quad \bar{N} = \frac{1}{n}\sum_{i=1}^{n} V_i \cos\theta_i$$

or if the instrument measures orthogonal cartesian components X_i, Y_i independently, it forms

$$\bar{E} = \frac{1}{n}\sum_{i=1}^{n} (X_i \cos\theta_i + Y_i \sin\theta_i)$$

$$\bar{N} = \frac{1}{n} \sum_{i=1}^{n} (-X_i \sin \theta_i + Y_i \cos \theta_i)$$

where θ_i is the instantaneous angle between the Y axis and North: n is chosen so as to reduce noisy contributions from the wave spectrum: a value of $nf_s^{-1} > 50$ sec is usual.

The averaged magnitude and direction are then given in the usual way by

$$\bar{V} = (\bar{E}^2 + \bar{N}^2)^{1/2}, \quad \bar{\theta} = \tan^{-1} (\bar{E}/\bar{N}).$$

As indicated above, preference is given to the cartesian rather than to the polar form of measurement. The reason is associated with the nonlinear nature of the rotational transformations: a nonlinearity in one part of the spectral response of a polar sensor will in general introduce errors throughout the spectrum of the averaged output. Inertial effects which degrade the high frequency response of a rotor and vane combination are an example of this. In contrast a similar deficiency in a component sensor merely degrades the high frequency response, leaving the mean unchanged.

Some of these points discussed can be illustrated by the simple example shown in Fig. 2.1, where (a) represents a hypothetical current consisting of a steady mean of 12 cm/s at 0°, on which is superimposed an oscillatory colinear flow of ±20 cm/s at 5 secs period. The broken line (b) represents output from a component sensor assumed to be aligned with the flow. The output lags the input due to a slow response time. Normally rotor response is characterized by a distance constant i.e. the length of fluid that must pass the rotor before it adjusts to the new speed: the time constant (τ) is the ratio of distance constant to speed. Distance constant and time constant are dependent on whether flow is accelerating or decelerating. Here, the rotor is assumed to have a response of the form $\exp(-t/\tau)$ to any sudden change in flow and a time constant $\tau \simeq 0.5$ sec. (b) shows the speeds registered by a perfect (solid line) and a lagging polar sensor (rotor) respectively. (c) illustrates the responses of a perfect vane (solid) and a lagging vane (hatched) with response to a step of the form $\exp(-t/\tau)$.

The following conclusions can be drawn:

(i) For the lagging component sensor (broken line in (a)) the performance is inadequate only if the oscillatory flow is itself of primary interest: the mean current will be registered correctly.

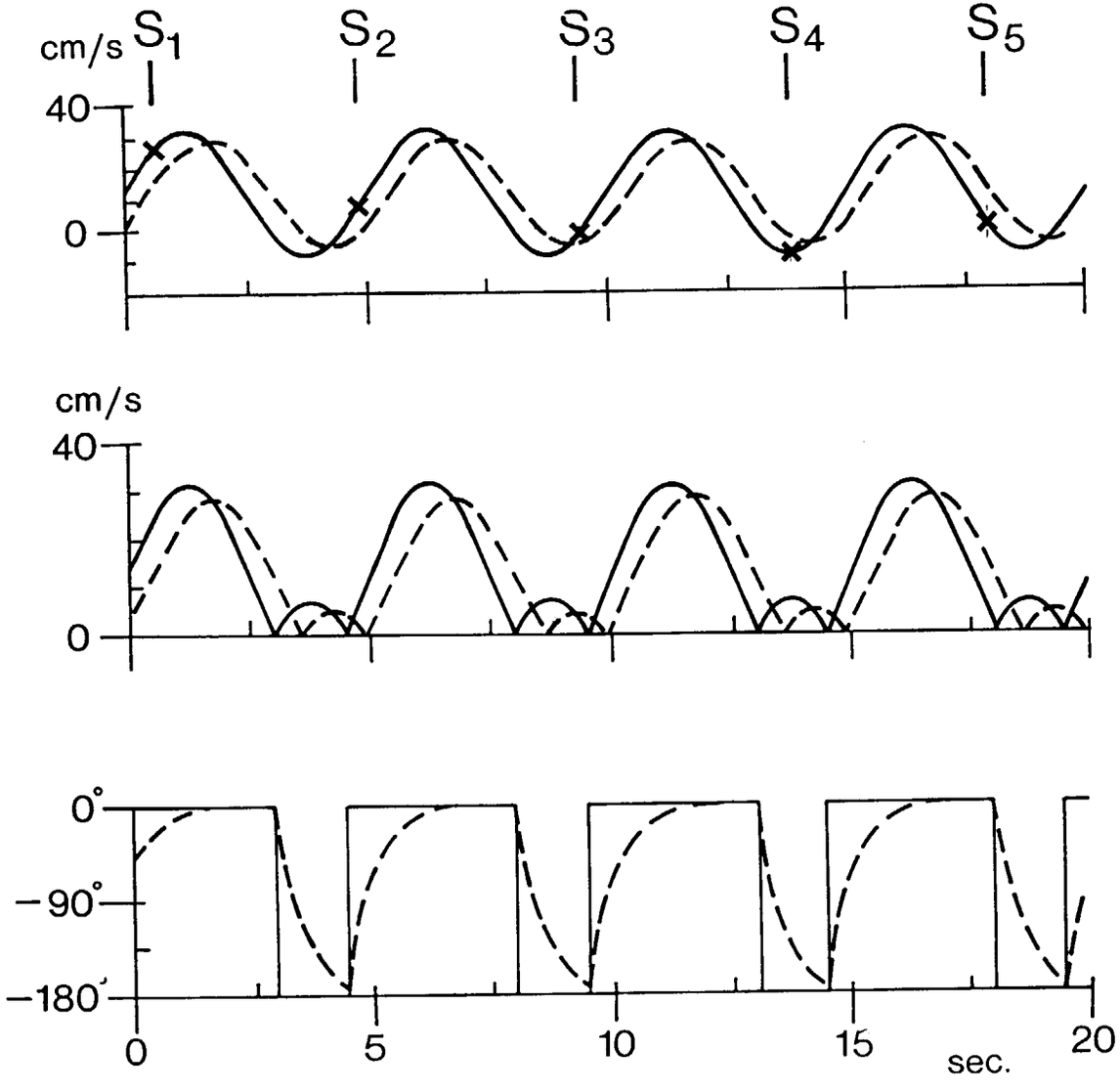

Fig. 2.1 Simple current meter responses

(ii) The lagging rotor/vane measurement (broken line in (b) and (c)), even when correctly resolved and vector averaged produces some error. The mean is 12.5 cm/s at -12°, a result which would be worse if rotor and vane time constants were widely different.

(iii) Independent averaging of magnitude and direction (polar averaging) even when the sensor response is ideal (solid line (b) and (c)) produces totally erroneous results: 15.2 cm/s at -53°. Independent averaging of polar components is fairly common practice in meteorology where the ratio of mean to fluctuating components is large, but is unacceptable when short period flow reversals are likely.

A sampling scheme in which scalar speed is measured and associated with a spot direction - a technique employed in a number of current meters - is clearly also a poor choice for oscillating flow conditions.

(iv) The result of sampling at too low a rate is shown in (a); where the sampled points S_1, S_2, S_3, S_4 ... clearly form part of a spurious low frequency current component.

2.2 Mechanical current meters

Many varieties of mechanical current meter are in existence, the majority of which make a polar measurement of current. With the advent of microprocessor technology, vector averaging schemes are now increasingly common. Three principal types of meter used for scientific observations, shown in Fig. 2.2, are the Aanderaa RCM7 and 8, the vector averaging current meter (VACM) and vector measuring current meter (VMCM). The characteristics of each differ substantially, as we now discuss.

2.2.1 Aanderaa

Originally equipped with a Savonius-like rotor (Savonius, 1931), the Aanderaa instrument (Aanderaa, 1964) senses scalar speed above a threshold of 2 cm/s and relies on a large vertical fin to orientate the entire instrument in the flow: freedom to pivot about a horizontal axis ensures that the instrument is vertical in steady conditions at mooring wire angles of up to 27° from the vertical. Until about 1987 a very simple sampling scheme was used: the number of rotor revolutions during a predetermined sampling interval was recorded on magnetic tape, together with a single spot measurement of meter orientation, derived from a mechanically clamped compass. Analogue to digital conversion of the six data channels available was effected by an electromechanical encoder controlled by a crystal clock. Aanderaa instruments now incorporate a vector averaging sampling scheme and solid state memory. Samples are taken every 12 seconds and are decomposed into E

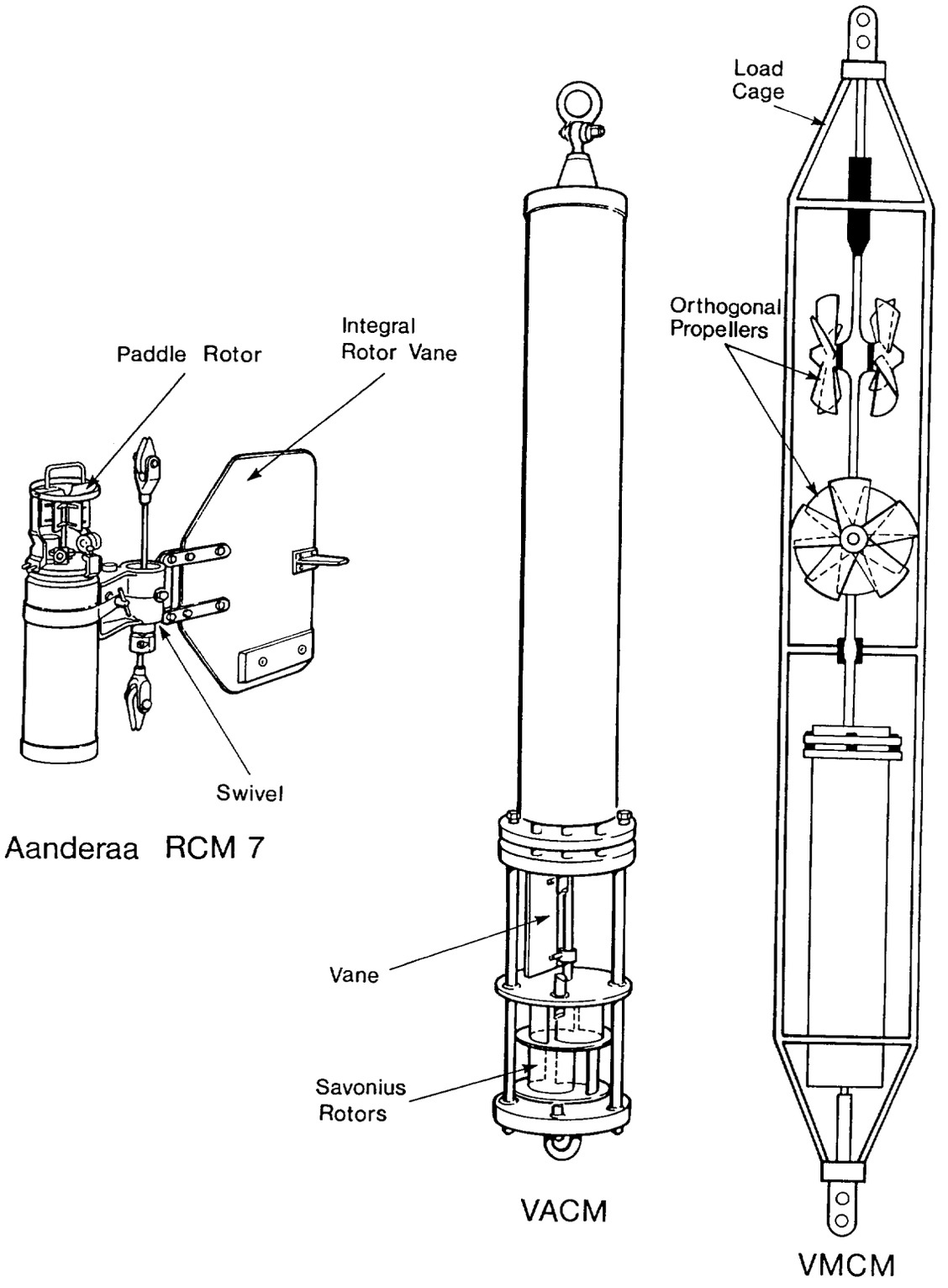

Fig. 2.2 Mechanical current meters in common use in oceanographic laboratories (VACM = Vector Averaging Current Meter, VMCM = Vector Measuring Current Meter)

and N components. Successive components are added and are recorded in EEPROM as speed and direction at the end of the recording interval. The capacity of the system is 10,900 sampling cycles which, for example, provides 75 days of operation at 10 min. sampling intervals. In addition to current speed and direction, provision is also made for measurement of conductivity, temperature and pressure (depth).

Over the years the Aanderaa current meter has established an enviable reputation for durability and reliability and it is relatively inexpensive. There is widespread experience of its use in the major oceanographic institutions and in industry. Though well suited to measurement in steady flow regimes, earlier versions were considered unsuitable for applications in or near the surface wave zone or indeed wherever appreciable instrument motion is likely to occur (Saunders, 1976; SCOR WG 21, 1974). The reasons - discussed above - were associated mainly with the scalar averaging of speed and with the inadequate sampling of direction. The replacement of the Savonius rotor by a paddle wheel design and modifications to the vane have improved performance in the near surface region, though prior to the introduction of vector averaging the fundamental limitations in directional measurement remained (Woodward, 1985). As yet there is relatively little information available on the effectiveness of the more recent changes, though Loder and Hamilton (1990) have reported on some effects of high frequency mooring vibration.

2.2.2 VACM

The VACM (McCullough, 1975), the first of the vector averaging instruments, offers a substantially improved performance over the Aanderaa current meter in non steady flows. The measurement is again made of polar components using a Savonius rotor, whose rotation is sensed eight times per revolution, and a 9 x 17 cm vane to indicate flow direction. At each rotor count the sine and cosine of the flow direction relative to magnetic north are computed from compass and vane follower measurements and are accumulated in east-west and north-south registers over the sampling interval so as to provide a vector averaged mean. Though representing a considerable improvement over current meters employing simple sampling schemes, the VACM falls short of ideal performance in oscillatory flow, due partly to inadequacies inherent in the rotor and vane dynamic response characteristics (Fofonoff and Ercan, 1967), and partly to rotor pumping. This last effect is the name given to the rectification of eddies shed by supporting structures and the instrument case, particularly when the instrument is subjected to strong vertical motions. Horizontal oscillatory flow can cause either underspeeding or overspeeding, dependent upon the characteristics of the flow and the amplitude of the fluctuations relative to the mean. The response of the Savonius rotor to a change in flow conditions may be characterized in terms of the filament length of the fluid that must pass through the rotor before adjustment to the new fluid speed is complete. The time constant is thus dependent upon fluid speed, the rotor responding more closely

to an increase than to a reduction in fluid speed. An estimate of the likely effects of rotor time constants on accuracy has been provided by Saunders (1980) who measured response lengths in both accelerating and decelerating flows. Application of these values in a simple rotor model of the form $\frac{dR}{dt} = \frac{S - R}{t}$ subjected to simple harmonic periodic forcing (where R is the rotor speed converted to apparent flow speed, S is the true speed and t is the rotor time constant) generated maximum fractional errors of ~10% when oscillatory and mean current values were comparable in magnitude.

A similar form of model was also used to examine vane and vane follower responses (Saunders, 1976). In this instance $\frac{d\theta}{dt} = \frac{\theta_i - \theta}{t}$ where θ_i, θ are, respectively, the instantaneous current and vane directions, and $t \geq 1.5$ sec is the combined vane and vane follower time constant. When applied to some representative near-surface current data, an overreading of currents of order 10% was predicted by the model. For a discussion of the importance of vane characteristics reference can be made to Kenney (1977). More recent work by Patch et al. (1992) considers the dynamic response characteristics of the VACM compass and vane follower.

2.2.3 VMCM

It was earlier pointed out that linear component sensors have advantages over polar sensors because the mean flow can still be correctly registered even if the sensor time response is slow. This fact underlies the approach adopted in the third instrument depicted in Fig. 2.2 in which the sensors are dual orthogonal propellers (Weller and Davis, 1980). The two components of the flow are measured directly, only a simple rotation of axes being required to transform the measurement to a cartesian geographical reference frame. The rotation of each propeller is detected by magneto-diodes - asymmetrically set so as to indicate the direction of rotation - which sense the passage of 4 permanent magnets embedded in an epoxy disc rotating with the propeller axle. The heading of the instrument is provided by a flux gate compass whose output is sampled at a 1 Hz rate. On the production of each pulse pair by the rotation of a propeller, sine and cosine of the heading angle are added to registers storing the East-West and North-South components, thus forming at the end of the sampling period a vector average of the flow. Preset sampling intervals between 1 and 15 minutes can be selected, the data then being written to cassette tape. The instrument is designed for in-line mooring, the exterior titanium frame - from which the instrument housing is isolated - carrying the mooring tension. The rotors are mounted in the frame so as to reduce flow disturbance in their vicinity caused by the instrument housing.

The development of the VMCM offers an example of the way in which modelling of complex dynamic sensor response and the feedback of results from tank testing have played a central role in achieving a near-optimum design. A simple model of propeller dynamics such as that advanced by

Davis and Weller (1980), though neglecting interactions between propeller blades, serves to identify parameters important in determining response; it also provides insight into the nature of the compromise that must be reached in selecting values for design parameters such as propeller pitch angle. In steady axial flow an ideal, frictionless propeller is accelerated until the lift and drag forces on its blades, which are quadratic in velocity V, are perfectly balanced at a given radius along the blade, and the sensor is essentially linear. Any off-axis flow component, or unsteadiness in the flow modifies the angle of attack of blade on fluid, thereby disturbing the dynamic balance, and hence includes contributions from the quadratic forces: a likelihood of non linear response then exists. Low pitch angles minimize the effects of off-axis components at the expense of increased bearing loads. However, response to unsteadiness in the axial component of the flow is also important, and can be described - as for the VACM - in terms of a distance constant L, which in this case is proportional to blade inertia and inversely proportional to sin (angle of attack). Good high frequency response therefore demands low blade inertia and high pitch angle, and a compromise has to be sought.

Tow tank testing and intercomparisons at sea are discussed in more detail later, but it can be remarked that the VMCM has been shown to perform well in near-surface conditions. Results from some of the more recent evaluations (Beardsley, 1987) suggest that the VMCM has the tendency to underread slightly, perhaps by -5% in a range of conditions in which a co-sited VACM overresponds by between 10% and 20%.

2.3 Acoustic travel time current meters

Acoustic current meters can be broadly classified into two types: those based on reverberation or backscatter techniques - described in Section 3 - and acoustic travel time (ATT) systems, the earlier development of which has been reviewed by McCullough and Gräper (1979).

ATT systems are based on the assumption that the resultant velocity of an acoustic pressure wave propagating at any point in a moving fluid is the vector sum of the fluid velocity at that point and the sound velocity in the fluid at rest. In essence the method involves the measurement of the difference in propagation time of an acoustic pulse along reciprocal paths in the moving fluid, although this basic principle can be realised equally in terms of measurement of phase or frequency difference.

For two transducers, A, B, separated by a distance x in fluid moving with velocity $\underset{\sim}{V}$ at an angle θ to the common axis, the travel time in one direction is

$$t_1 = \int_A^B \frac{dx}{c \cos \alpha + \underset{\sim}{V} \cos \theta}$$

where c is the sound velocity in the fluid at rest and $\alpha = (V \sin \theta)/c$.

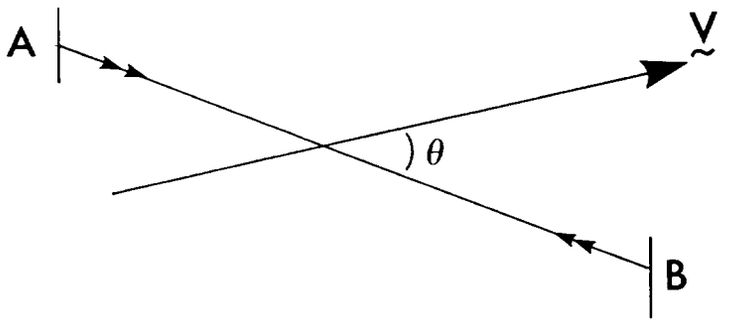

Fig. 2.3

For the reciprocal path

$$t_2 = \int_A^B \frac{dx}{c \cos a - \underset{\sim}{V} \cos \theta}$$

The propagation time difference is then

$$\Delta t = t_2 - t_1 = 2 \int_A^B \frac{\underset{\sim}{V} \cos \theta}{c^2 \cos^2 \alpha - V^2 \cos^2 \theta} dx$$

$$\simeq \frac{2x \ \overline{\underset{\sim}{V} \cos \theta}}{c^2} \text{ given that } V << c.$$

For a known transducer geometry, the measurement of fluid velocity component thus depends solely on the measurement of time difference, and on a knowledge of sound velocity, which can be derived from the two-way travel time, $t_1 + t_2 \sim 2x/c$. The current vector is obtained by using two or more sound paths.

Measurement of phase difference requires the use of continuous wave (cw) or continuous wave burst transmissions. The analogous phase expression to that above is:

$$\Delta f = \frac{4\pi f x \overline{V \cos\theta}}{c^2}$$ where f is the transmission frequency.

The frequency difference technique, as applied to a pulse system, measures the difference in upstream and downstream pulse repetition frequencies, f_1 and f_2, each pulse being triggered in a given direction by the arrival of the preceding pulse.

The difference pulse repetition frequency, $f_1 - f_2$, is then related to the mean velocity component along the axis by

$$\Delta f = \frac{2 \overline{V \cos\theta}}{x}$$

Each of the three techniques presents a different set of design constraints, accompanied by both advantages and disadvantages. In a self-recording current meter, for which the acoustic path length is typically of order 10 cm it follows from the expression for Δt that the resolution of currents to better than 1 cm/s by the time difference method requires time discrimination to about 10^{-9} sec. This emphasizes a need for highly stable, wideband detection of pulse arrivals, a critically important factor in achieving a successful design. Aspects of the design and performance of an acoustic travel time sensor are discussed by Gytre (1976, 1980). In contrast, phase detection of continuous wave signals is effected within a narrow bandwidth, thereby relaxing the front end circuit design requirements. Accurate phase difference measurement at frequencies of order 1 MHz is difficult, but the application of heterodyning techniques so as to make the comparisons at a few kHz baseband frequency results in a relatively simple system. Phase measurement provides good zero stability and low power consumption, but the need to avoid phase ambiguity can affect selection of path length.

As is also the case with the travel time methods, the phase measurement technique can in principle be implemented either by using two pairs of independent transducers for simultaneous transmission and reception along each path, or else by combining these functions in two single transducers, and separating reciprocal cw burst transmissions in time (Brown and Lawson, 1980). Another implementation has been tried which, however, demands considerable attention to front end isolation. In this method simultaneous transmission and reception of two cw signals takes place through single transducers, relying on the frequency separation to achieve discrimination (Lawson et al., 1976).

The frequency difference method has some advantage in that independent measurement and explicit corrections of temperature induced changes are not required, though with the advent of microprocessor based instruments the advantages are probably slight nowadays.

Whichever of the three basic methods outlined above is chosen, hydrodynamic considerations are likely to be critically important in achieving accuracy of measurement. The principal difficulty arising in the case of acoustic current meters is that of providing rigid mounting arrangements for the transducers, which are typically of order 1 cm in diameter, at each end of an acoustic path of perhaps 10-15 cm without significantly disturbing the free stream flow. Various approaches have been adopted or suggested (McCullough and Gräper, 1979) in order to minimize disturbance, including the use of mirrors so as to route the sound path away from regions likely to be influenced by wakes generated by transducer supports (Fig. 2.4). Latterly the development of microprocessor technology has enabled use to be made of redundant paths, so that for a given instrument orientation, the least disturbed paths can be selected in subsequent processing.

The basic ATT techniques have been implemented in various forms for a range of applications. As in the case of electromagnetic sensors applications include miniature probes for use in laboratory wave tanks, profiling instruments, self recording current meters and buoy mounted instruments specifically intended for use close to the sea surface. Examples of in situ recording instruments in common use which employ the transit time and cw burst techniques are the Simrad UCM and the Smart Acoustic Current Meter manufactured by EG & G Inc. The frequency difference method seems to be less widely used, although Mahrt (1980) has described a miniature profiling sensor which operates in this mode at 5 MHz. The technique has also been used in a long path acoustic sensor designed to measure near surface currents (Fig. 2.5), in which the transducers were mounted approximately 3 m apart on spars beneath a 7.6 metres diameter data buoy (Rusby et al., 1978). This technique proved to be very effective and more than five years of nearly continuous operation of the instrument were obtained at two sites in the vicinity of the British Isles. More recently ATT techniques have been extended to path lengths of tens of kilometres in order to provide measurements of transport in the open sea. These techniques are considered in Section 6.

In summary ATT current meters offer the advantages of well defined spatial averaging, high resolution of current ($\leq$1 mm/s), potentially good linearity and excellent high frequency response. The main problem, tackled with varying degrees of success in individual types of instrument, seems to be associated with disturbance of the flow in the acoustic path by transducers, support struts and instrument housing.

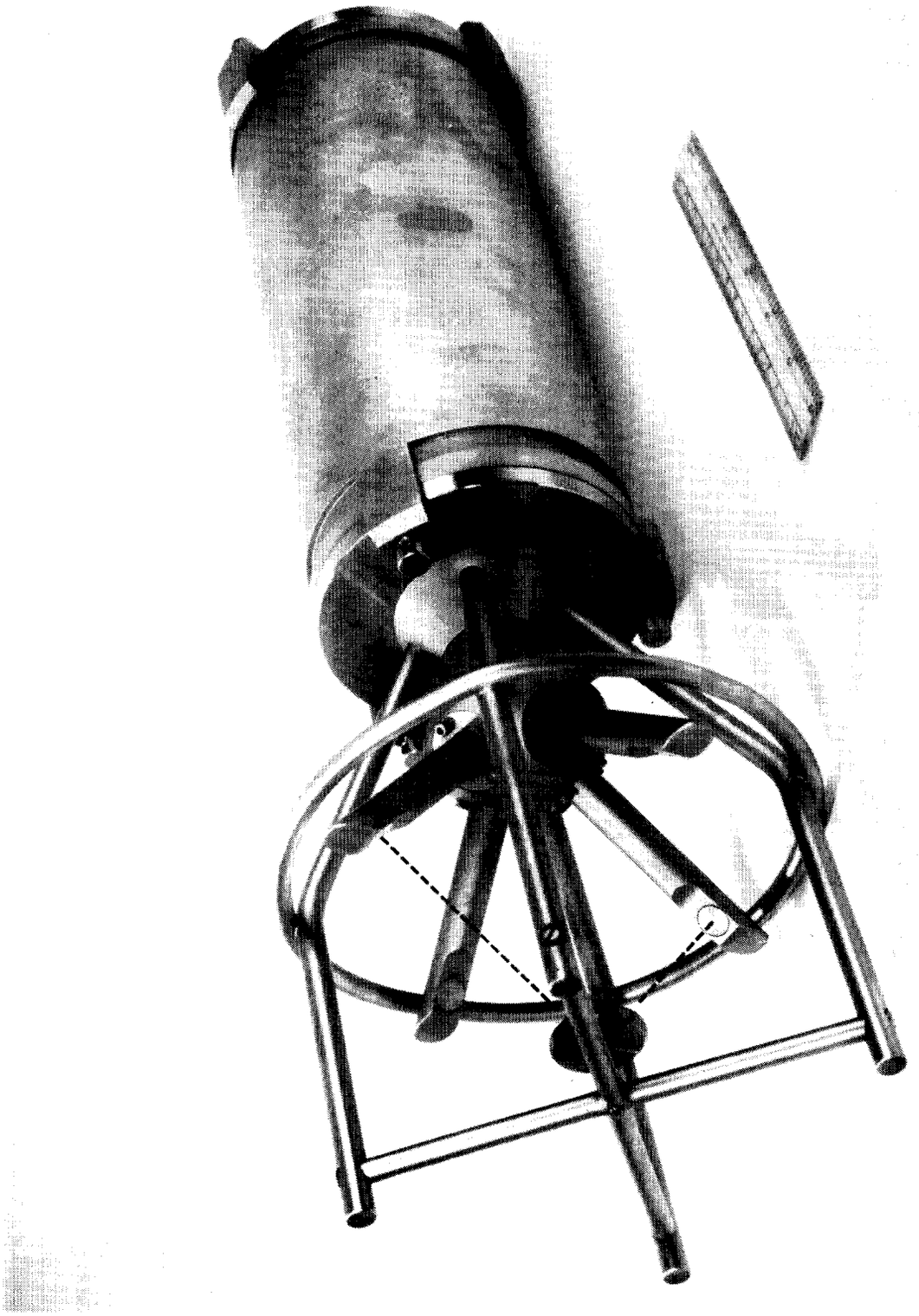

Fig. 2.4 Acoustic travel time current meter (original Christian Michelsen Institute design). Hatched line shows one of the two orthogonal acoustic paths via a reflector.

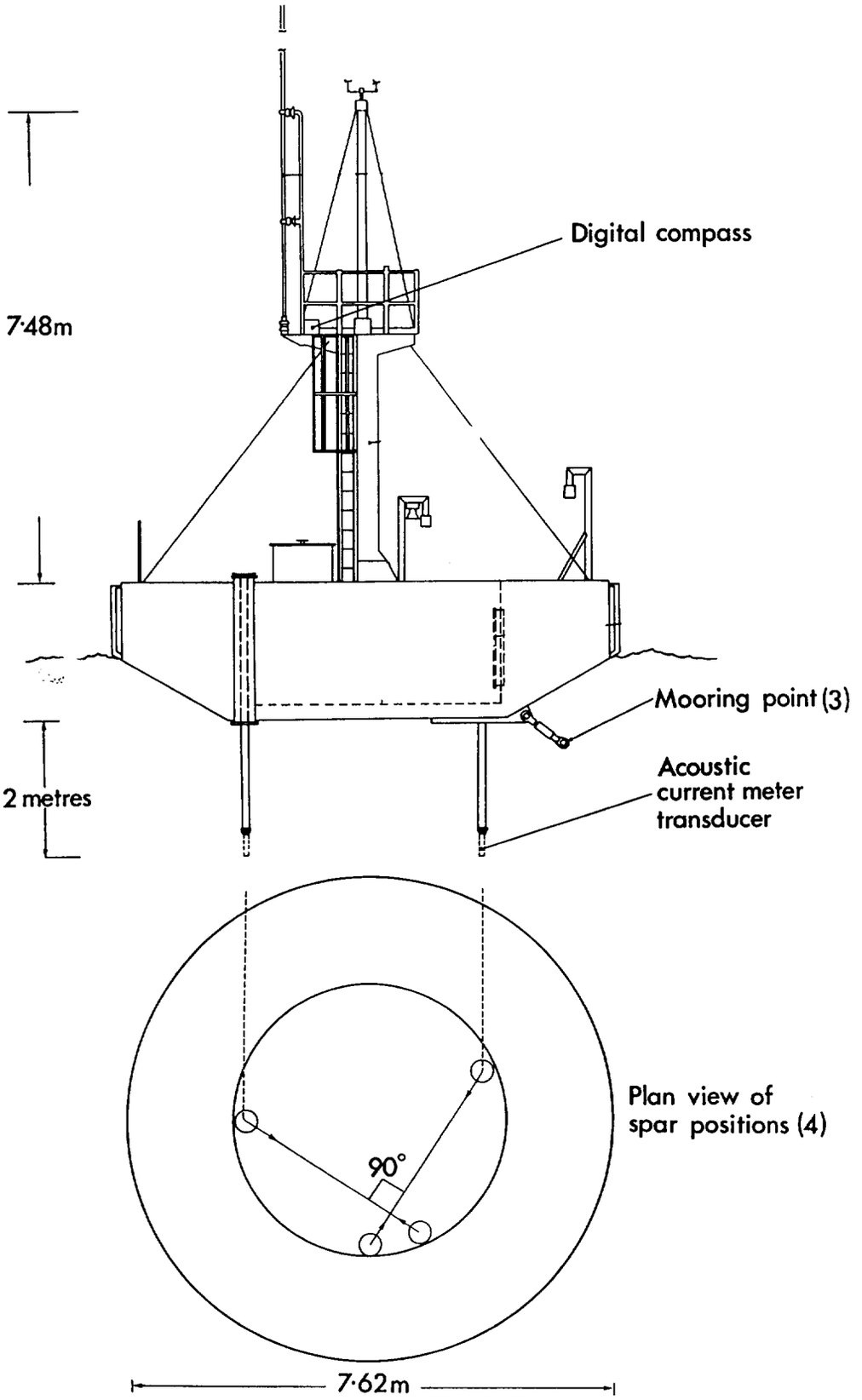

Fig. 2.5 Long path acoustic current meter mounting arrangement on UK Data Buoy, DB1.

2.4 Electromagnetic Current Meters

The operation of electromagnetic current meters is based upon the Faraday Effect: when a magnetic field is applied to moving fluid - for example in the z direction in fig. 2.6 - electric potentials are generated in the fluid, dependent upon the fluid velocity. Thus, in the z = 0 plane potential gradients in the x and y directions are proportional to the flow components V_x, V_y.

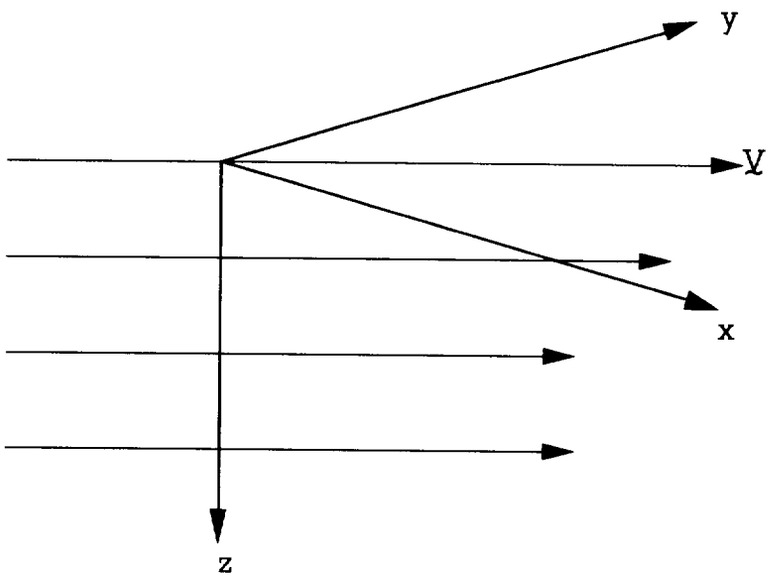

Fig. 2.6

In practical e.m. current sensors the magnetic field is impressed on the fluid using a coil buried in the sensing head and measurements of the potential gradients are made using orthogonally mounted pairs of electrodes. Instruments are usually configured for measurement of two horizontal current components, but there is no reason in principle why measurement should not be made of 3 dimensional flow. The impressed magnetic field may be either a.c. or switched d.c. Some electromagnetic techniques make use of the Earth's magnetic field (Section 4) but in self-contained instruments the use of d.c. excitation is avoided because variable polarisation potentials at electrodes, and stray d.c. potentials in the water, can easily exceed flow generated potentials by two orders of magnitude. A.c. excitation produces induction e.m.fs in the electrode leads, though these can be balanced out. Tucker (1972) found that on occasion the a.c. technique produced the greater sensitivity to the presence of inhomogeneities such as bubbles, struts or a surface, and for these reasons adopted switched d.c. (square wave) excitation, in which transients are allowed to die away before the electrode voltages are sampled, using a phase sensitive rectification technique. The main disadvantage of this technique is that noise is accepted in a number of bands centred on odd harmonics of the excitation frequency: the signal to noise ratio is then theoretically worse than for a cw system.

The basic theory of electromagnetic flow meters has been discussed by Shercliff (1962). The starting point is provided by Maxwell's equations:

$$\nabla \times \underset{\sim}{E} + \frac{\partial B}{\partial t} = 0$$

$$\nabla \times \underset{\sim}{B} - \frac{\partial B}{\partial t} = \mu \underset{\sim}{J}$$

and the relationship (Ohm's Law) $\underset{\sim}{J} = \sigma(\underset{\sim}{E} + \underset{\sim}{V} \times \underset{\sim}{B})$

where B is the magnetic flux density; D the electric displacement; J the current density vector. The term $\underset{\sim}{V} \times \underset{\sim}{B}$ represents the e.m.f. induced in the fluid moving with velocity V, whose permeability and conductivity are denoted by the scalar quantities μ and σ.

The choice of frequency for a.c. driven systems - or field reversal rate in the case of switched d.c. drives - is somewhat dependent on application. In oscillatory flows the drive frequency should be several times higher than the highest frequency of interest in the flow, in keeping with the requirements of the sampling theorem, but should not be so high that skin effect or dielectric relaxation become important. At angular frequencies $\omega << \frac{\sigma}{\varepsilon}$, where ε is the dielectric permittivity, dielectric relaxation is essentially instantaneous, and displacement current D can be neglected. Likewise, for $\omega << \frac{2}{L^2\sigma\mu}$, where L is a characteristic dimension of the sensor, generally ~5-50 cm, self induction manifest in the classical skin effect can be neglected. In practice drive frequencies lie between about 10 Hz and 1 kHz or so. Substitution of appropriate values of $\varepsilon \approx 81$ x permittivity of free space $\approx 81 \times \frac{1}{36\pi} \times 10^{-9}$, $\sigma \sim 4$ Siemens/m for seawater, and $\mu \sim 4\pi.10^{-7}$ shows that conditions for neglect of terms in $\frac{\partial D}{\partial t}$ and $\frac{\partial B}{\partial t}$ in Maxwell's equations are then comfortably met.

Since these $\nabla \times \underset{\sim}{E} = 0$, a potential ϕ can be defined such that $\underset{\sim}{E} = -\phi$, while from Maxwell's second equation, $\nabla.\underset{\sim}{J} = 0$.

Substituting from the third equation,

$$\nabla.\underset{\sim}{J} = \sigma(-\nabla.\nabla\phi + \nabla.(\underset{\sim}{V} \times \underset{\sim}{B}) = 0.$$

The properties of the e.m. current sensor are thus described by solutions of the Poisson equation

$$\nabla^2\phi = \nabla.(\underset{\sim}{V} \times \underset{\sim}{B})$$

with appropriate boundary conditions. This effectively describes the potential distribution arising from a continuum of elements $(\underset{\sim}{V} \times \underset{\sim}{B})$, contributions being everywhere perpendicular to the local

field and to the local flow vector. Note that the problem can be reduced to a time independent or d.c. situation, in which the ideal form of solution for the potential difference between electrodes is:

$$\nabla\phi = B\,V\,L.$$

Typical sensitivities are generally within the range $10\text{-}10^2$ μV/m/sec.

Bevir (1970) has extended e.m. current meter theory in terms of a 'weighting function' concept, which provides insight into the way in which the regions surrounding the sensor head contribute relatively to the overall sensitivity. According to Bevir the potential difference measured between the electrodes of a sensor is:

$$\nabla\phi = \int \underline{V}.(\underline{B} \times \underline{W})\, d\tau$$

where τ is volume and W is the local current vector resulting from unit virtual electric current injected into the sea at one electrode and recovered at the other, in the absence of flow in the fluid. In principle, it is thus possible to compute the sensitivity of a sensor possessing a particular electrode configuration, provided that the magnetic field and flow field distributions are known. Evaluation of the virtual current distribution can be done in terms of a current potential distribution using, for example, relaxation methods to solve Laplace's equation numerically.

The flow field around a sensor head, established to a large extent by the head geometry, is of critical importance in that it determines the degree of linearity that can be achieved as well as the nature of the directional response. Characteristics of the flow that are important include the thickness and velocity-dependence of the surface boundary layer, especially in the proximity of embedded electrodes; also the existence of flow separation effects which create complex flows capable of generating substantial non-linearity in the sensor output. Modelling techniques, when applied to flow conditions and sensor response, can provide a basis for understanding sensor behaviour and for prediction when seeking an optimum head design. Bevir's method lends itself to numerical evaluation of sensor response, although as yet it does not seem to have been widely used in oceanographic sensor design. In contrast Cushing (1976) has constructed analytical models in order to compare the responses of different head geometries.

Forms of head shape that have been considered or used include various solids of revolution, such as spheres, cylinders, and ellipsoids. Although the hydrodynamic performance weighs heavily in choice of shape, this may be balanced in individual cases by considerations such as ease of fabrication and durability. The sphere has proved particularly attractive in that it possesses three

dimensional symmetry and might therefore be expected to exhibit good responses to off-axis flows. However, any sensor head inevitably disturbs the free stream flow and introduces the risk of flow separation as the following example (Fig. 2.7) illustrates.

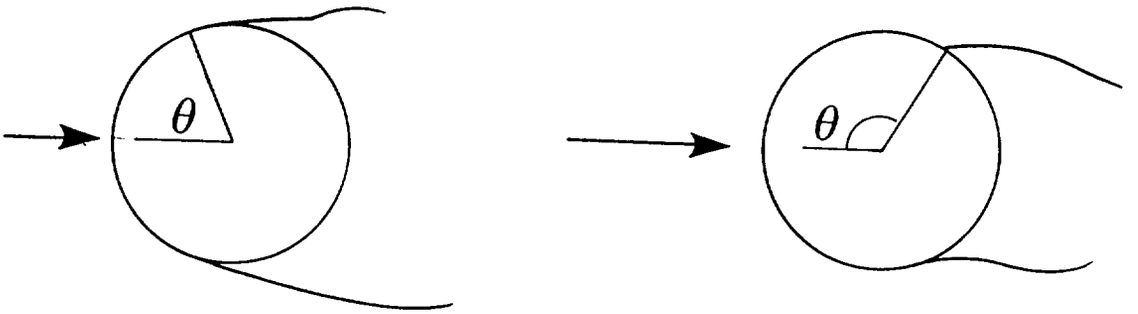

(a) (b)

Fig. 2.7 Flow around a sphere for
(a) Reynolds number $<4 \times 10^5$
(b) Reynolds number $>5 \times 10^5$

The flow regime around a solid body depends upon the dimensionless Reynolds Number, $R_e = VL/\upsilon$, where V is fluid velocity, L is a characteristic dimension and υ is the kinematic viscosity. For a sphere at very low values of R_e flow in the equatorial plane is laminar and fully attached at all azimuth angles θ (here defining $\theta = 0^\circ$ as the forward stagnation point, where fluid pressure is greatest). For $10 < R_e < 3.5.10^5$ flow in the equatorial plane separates shortly before the point of minimum pressure is reached, at $\theta \sim 70^\circ$ (Fig. 2.7(a)). The flow is still laminar and though a regular vortex street is established in the range $70 < R_e < 5000$, the wake does not become fully turbulent until $R_e > 5000$. Throughout the range $10 < R_e < 10^5$ at angles $\theta > 70^\circ$ the flow in the boundary layer close to the sphere surface is reversed as a result of the increasing pressure towards the rear of the sphere. Flush electrodes embedded in the equatorial plane would thus experience this reverse flow component. As the Reynolds Number increases beyond 4.10^5, the point is reached within the range 4.10^5 - 5.10^5 at which the boundary layer begins to become turbulent. Laminar separation begins but turbulent reattachment takes place. The fluid sheets nearest the surface possess increased momentum and are better able to flow against the positive pressure gradient along the rear of the sphere. In consequence the flow remains attached until final separation occurs at angles exceeding 120° (Fig. 2.7(b)). As R_e increases further the point at which turbulent reattachment takes place moves closer to the forward stagnation point.

The shape and dimensions of the sensor head are clearly important: the design must avoid the critical range of Reynolds Numbers if changes in sensitivity and response are not to occur (Griffiths et al., 1978). Some degree of immunity from the problems caused by changes in flow

regime around a solid of revolution can be obtained by mounting the electrodes out from the surface. This technique has been adopted in the Marsh McBirney instruments, an assessment of which has been made by Aubrey and Trowbridge (1985). Another development has ingeniously circumvented the problems associated with Reynolds Number transitions. The InterOcean S4 meter (Lawson et al., 1983) incorporates the entire instrument within a spherical housing which can be inserted directly into a mooring line. The resulting instrument dimensions would normally yield critical Reynolds Numbers at some point within the working range, but this is forestalled by use of surface ribsr so as to induce a fully turbulent boundary layer throughout the working speed range. Good linearity is thereby achieved.

The alternative to using solids of revolution in the design of electromagnetic sensor heads is to adopt an open form of construction, thereby minimising disturbance to the flow as far as is practicable. This approach, investigated earlier by Olsen (1972), has been adopted at IOS in work on the measurement of mean current in the wave zone. Head shapes such as the discus form, developed earlier for use in a ship's log (Tucker et al., 1970), and used successfully also for current measurement in near-rectilinear flows (Thorpe et al., 1973) do not perform adequately in three dimensional flows (Griffiths et al., 1978). In the open head construction, an example of which is shown in Fig. 2.8 together with discus and spherical forms, the magnetic field coil is contained in an epoxy moulding of ellipsoidal cross section so as to minimize disturbance when flow is mainly in the plane of the coil. Four electrodes are mounted within the annulus, and screened electrode leads and coil drive conductors are led away through the tubular support arms. It has been the practice in IOS-designed sensor heads to use Monel as the electrode material, though other materials used elsewhere include carbon and silver. Variants of this form of head construction which was developed at IOS for a vector averaging current meter (Clayson, 1983) include a 45 cm diameter sensor designed for mounting beneath a surface buoy (Collar et al., 1988); a miniature 4 cm sensor for small scale resolution; and an experimental sensor incorporating two field coils and pillar-mounted electrodes (Fig. 2.9) intended for simultaneous measurement at four levels within 0.5 metres of the sea surface. For each of these open forms, extensive tow tank tests (Griffiths et al., 1978) have shown that excellent linearity and off axis response obtain: the maximum departure from linearity for the 15 cm diameter head for example is less than ±2 mm/s in a 1.5 m/s speed range. Perhaps the main relative disadvantages of this form of construction compared with solid heads are the complexity of construction and their fragility, which often requires some form of protective ring or cage to be mounted around the sensor.

Sensor head design affects other aspects of performance. For example head sensitivity - which is of order 20μV/m/s for 1 watt dissipation - increases as the square root of both the power dissipation in the coil and a characteristic linear dimension of the coil. Head shape rather than size, on the other hand, is generally more important in determining noise level. With the possible

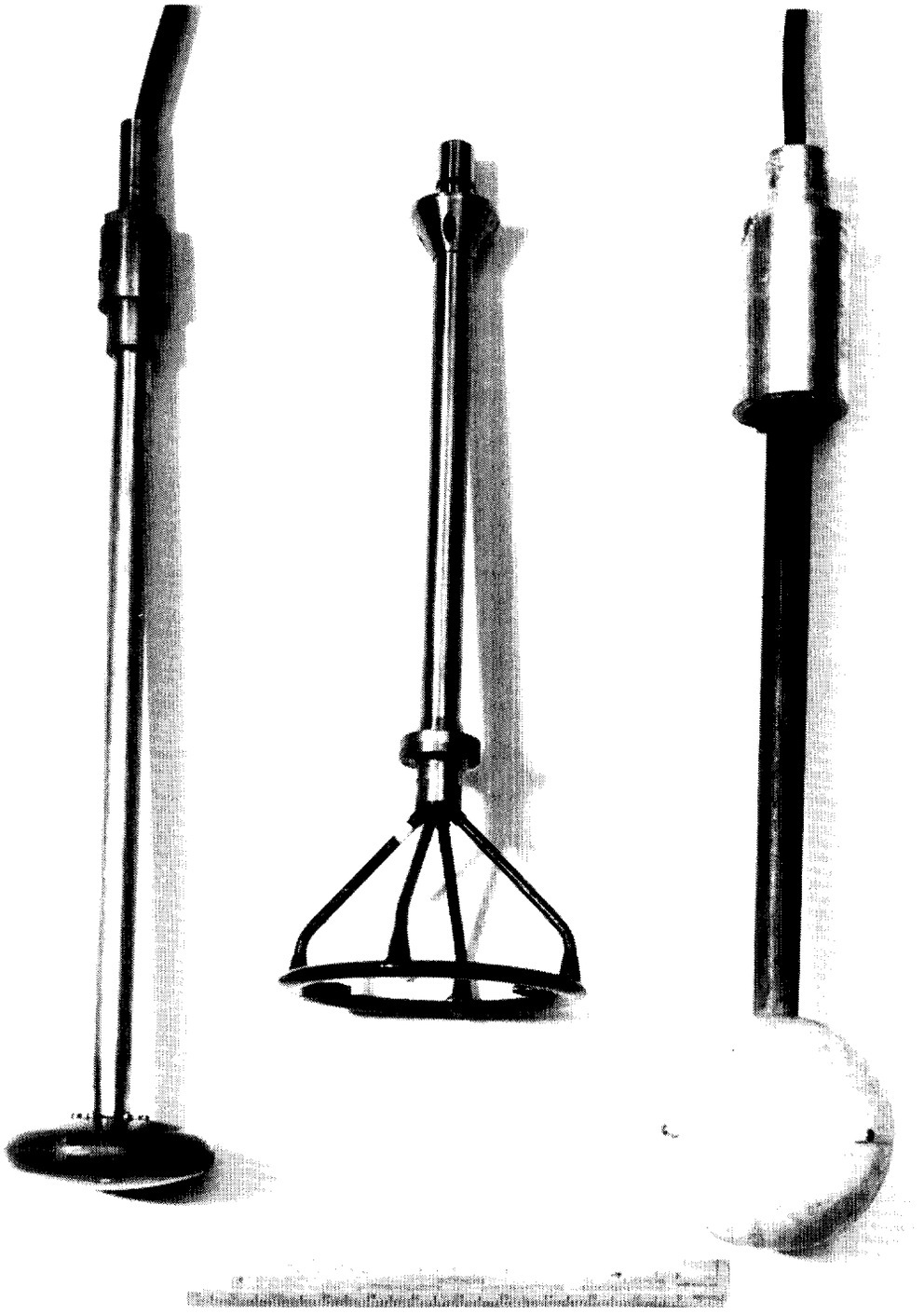

Fig. 2.8 Three forms of electromagnetic sensor head

Fig. 2.9 Experimental electromagnetic sensor intended for simultaneous measurement of currents at four levels within 40 cm of the sea surface. The inflated tube provides coupling to the sea surface. Orthogonal pairs of electrodes are distributed along the pillars which separate the field coils.

laminar flow around streamlined head forms such as the ellipsoid, flow induced noise is likely to provide the dominant contribution to sensor noise level. Wherever in the spectrum this is true, signal to noise ratio cannot be improved merely by increasing coil input power. This situation obtains for the open sensor in Fig. 2.8. A series of tow tank measurements (Griffiths et al., 1978) showed that this has associated with it an rms noise level of ~0.6 cm/s at 50 cm/s within a nominal bandwidth of 5 Hz. The thermal noise within the same bandwidth is of order $(1.7.10^{-20}.RB)^{1/2}$ where B is the bandwidth and R is the electrode source impedance. In fresh water R ~ 3kΩ, in sea water ~ 70Ω; thermal noise therefore results in noise in the current signal of ~0.07 cm/sec and ~0.01 cm/s respectively. Noise levels measured for the discus sensor were only slightly greater than the thermally induced noise and were related to fluctuations in carriage speed. In practice the bandwidth required for most measurements is much smaller than that available, and prefiltering is possible. Noise levels are also reduced by taking vector averaged values over a minute or two, yielding a current resolution typically <1 mm/s.

For many purposes power dissipation levels need not exceed a few tens of milliwatts, though at these levels difficulties can sometimes be experienced in calibration in fresh water tanks, where the sense head source resistance is relatively high and stray potentials are often present in the water as a result of electrical activity in surrounding buildings. In such cases careful attention to earthing arrangements is essential but is usually enough to overcome any problems. The mains supply frequency can be intrusive in this respect, and is usually evident in the form of an unwanted low frequency beat at the output of the instrument. For this reason the choice of head drive frequency should avoid the mains frequency, its harmonics and sub harmonics: otherwise a spurious d.c. offset in the calibration may result.

Unlike mechanical current meters, electromagnetic instruments have no zero velocity threshold. Response down to zero velocity is, however, of little value unless the output is stable. Potential causes of instability include electrode contamination, biological fouling of the sensor producing a major disturbance of the boundary layer, and changes in the insulation resistance between the magnetising coil and the water: electronic drift, once a problem, can now generally be made insignificant. Experience suggests that the first cause is generally not a problem in measurement at sea, although care is required when heads are first put into the water for calibration. The water surface in a tow tank frequently carries a thin, almost imperceptible greasy film. The prior addition to the water of a drop or two of detergent has been found to eliminate this nuisance. The second cause is site- and time-dependent, but in the open sea has not generally been found to present any problem. The third potential cause of instability arises because the coil-water resistance path forms a potential divider with the electrode source resistance, thus permitting a proportion of the coil drive voltage to appear at the output. The need for adequately high ($\geq 10^9\Omega$)

coil insulation resistance is particularly acute in the form of construction adopted for the annular head, but with care stabilities to within a few mm/s over periods of several months can be realised.

Overall electromagnetic sensors potentially possess many of the same advantages as acoustic travel time instruments, particularly of fast response and good linearity, though sensor head design probably represents a more critical area for electromagnetic sensors than for acoustic instruments. Interaction of the flow with the sensor head is clearly of fundamental importance. While much evaluation work has been done in laminar flow conditions, knowledge of response to turbulent conditions is less well developed. This is a difficult area in which to work, partly because turbulence characteristic of the sea is difficult to create in the laboratory tow tank or flume - and partly because, unlike ATT instruments which possess a well defined linear averaging scale, the electromagnetic sensor yields a weighted, volumetric average. Evidence from the few investigations reported in turbulent flow is conflicting, though this may result from the nature of the flow around differing head shapes. Bivins (1975) found up to 20% changes in sensitivity when a cylindrical sensor was subjected to grid induced turbulence. The preliminary results of Aubrey and Trowbridge (1985) using a Marsh McBirney spherical sensor were not conclusive but showed some evidence for a decreased sensitivity. Griffiths (1979) on the other hand found no evidence for change in experiments using an annular sensor in turbulence created either by a towed cylinder or by a submerged jet.

2.5 Measurement of Direction

The directional reference for measurement of current is invariably supplied by a magnetic compass, two main types of which are in common use. The first is the traditional bar magnet, perhaps mounted on an optically read encoded disc, or, as in the case of the Aanderaa compass clamped on sampling to a potentiometer providing an analogue output. The entire assembly is usually mounted on jewelled bearings, and arrangements are made for damping and gimballing. The second class of sensor is the flux gate type in which a soft magnetic core is driven into saturation by an a.c. signal. Orthogonal secondary windings detect the out of balance harmonic signals caused by the polarising effect of Earth's field and, from an appropriately summed output, the orientation of the sensor relative to Earth's field can thus be derived. For current meter applications it is usual to use a two component system suitably gimballed in order to provide a horizontal reference: in the S4 current meter, for example, the core is floated in an inert heavy liquid within the sensor assembly, and windings are situated on the outside. For a detailed discussion of compass design and construction the reader should consult Hine (1968).

Compass performance has at times in the past suffered neglect by comparison with the scale of development effort put into the current sensor itself. Again, the most stringent requirements

arise in situations where appreciable instrument motion is encountered, such as in the surface wave zone. The dynamic response of the gimballing system and of the compass itself, if of the moving magnet type, must be able to cope with both rotational and translational motions across a wide range of excitation frequencies. At the same time, in a vector averaging system, the compass response time has to be sufficiently short that compatibility with the sampling frequency is achieved. Few data relating to the dynamic behaviour of compasses have been published, although Patch et al. (1990) have carried out simple laboratory experiments on the VACM instrument.

The static calibration of the compass is important and should be carried out in a region free from stray fields using a precisely orientated compass table equipped with an accurately graduated scale. Non linearities in compasses can produce significant errors. In strong tidal or inertial flows, errors in the residual circulation can amount to 1% of the mean scalar speed per degree of compass non linearity (Gould, 1973). Considerable care must therefore be taken to avoid unwanted stray magnetic fields in the vicinity of the compass - and there are many pitfalls for the unwary. Instances have arisen where battery packs have been found to possess a significant magnetic field, while some years ago a pressure dependent error was discovered in Aanderaa current meters (Hendry and Hartling, 1979). This resulted from the magnetisation, at high pressures, of a nickel coating on the meter case by the compass magnet. Errors of up to 10° were observed at pressures of 2800 dbar: sticking of the compass took place above 4200 dbar.

2.6 Calibration, evaluation and intercomparison

The calibration, evaluation and intercomparison of current measuring instruments and techniques are all closely related and are central to the issue of data quality assurance. Calibration is usually carried out either in a tow tank of nominally still water by moving the sensor at a constant, independently determined velocity, or in a flume in which water is pumped past the stationary instrument. In tow tanks care must be taken to avoid residual circulations - settling times between calibration runs can be lengthy - but unlike the case of the flume a direct measurement is made of the fluid velocity relative to the instrument under test. The 50 x 2 x 2 metre freshwater towing tank at the Institute of Oceanographic Sciences Deacon Laboratory, shown in Fig. 2.10, is typical of several such installations. The carriage on which sensors are mounted is powered by hydraulic motors, and operates at preset speeds within the range 0.01 - 2 m/s. Carriage speed is obtained by interrupting a light source-detector path with a slotted wheel, geared to a ground steel wheel spring loaded on the running rail. The pulses are counted synchronously with current sensor outputs. All data sampling, processing, recording and display activities are handled by an IBM PC based system.

Amongst current meter users there is a variety of practices relating to routine calibration, ranging from calibration checks before and after every deployment of the instrument to almost

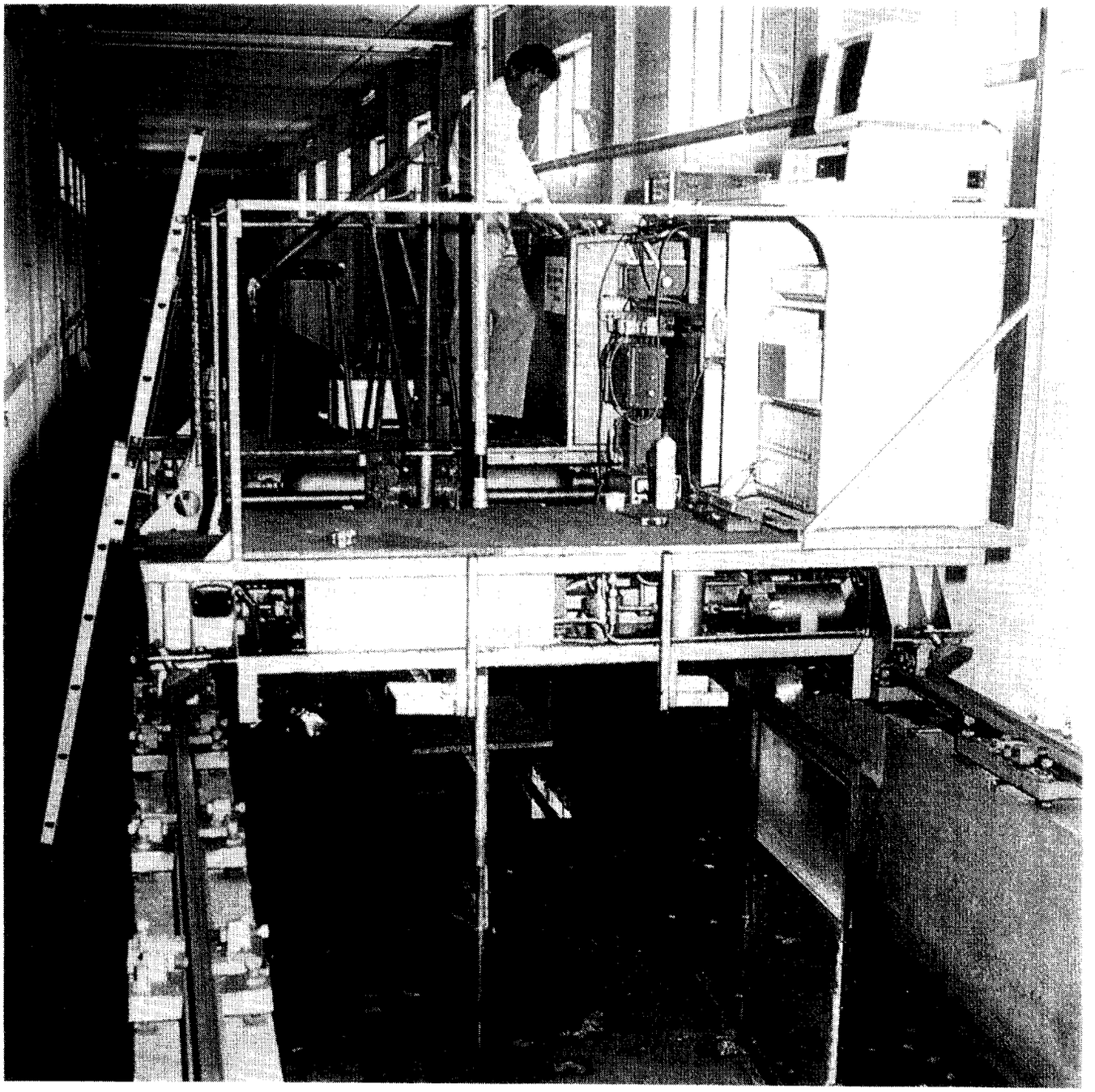

Fig. 2.10 Towing tank at the Institute of Oceanographic Sciences Deacon Laboratory

complete lack of any checks. There is also divergence of opinion as to what is necessary. In the case of mechanical sensors some argue that all instruments of one type have identical rotors, hence identical time-invariant calibrations - and that a simple in-air test to ensure free revolution of the rotor is sufficient. The new generation of current meters, electromagnetic, acoustic, also, should have stable sensitivities because these are determined by physical dimensions and stable electronic gains. However experience at IOS suggests strongly that individual instruments require pre and post deployment calibration checks, including linearity, compass calibration, and checks of ancillary parameters such as temperature.

Fortunately most current meters in fact behave well in steady flows: it is generally only when near-surface measurements are required - or appreciable mooring/platform motion is present - that problems arise. Substantial differences often occur in measurements made by different instruments used at the same place and time after calibration in steady flows.

The reasons lie in the differing instrumental responses to the complex broadband fluid motions experienced in the ocean, but which cannot be reproduced satisfactorily in the laboratory. There are as yet neither standard instruments nor standard laboratory procedures for comprehensive instrument calibration, though in recent years some progress has been made in this respect. Efforts have also been made in some instances to model the errors generated by specific instruments with a view to predicting performance in the sea from data acquired in the laboratory (Mero et al., 1982).

The Current Measurement Technology Committee of the IEEE Council on Oceanic Engineering has considered the establishment of standards for current measurement. As yet Eulerian techniques alone have been discussed. An initial framework of tow tank tests which might be considered appropriate, based on tests found useful by a number of investigators, have been published (Appell et al., 1983). Examples are:

Linearity

Horizontal plane azimuth response

Tilt response

Zero flow - threshold - mechanical sensors

Zero stability - acoustic (ATT)/electromagnetic sensors

Direction - distance constant (polar sensors)
- vane threshold

These are carried out in steady flow and provide a baseline check on instrument performance. Dynamic tests simulate the unsteady flows to which sensors may be subjected, either real - as for example in the wave zone - or induced by mooring motion. These include circular motion of the

sensor in a vertical plane (vertical cosine response), which tests the ability of the sensor to resolve horizontal flow when an appreciable vertical component due to wave orbital motion is present; and linear oscillatory motion, horizontal and vertical, at frequencies generally below 1 Hz, which simulate mooring motion. Some tests have been done on the response of electromagnetic sensors to turbulence at frequencies above 1 Hz though no recommended procedures for these have yet been suggested.

A considerable amount of work has been done in connection with the laboratory evaluation of current meters of various types, much of which is unpublished and some of which appears in the 'grey' literature. A further difficulty is that manufacturers may often respond positively to some previously unsuspected design problem revealed on testing, by modifying the instrument, and thereby rendering the earlier test data obsolete. With these caveats, some examples of tow tank test results for a number of commonly used instruments are given in Table 2.1 though these are far from exhaustive. Other relative references can be found within the text.

Table 2.1

Mechanical	Aanderaa, Braystoke and others	Hammond & Collins (1979) Hammond et al. (1986)
	VACM	Woodward & Appell (1973) Saunders (1976) (1980)
	VMCM	Mero (1982) Weller & Davis (1980)
Acoustic (ATT)	Christian Michelsen Institute (Simrad precursor)	Collar & Gwilliam (1977)
	Neil Brown Instrument Systems Ltd (ACM-1) (ACM-2)	 Appell (1978) (1979) Mero et al. (1982)
Electromagnetic	(IOS sensor heads)	Griffiths, Collar & Braithwaite (1978)
	(Marsh McBirney)	Aubrey, Spencer & Trowbridge (1984) Appell (1979)

Laboratory tests in controlled conditions provide a means for identifying any major deficiencies in response. Alone, however, they represent a 'necessary but insufficient' basis for judging performance, and it is common practice to compare the data from an instrument, when initially used at sea, with those obtained from other longer established instruments simultaneously subjected to similar conditions. Such intercomparisons are carried out quite frequently, but

- require careful selection of the test site,
- require good understanding of the conditions prevailing,
- are inevitably imperfect, not least because there are no standard sensors,

- may be improved by combining with laboratory tests based on the major characteristics of the flow regime at the test site,
- are very expensive.

Not surprisingly most of the impetus for the evolution of both laboratory and in situ tests has come from the scientific sector of the oceanographic community: the costs of providing other than basic performance data in controlled flow conditions is, with some justification, considered prohibitive by most commercial manufacturers. Extensive information is available on the performance of instruments of many types in the scientific literature, though cheaper instruments with the exception of the Aanderaa current meter are generally less well represented.

A survey of intercomparisons carried out at sea on a variety of instruments prior to 1980 has been made by Halpern (1980). Table 2.2 complements this and provides details of some intercomparisons reported within the past few years, though it is far from exhaustive.

Table 2.2

Reference	Instruments	Conditions
Howarth (1981)	VACM, Aanderaa	Shallow water/strong tides
Beardsley (1987)	VACM, VMCM	Near surface
Magnell & Signorini (1986)	Neil Brown Smart Acoustic CMs VMCM Marsh McBirney Aanderaa, Grundy RD Inst. Acoustic Doppler Profiler	Shallow water
Beardsley et al. (1986)	VMCM, InterOcean S4	Near surface, shallow water
Halpern et al. (1981)	VACM, NBIS, ATT, VMCM	Upper ocean
Sherwin (1988)	Aanderaa, VMCM, Suber	Near-surface
Halpern (1987)	VACM, VMCM	Upper ocean
Johnson & Royer (1986)	Aanderaa, VMCM	Near-surface

The assessment of Lagrangian methods or systems based on the newly emergent remote measurement techniques such as Doppler sonar, h.f. backscatter radar, long path acoustic travel time and acoustic tomography present different problems. Each requires differing physical assumptions to be made in deriving current. In no case is the measurement directly comparable with a single fixed point measurement. The h.f. backscatter technique for example averages over horizontal motion scales as large as 1 km, and a vertical scale of metres. Nevertheless, intercomparison at sea is the only way to proceed, although comparison with theory can be useful. Assessment of these methods is discussed at the appropriate section in the text.

2.7 Current Meter Moorings

Mooring configuration and design are of crucial importance in making accurate and reliable current measurements, though in the past these have sometimes suffered from relative neglect. In some instances mooring configuration now probably provides the ultimate limitation on the accuracy of measurement that can be achieved: a badly thought out mooring can completely negate the improvements in performance that the most refined of current meters has provided.

A number of factors influence the configuration and design of a mooring. These may be listed as:

- scientific objectives
- availability of instrumentation
- current regime in the area of deployment
- capabilities of deploying vessel
- nature and topography of seabed at mooring site
- fisheries activity (principally in continental shelf seas)
- materials.

Various types of mooring are in common use. For the most part these are single leg moorings, supported by a surface buoy, subsurface buoyancy or a combination of both methods (Figs. 2.11a,b,c), though a 'U' configuration is frequently adopted for measurements in shallow shelf seas. Where no surface buoy is used, an acoustic command release system is used to shed an anchor weight and bring the mooring or instrument package to the surface.

Because it is the most efficient shape for withstanding external pressures, and also possesses minimum surface area for a given volume, the sphere is the most frequently used form of subsurface buoyancy. Materials used include steel, aluminium and glass. It has been the practice at IOS to use steel spheres at relatively shallow depths. As the working depth increases, aluminium becomes a more efficient material, while at great depth glass spheres provide the greatest buoyancy for a given weight.

Mooring lines comprise a wide variety of rope types and materials, depending on application and cost. Steel wire ropes - sometimes plastic covered for improved corrosion protection - are used where abrasion resistance is required or wherever fish bite may be a hazard - and tend to provide more resistance to being trawled by fishermen and to other unwanted human attentions. Steel is by far the heaviest material, but also the strongest, though parallel fibre Kevlar rope approaches steel in strength and low stretch characteristics at a fraction of the weight. Other

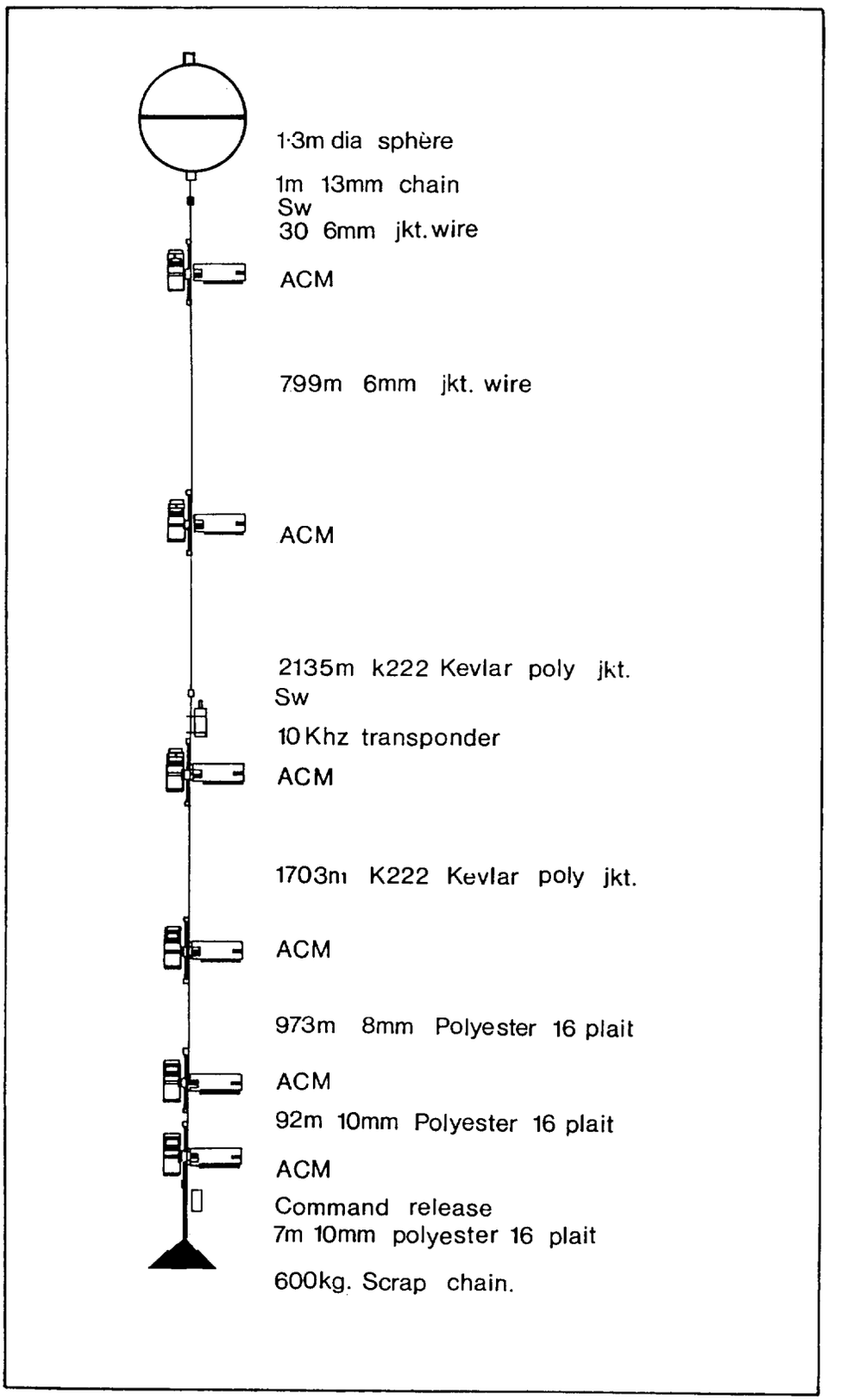

Fig. 2.11(a) Deep ocean mooring for which all components are subsurface and release is effected by acoustic command system. Maximum currents of order 10 cm/s.

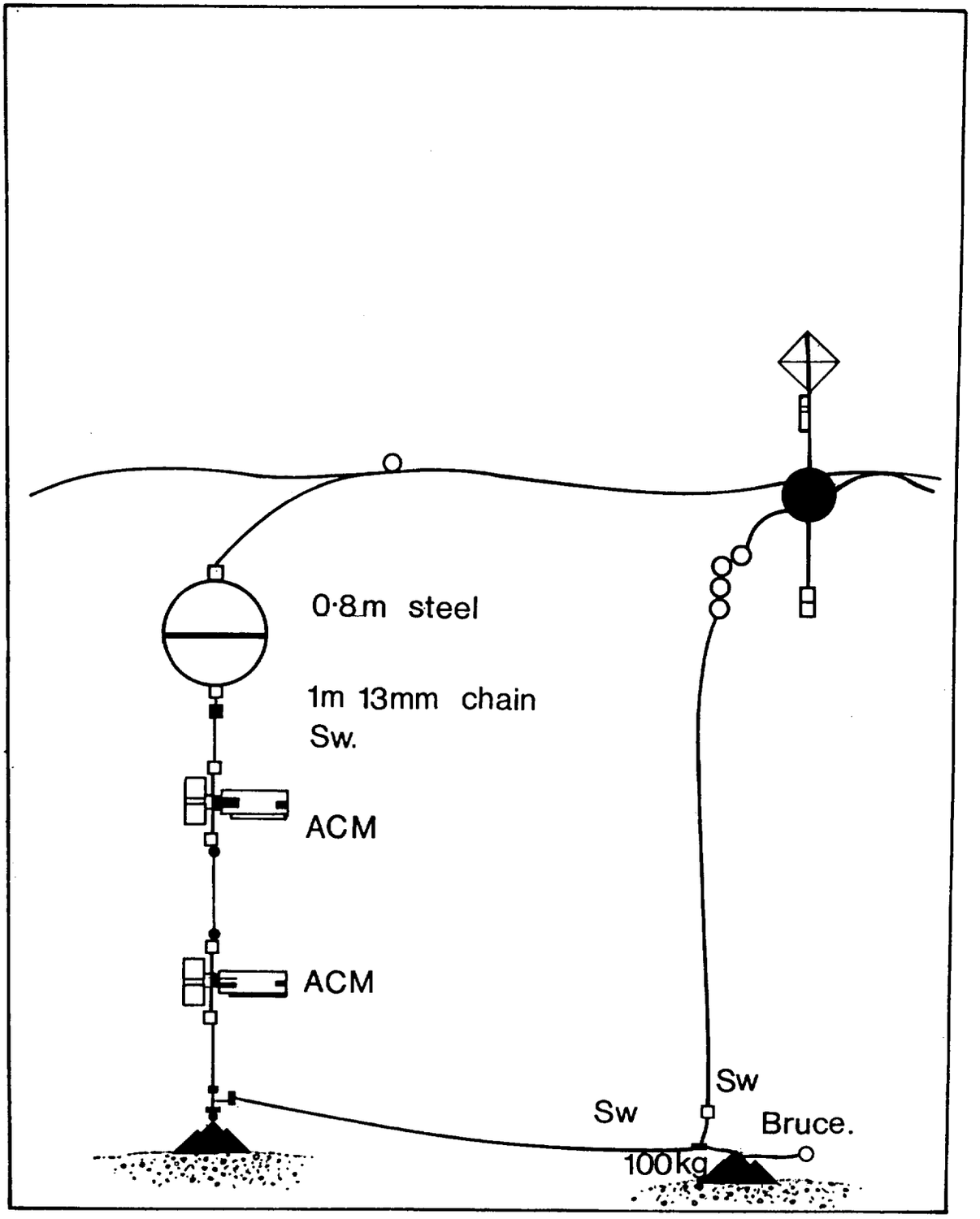

Fig. 2.11(b) U-shaped mooring for application in Continental Shelf waters

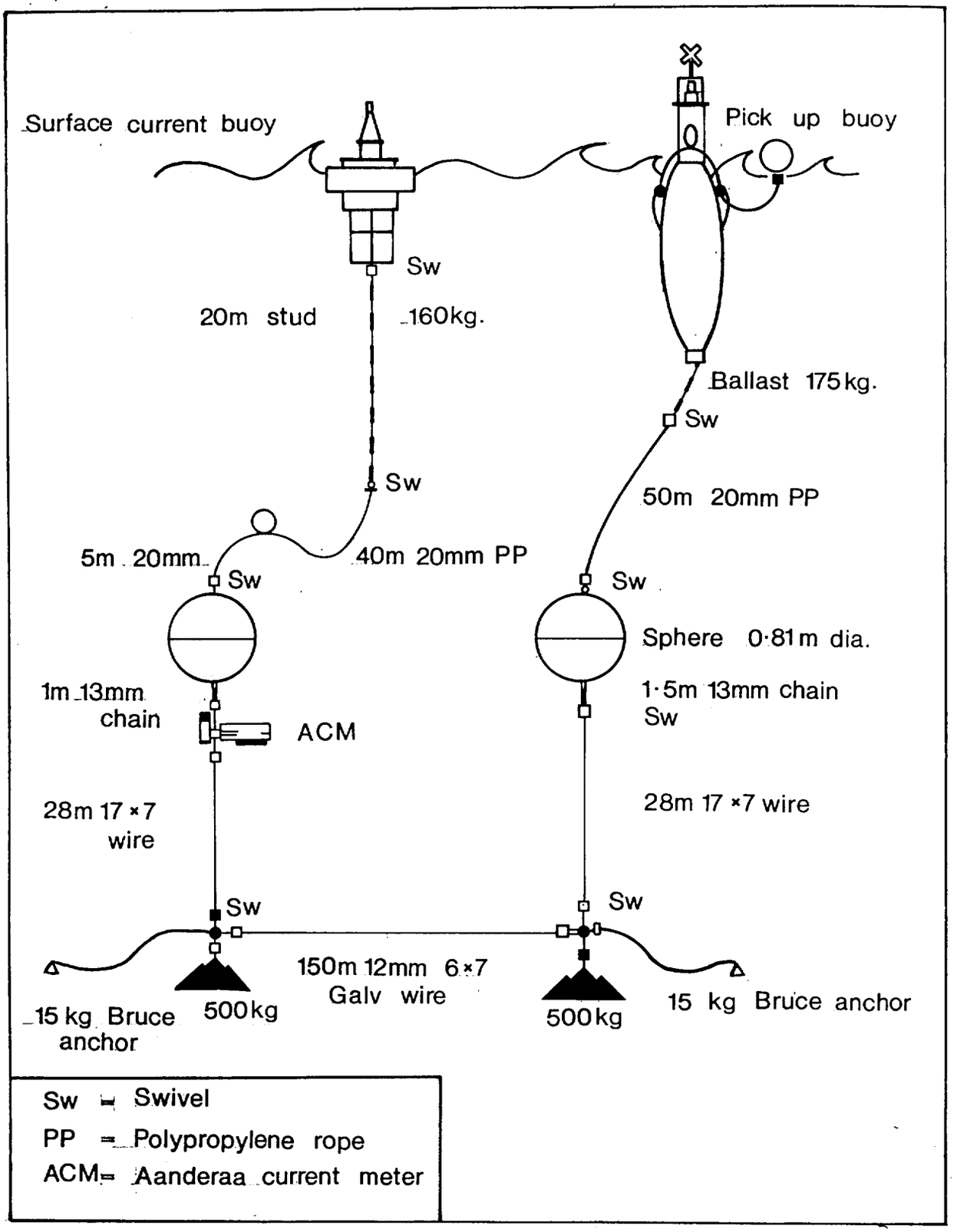

Fig. 2.11(c) Form of mooring used for surface current measuring buoy in North Sea off Flamborough Head. Depth of water 50 m; maximum currents (tidal) ~1 m/sec. This type of mooring has been used successfully for deployments in water depths to 200 m over periods of several months.

man-made fibre materials include polypropylene, polyethylene, nylon and polyester. Of these, polypropylene and polyethylene rope are not relatively strong, but are buoyant, which can be useful in some applications; nylon is the most compliant and is useful in absorbing transient or shock loads; polyester ropes have the best fatigue characteristics.

In situations in which the horizontal component of the mooring line tension at the sea bed is low, the anchor takes the form of a ballast weight - clumps of scrap chain are normally used at IOS - of about twice the excess buoyancy force. In high current regimes, where the drag force is an appreciable fraction of the anchor weight it is common practice to attach a self-burying anchor to the clump weight. Further discussion of practical aspects of mooring construction and use are to be found, for example, in Gaunt et al. (1975); Berteaux (1976); Berteaux and Walden (1969).

2.8 Static design

Design involves essentially two aspects, the first of which is the steady state performance of the mooring under loads imposed by current, waves and, possibly, wind. This is important in a number of respects; for example the overall shape of the mooring is dependent on current speed - and will therefore modify the depth at which a current measurement is made. The performance of many sensors degrades with increasing angle to the flow as the mooring leans over due to the current, so the designer must be able to estimate the wire angle at the location of each sensor. If surface buoys are to be used the effects of wind, waves and tides need to be quantified in order that the drift distance of the buoy from the anchor can be estimated; it needs to be established also whether the buoy has sufficient buoyancy to remain on the surface under all conditions. The horizontal and vertical loads on the anchor need to be calculated in order to make the right choice of anchor thus ensuring that the whole mooring does not move. Variations in line tension require evaluation if long lengths of rope or elastic rope sections are employed, so that the rope stretch can be estimated.

Design in steady state conditions in general presents relatively little difficulty once values for the parameters required in the calculations have been established. Mooring shape and line tensions are determined by the balance of weights, buoyancy and drag forces acting on the instrument packages and on the cable itself, the cable drag predominating in the case of deep sea moorings.

The drag force, F, on a body in a fluid is expressed as

$$F = \frac{1}{2} C_D \rho A V^2$$

where ρ is the density of the fluid (kg/m^3)

A is the projected area exposed to the fluid

V is the relative fluid velocity.

The drag coefficient, C_D, is a characteristic dimensionless number dependent on the Reynolds number $R_e = \frac{Vd}{\upsilon}$, where d is a characteristic dimension of the body, υ the kinematic viscosity. Details of drag coefficients for simple shapes, to which mooring components approximate, can be found in Hoerner (1965) and Myers et al. (1969), though Finke and Siedler (1986) have determined drag coefficients directly for certain mooring components, finding departures in practice of up to 50% from values based on simple shapes. Drag coefficients for cables are likely to exceed static values appreciably due to the effect of cable strumming (Griffin et al., 1982).

Various numerical mooring design programs have been produced, of which the two dimensional analysis SHAPE program (Barber, 1971) developed at IOS is an example. In this the mooring catenary is divided into a number of idealized sections each characterized by mass, dimensions, current speed and drag coefficient. The analysis uses the cable loading functions proposed by Eames (1968) and integrates step-wise along the mooring catenary using a predictor-corrector method, a number of iterations being allowed for overall convergence.

2.9 Effects of mooring dynamics

The second aspect relating to mooring design concerns the more difficult problem of dynamic response to wave forcing, to changes in the current regime and to excitation brought about by vortex shedding. The effects of mooring motion can have serious consequences for the accuracy of current measurements. In oceanic depths, for example, drag forces on non-taut moorings can produce substantial horizontal excursions of the moored instruments, with the consequence that underreading will occur. It can be shown, using a simple dimensional argument, that percentage error in an oscillatory current of period T is $\sim\frac{4s.U}{T.B}$ where s is the mooring scope, U the current speed and B is the net buoyancy. Experience suggests that for a mooring in 3,000 m depth a 10% error is easily incurred; the remedy is to increase the ratio of buoyant to drag forces. It should be remembered, however, that the introduction of errors into the measurement by mooring motion is generally a non-linear process. In the example given above the forcing of the mooring is proportional to $u|u|$, and this will therefore produce errors at a series of higher order harmonics. Briscoe (1982) discusses in semi quantitative terms the impact of the mooring movement problem on the spectral distribution of currents. For a review of modelling methods the reader is referred to Dillon (1973): Skop and Rosenthal (1979) discuss use of some approximation techniques for the effects of strumming and for the dynamics of single point taut moorings.

The effects of wave forcing on mooring motion can effectively, if somewhat arbitrarily, be separated into two classes, dependent on whether the measurement is being made in the wave zone or at greater depths. Measurement in the wave zone is additionally complicated by presence of the strong wave orbital shear flow and the related consequences of departure from an Eulerian frame of reference.

Errors in measurements made below the wave zone, but where surface forcing of the mooring is involved, have received considerable attention (Gould and Sambuco, 1975; Chhabra, 1985) and use of modelling techniques has led to the development of correction schemes (Chhabra, 1977). At depth the problem is eased because much of the horizontal motion of the mooring may be expected to be damped out. The transfer of vertical excursions, though dependent on the elasticity of the line, probably represents the greatest source of error when coupled with inadequacies in the sensor responses to off-axis flow (dynamic vertical cosine response). Where possible, exclusive use of sub-surface buoyancy is a better practice to adopt than suspending instruments at depth beneath a surface buoy.

With only rare exceptions, such as platform based measurements - when flow disturbance caused by supporting structures may present difficulties - Eulerian measurement in the wave zone is generally not practical, and some form of surface mooring is necessarily employed. Accurate measurement is then dependent upon the relationship between the cyclic motion of the sensor and the local wave orbital velocity (Pollard, 1973).

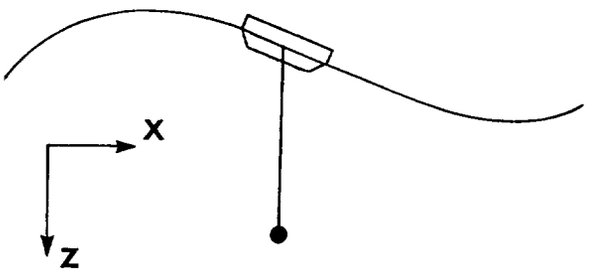

Fig. 2.12

Consider for example a sensor moving vertically only beneath a surface buoy which follows the two-dimensional wave profile $\eta = a \sin(kx - \sigma t)$ but with a phase angle ϕ. The mean position of the sensor is x_o, z_o (assuming two-dimensional waves for simplicity): its instantaneous position is $x = x_o$, $z = z_o - a \sin(kx_o - \sigma t + \phi)$ ($\sigma = 2\pi/T$, $k = 2\pi/\lambda$ where T is wave period)(Fig. 2.12).

It measures the horizontal orbital velocity

$$u = a\sigma \sin(kx - \sigma t)e^{-kz}$$

and so will measure

$$u = a\sigma \sin(kx_o - \sigma t) \exp(-kz_o + ak \sin(kx_o - \sigma t) + \phi)$$

Integrating this over one wave period gives

$$\overline{u} = \frac{\sigma}{2\pi} \int_o^{2\pi/\sigma} u dt = \frac{a^2 \sigma k e^{-kz_o}}{2} \cos\phi \quad (\text{for } ak << 1)$$

i.e. the sensor measures a spurious non-zero velocity dependent upon the angle ϕ. If the buoy follows the wave perfectly, $\phi = 0$ and the instrument experiences a larger forward velocity when the buoy is at the wavecrest than the backward velocity when it is in the trough.

But had the buoy been moving at 90° out of phase with the surface - as might happen with a spar buoy near heave resonance - the recorded current would be zero.

In the event that the motion of the sensor is in phase with the wave amplitude and includes a cyclic horizontal component x - as might be the case for a current meter suspended beneath a surface following buoy - the recorded wave-induced current becomes $\overline{u} = \left(\frac{a + x}{2}\right) \sigma k e^{-kz_o}$.

Note that this apparently spurious component of the flow is related solely to wave properties: the magnitude is of similar order to the Stokes drift (Section 1.2) which would be recorded in a Lagrangian reference frame, though differing from it (for x = a) by a factor e^{-kz_o}.

The lack of an adequate frame of reference for the measurement can clearly induce substantial errors in measurements close to the sea surface. Indeed Pollard (1973) estimates that these can easily attain 10-20 cm/s in the uppermost few metres in storm conditions.

Notwithstanding the predictions of the above equations practical methods for measuring currents within the near surface region generally involve hanging instruments beneath surface following buoys. Spar buoys offer the possibility of approaching the Eulerian fixed point measurement but need to be of sufficient length to achieve adequate decoupling from wave motion and are therefore not suitable for measurements in the upper part of the wave zone. Also, handling problems increase as the length of the spar increases. Techniques in common use for measurement at midwater depths, viz. attachment of an instrument to a mooring line held vertically by subsurface buoyancy is not considered feasible at distances beneath the surface of less than ~30 metres, due to the effects of wave action on the subsurface buoy. Techniques presently under investigation involve

the use of Doppler sonar instruments mounted either downward-looking in a surface following buoy, or in an upward-looking attitude at the top of a subsurface mooring, immediately beneath the wave zone. The latter configuration should produce a near Eulerian measurement provided that mooring sway can be kept within acceptable bounds: initial testing of the idea shows some promise (Griffiths, 1986).

For measurements in the uppermost 3 metres or so, Collar et al. (1983) analyzed the situation in which a current sensor is rigidly attached to a waveslope following buoy, thus effectively using the instantaneous surface as a reference. The analysis shows that because the buoy, while following a closed orbit, tends to follow water particles through a wave cycle, a sensor mounted at depth h in waves of length λ below a buoy of diameter D, measures a quantity S related to the surface value of Stokes Drift, S_o, by:

$$S = S_o\left\{\cos\frac{kD}{2}.e^{-kh} + \frac{\sin kD/2}{kD/2}\left[\left(\frac{hk - 1}{2}\right)e^{-kh} + \frac{1}{2}\right]\right\}$$

where k, wavenumber = $2\pi/\lambda$.

The effect of buoy diameter is to cause the buoy to act as a low pass spatial filter at shorter wavelengths and so the sensor will register a lower value of Stokes Drift than it should do. At the same time error increases rapidly with increasing sensor depth, h, and this means that the shear cannot be determined in this way. The effect is shown in Fig. 2.13 for a current meter mounted beneath buoys of 1, 5 and 7 m diameter respectively in waves of period 5 seconds. This simple model has been tested in unidirectional regular waves in a wavetank and has been found to provide a reasonably accurate description of the errors encountered. Experiments carried out at sea suggest that the model may be appropriate in sea waves. It is already known from earlier comparisons that a sensor rigidly attached to a surface buoy provides equivalent accuracy to that of an instrument moored below the surface wave zone.

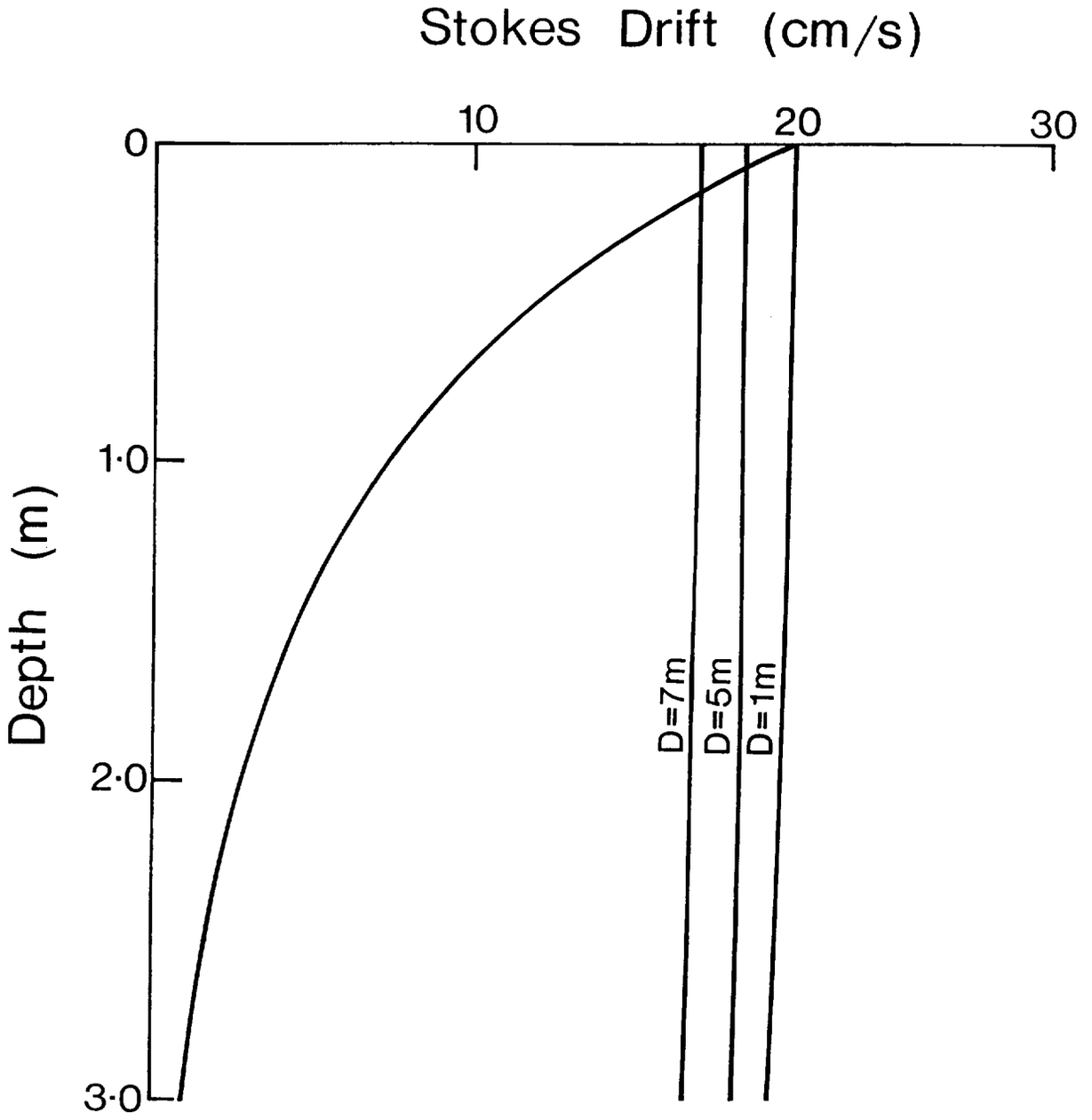

Fig. 2.13 Profile of Lagrangian velocities associated with Stokes Drift in regular two dimensional waves of period 5 sec, amplitude 0.5 m; also the profiles which would be expected to result from current sensors mounted at various depths beneath buoys of 1, 5 and 7 m diameter.

3.0 ACOUSTIC DOPPLER CURRENT PROFILERS (ADCP)

Doppler sonar techniques, which enable profiles of currents to be obtained at distances up to several hundred metres from the instrument, were investigated several decades ago but have been adopted in oceanography only comparatively recently - initially in shipboard installations, then, as low power microprocessors became available, in self recording moored instruments. These developments are presently receiving considerable stimulus from requirements for research in upper ocean processes in the context of climate research, while in the shallow shelf seas, current profiles are needed in connection with the proving of three dimensional circulation models, navigation, sediment transport and fluid loading of structures. Gordon (1990) provides a useful bibliography relating to a variety of acoustic doppler current profilers.

The principle upon which Doppler profilers operate is as follows: a pulse of sound is transmitted within a narrow beam through the water at a known angle to the horizontal, downwards from a ship based installation, from a moored instrument or from a sea bed instrument package (Fig. 3.1). Sound is backscattered from particulate matter, from organisms in the water and, near the surface, from air bubbles. It is received as a function of time at the transmitting transducer, now operating as a receiver. The water motion introduces a Doppler shift proportional to the component of velocity resolved along the beam, whose sign is positive or negative depending on whether the velocity is towards or away from the transducer. By examining the signal within discrete preselectable time intervals (range-gating) and measuring Doppler shift within each cell a horizontal component of the water velocity can be deduced. Construction of the current vector is generally achieved by combining independent radial measurements of orthogonal components, a sampling procedure which carries an implicit assumption of uniformity in the flow field throughout the insonified regions. Some implications of beam geometry have been considered by Theriault (1986b).

The physical properties of the transmission medium have a profound effect on system design. Besides simple spherical spreading a number of frequency dependent loss mechanisms are involved in acoustic signal propagation, the effect being to produce a rapid increase of attenuation with frequency (Urick, 1982). Thus, although it is desirable to operate at high frequency in order to improve Doppler frequency resolution, the working frequency is generally set by the maximum range required.

Understanding of the way in which the properties and behaviour of individual scatterers determine backscattering properties is as yet incomplete in several respects. Acoustic scatterers at depths in the ocean well below the surface are of biological origin and scattering strength is therefore dependent upon productivity. This can vary spatially and temporally, being enhanced in

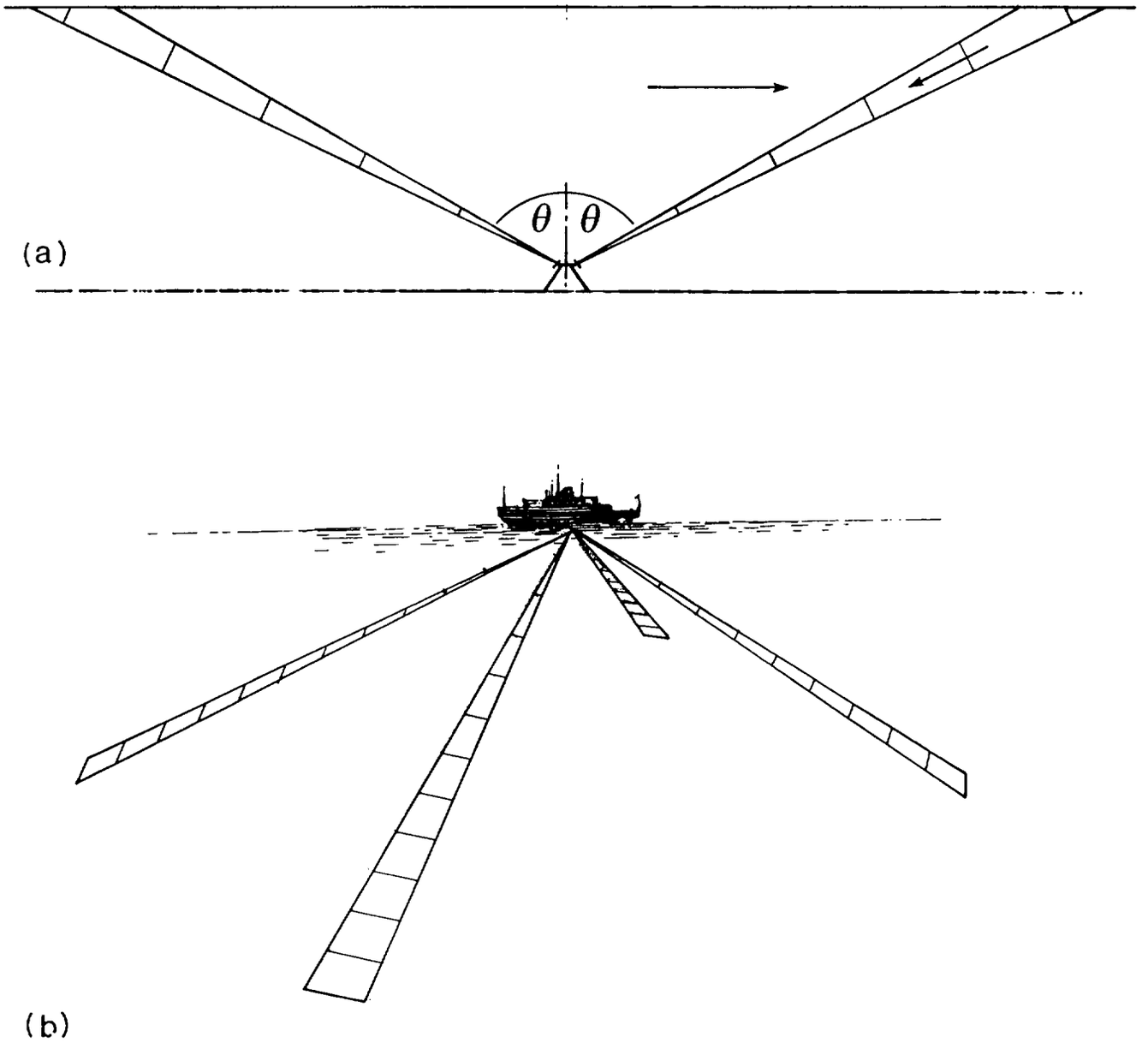

Fig. 3.1 Bottom mounted and shipboard acoustic doppler current profilers. A change in horizontal velocity ΔV produces a change in received frequency of $\frac{2\Delta V f \sin\theta}{c}$. Use of bi-directional beams (Janus arrangement) permits reduction of errors due to inadequate levelling (a) and ship pitch and roll (b). θ is typically 30°.

regions of upwelling and in the well defined scattering layers. Entrained bubbles can provide a substantial scattering mechanism within 10-20 metres of the sea surface (Thorpe, 1986), while in areas of strong tidal mixing in continental shelf waters - for example the southern parts of the North Sea - suspended sediment may provide the greatest source of backscatter. Volumetric backscattering strength may be defined as $S_s = 10 \log \frac{I_s}{I_i}$, where I_s, I_i refer to incident and scattered sound intensities. Values may vary greatly, but generally lie within the range -60 to -90 dB (Urick, 1982). At the lower end of the range returned signals may be sufficiently weak as to restrict the maximum range attainable.

Relatively little investigation seems to have been carried out of the frequency dependence of S_s, though the observations available suggest that this is reasonably constant in frequency bands where doppler current meters operate.

Small scale motions of scatterers relative to each other are of fundamental importance, for these produce changes in the relative phases of individual echoes, with the consequence that the phase signature from the ensemble will evolve with time, eventually becoming decorrelated from the initial situation. The characteristic time τ_c during which this process occurs is defined as the scattering correlation time, and is a function of the acoustic wavelength, scattering volume and velocities of the insonified scatterers. In most practical measurement situations the two-way pulse travel time greatly exceeds τ_c as a result of the relatively slow acoustic propagation velocity, and this initially caused non-coherent processing to be adopted, i.e. the signal frequency is estimated each time from the echo from individual transmitted pulses. Coherent processing is, however, possible in principle and techniques based on multiple pulse, or coded transmissions have since been developed: these are reviewed later in the section.

3.1 Incoherent scatter

For a single pulse system range resolution and velocity resolution are closely related: in a system in which a pulse is transmitted at angle θ to the vertical, a change in horizontal velocity ΔV is given in terms of doppler shift Δf by $\Delta V = \frac{c}{2f \sin\theta} \Delta f$ where f is the transmitted frequency. The Fourier transform of a transmitted rectangular pulse of length T has width $1/T$. If this is assumed to represent the minimum detection bandwidth within which Δf cannot be resolved then the velocity resolution can be rewritten as $\Delta V = \frac{c}{2fT \sin\theta}$.

Now $\Delta R = \frac{cT \cos\theta}{2}$,

$$\text{hence } \Delta V.\Delta R = \frac{c^2}{4f \tan\theta'}$$

i.e. increasing the pulse length improves the resolution of currents but simultaneously reduces resolution in range. A limit to this process occurs when the pulse length equals the scatterer correlation time: thereafter range resolution decreases without any corresponding benefit in current resolution. Note also that the resolution product improves with increasing frequency.

A more optimistic lower bound on the attainable measurement accuracy has been derived by Theriault (1986a) based on the Cramer-Rao criterion. In an ideal, reverberation-limited situation the standard deviation in a measurement of velocity

$$\sigma_v \geq \frac{c}{4p\sqrt{2}\,Tf\sin\theta}$$

Analysis of the performance bounds for practical systems have been made by Hansen (1985), applying several types of velocity estimation algorithm in current use to a series of oceanic and simulated data sets. The asymptotic performance was found to be approximately 25% higher than the theoretical lower bound predicted by the Cramer-Rao criterion.

The use of coded pulses as a means of reducing velocity variance has been proposed by Pinkel and Smith (1992); and independently by Trevorrow and Farmer (1992).

Extraction of the mean Doppler frequency from the backscattered signal can in principle be achieved in several ways. However, the need for real time processing in low powered, self contained instruments has tended in practice to encourage use of either Fast Fourier Transform (FFT) or complex autocorrelation methods. Crocker (1983) has investigated also an axis crossing counting technique in which returned signals were first heterodyned with closely spaced digitally synthesised local oscillators to produce a narrow baseband frequency, but the method was found to be unsatisfactory, due possibly to the large dynamic ranges encountered in received signals.

In the FFT method, a well-established algorithm derives the n^{th} spectral estimate of the discrete Fourier transform:

$$S_n = \frac{1}{N}\sum_{k=0}^{N-1} x_n \exp(-j2\pi nk/N)$$

The mean Doppler frequency shift Δf is then assumed to be the first moment of the discrete power spectrum, namely:

$$\overline{\Delta f} = \frac{1}{T} \frac{\sum_{n=-N/2}^{N/2} n |S_n|^2}{\sum_{n=-N/2}^{N/2} |S_n|^2}$$

In the complex autocorrelation or autocovariance method, the autocorrelation of a sequence of complex samples $\{x_n, n = 1,N\}$ is evaluated at a one-sample lag, τ

$$\text{i.e. } R(\tau) = \frac{1}{N} \sum_{n=0}^{N-1} x_n(t)\, x^*_{n+1}(t)$$

where x_n^* is the complex conjugate of x_n, and $x_n(t) = a_n(t) + jb_n(t)$

The mean frequency is simply given as

$$\overline{\Delta f} = \frac{1}{2\pi\tau} \arg R(\tau) = \frac{1}{2\pi\tau} \tan^{-1}\left\{\frac{b_n(t)a_{n+1}(t) - a_n(t)b_{n+1}(t)}{a_n(t)a_{n+1}(t) + b_n(t)b_{n+1}(t)}\right\}$$

The FFT algorithm provides a description of the spectrum of the received signal, but requires rather more computation than does the complex autocorrelation method, which is implemented very easily. The complex autocorrelation method appears to perform better particularly at low signal to noise ratios (Sirmans and Bumgarner, 1975).

Realization of an optimum Doppler profiler is thus very dependent upon the nature of the problem under investigation. Discussion of the fundamental constraints can be found in Pinkel (1980). An idea of the performance of typical Doppler sonar systems can be obtained from Table 3.1 in which specifications are shown for short and intermediate range (250 kHz) systems developed at IOS (Griffiths and Flatt, 1987; Flatt, Griffiths and Howarth, 1988). The characteristics quoted for the long range system are those of the RD Instruments ship mounted profiler (high power version).

Table 3.1

Performance specification for ADCP developments

	(IOS) Short Range	(IOS) Intermediate Range	RDI Ship mounted Long Range
Frequency (kHz)	1048	250	75
Max. radial range (m)	R>20	80<R<120	700
No. of cells	10	24	<128
Cell size (m)	1.9	2,4,6 or 8	1-32
Beams	2	2	4
-3 dB beamwidth (deg.)	1.5	3	-
Ping frequency	0.1 Hz	1	0.01-20
Averaging time (sec.)	500	600-900	1-64000
Velocity range (m/s)	±2	1	±10
R.M.S. velocity error (m/s)	0.02	0.01	0.08 for 32 m cell 0.3 for 8 m cell

3.2 Intercomparison and Evaluation

As in the case of other types of current meter, aspects of acoustic profiler system performance can in principle be evaluated by applying several different techniques. Most have involved comparison with independent forms of measurement. However, an important step forward has been the development of system modelling techniques (Chereskin et al., 1989; Chereskin and Harding, 1993). As noted by Chereskin and Harding (1993) this approach, when applied in conjunction with signal simulation, enables the performance of individual parts of the system to be analyzed and allows the relationship between system parameter choice and measurement error to be investigated.

Many of the intercomparisons carried out so far on acoustic Doppler profilers have been associated with upward directed instruments deployed on the seabed in shelf seas, and particularly in coastal areas, although Schott (1986), Schott and Johns (1987), Johns (1988) have investigated the use of profilers in deep water for the purpose of obtaining long time series of currents.

For the most part intercomparisons have been made using data from moored current meters of various types, although Griffiths (1986) has also compared current profiles derived from a Doppler sonar with the predictions of a shallow water tidal model, and has found a excellent measure of agreement.

Fig. 3.2 shows current amplitude profiles measured at 3 hours after high water over a number of successive tidal cycles. These have been normalized to water depth D and depth mean current $\bar{u}$ and show clearly the classical form associated with a logarithmic bottom boundary layer for which

$$u(z) = \frac{u^*}{k_o} \ln(z/z_o)$$

where k_o = von Karman's constant
= 0.4 in clear water
z_o = a roughness length constant
z = height above bottom
u^* = shear velocity

Close agreement is evident between the measured profile, the output from an analytical tidal model and independent bottom observations. The slight offset between the adcp output and the model has been attributed to inaccuracy in extracting a true depth mean current from the adcp data.

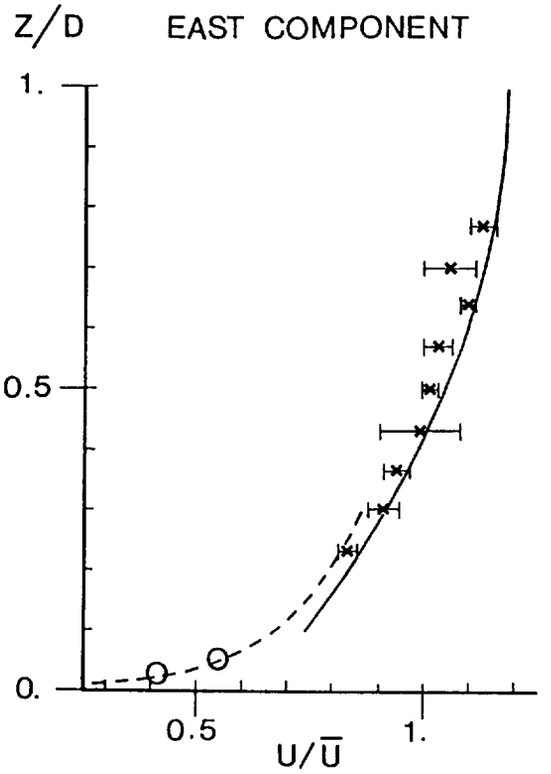

Fig. 3.2 Normalized current amplitude profiles obtained from a bottom mounted adcp in shallow water.
*adcp with 95% confidence limits
Analytical model ————
Theoretical boundary layer - - - - - -
Bottom current meter measurement
$\bar{u}$ = depth mean current, O = water depth

The results of other instrumental comparisons published so far broadly suggest that below the surface wave zone incoherent acoustic doppler provides comparable accuracy of measurement to that of vector averaging discrete instruments, although Magnell and Signorini (1986) found some discrepancies between data from an ADCP and moored instruments at periods outside the main tidal bands. In another study Pettigrew et al. (1986) found generally excellent agreement between a bottom mounted ADCP and moored VACM and VMCM data: differences observed within 20 m of the surface were consistent with motion induced errors previously identified in laboratory studies on VACM and VMCM instruments. A more recent study (Freitag et al., 1992) has shown that ADCP speeds can in some circumstances by biassed low in comparison with speeds recorded by moored instruments. This is attributed to the presence of fish in the ADCP beams.

Provided that adequate levelling of the instrument can be arranged the use of bottom mounted ADCPs provides substantial advantages over strings of moored current meters in determining vertical profiles of currents. The reasons include the following:

- the flow is completely unobstructed by the sensor;
- measurement is not contaminated by instrument motion;
- any compass-related errors are common at all levels;
- relative errors arising from this cause should be small;
- the instrument is probably more secure than a moored string of current meters;
- costs, including maintenance, are lower than those relating to an equivalent series of discrete instruments.

Errors resulting from instrument tilt have been considered by Pulkkinen (1993).

The main problems arise in making measurements close to and within the surface wave zone, in which fluid motions are sheared and are highly variable in magnitude and direction. The instantaneous surface provides a strong acoustic target, as do also the air bubbles carried down by breaking waves (Thorpe, 1986). Backscattered returns may in consequence suffer spectral broadening or distortion and if the transducer has a near-vertically directed side lobe which is inadequately suppressed, signals at longer ranges may be masked by strong, unwanted surface returns. Errors may also be generated in determining Doppler shift in high shear flows (Pullen et al., 1992). As yet relatively little effort seems to have been devoted to near surface adcp applications, although some preliminary work has been done at IOS using an upward looking adcp moored at about 20 m depth. Several downward looking, buoy-mounted systems are known to be under development.

3.3 Shipboard profilers

The vector difference between a ship's dead reckoning and its true position has long been used to provide a measure of surface current and over the years a large data bank of surface current statistics has been built up (e.g. Duncan and Schadlow, 1981). Satellite based navigation systems and the development of accurate ships' logs have enhanced both resolution and accuracy of measurement. The arrival of acoustic doppler current profilers (ADCPs) has enabled the technique to be extended to the measurement of currents to depths of several hundred metres.

The development of shipboard ADCPs - a logical extension from Doppler navigation systems which operate on the signals returned from the sea bed - began more than a decade ago and a number of successful applications of the technique have since been described in the literature. Surveys using shipboard profilers provide detailed information about the spatial structure of currents in a way that cannot be matched by moored instrument arrays. Such systems can provide a powerful tool in large scale international campaigns such as the World Ocean Circulation Experiment, particularly if systems can be made suitable for use on Ships of Opportunity (Cutchin et al., 1986).

Evaluations of the shipboard ADCP technique conducted so far have included both error analyses and comparative observations made with profiling current meters and moored instruments in both shallow and deep waters; these have generally shown good agreement between the respective techniques, though data on performance in severe surface conditions is as yet limited. Some recent comparisons, which include both moored and shipboard ADCP observations are tabulated in Table 3.2.

Apart from the physical characteristics of the acoustic medium, discussed earlier, factors which have been considered in assessing the accuracy attainable in current shear measurement can include various components of ship motion, imperfections in the acoustic geometry (beam pattern, beam orientation) and acoustic noise generated by the ship itself (Joyce et al., 1982; Crocker, 1983; Didden, 1987; Kosro, 1985; Kosro et al., 1986; Joyce, 1989). Velocity quality screening techniques are an important aspect in obtaining maximum accuracy from shipboard ADCPs. Real time methods have been discussed by Zedel and Church (1987). In measurement of absolute current the rate of change of ship position with time over the Earth's surface must be known to a higher precision than that required of the current measurement; this represents a major constraint at present (Trump, 1986), though with full implementation of improved satellite based position fixing systems, such as GPS, the level of accuracy attainable should show marked improvement.

Table 3.2

Intercomparisons involving ADCPs

	Instruments	Conditions	Mode
Chereskin et al. (1987)	RD Instruments ADCP (300 kHz) VACM	Deep (160 m max.)	Ship
Magnell and Signorini (1986)	RD Instruments (DR1200) VACM, Grundy VMCM, Aanderaa Neil Brown Instr. Systems SACM Marsh McBirney Electro-magnetic CM	Shallow	Bottom mounted
Didden (1987)	Ametek-Straza ADCP	Shallow waters <200 m	
Pettigrew et al. (1986)	RD Instruments ADCP (DR 0300) (300 kHz) VMCM VACM	Shelf waters <200 m	Bottom mounted
Schott (1986)	RD Instruments ADCPs (150 kHz; 75 kHz) Aanderaa CM	Deep	Upward looking/ moored
Appell et al. (1985)	Ametek-Straza ADCP DCP 4400/300 RD Instruments SC1200 Surface drifters VMCM	Shallow water	Bottom mounted
Griffiths (1986)	IOS ADCP (1.2 MHz) IOS surface current meter	Shelf waters <200 m	(a) Moored (Near surface)
	Tidal flow model predictions	Shallow waters <20 m	(b) Bottom mounted
Delcroix et al. (1992)	RD Instruments RDVM-150 (153 kHz) Profiling Aanderaa RCM-7	300 m	Ship

3.4 Coherent processing

Coherent processing is a comparatively recent development in oceanographic applications of sonar, though the techniques are well established in atmospheric sounding radars (Mahapatra and Zrnic, 1983). A multiplicity of pulses is transmitted, while maintaining phase coherence in the transmitted signal. Doppler shift is evaluated from the pulse-to-pulse change in phase of the received signal, with a frequency resolution that depends upon the total dwell time. Since Doppler resolution is no longer dependent upon individual pulse length - in contrast to non-coherent processing - pulse lengths can be selected to provide a desired range resolution, system or transducer bandwidth and signal to noise considerations alone providing a practical lower limit. As a result, coherent systems provide greatly enhanced velocity and range resolution. Recently

developed profilers (Rowe et al., 1983; Lohrmann et al., 1990) can provide precision in current measurement of a fraction of a cm/s, resolution of spatial scales to 20 cm (Lohrmann et al., 1990), thereby offering an improvement of two orders of magnitude over non coherent systems.

Multipulse coherent systems are, however, restricted by ambiguities in both velocity and range. The velocity ambiguity arises because the returned signals are effectively sampled at the pulse repetition frequency, f_t, and the usual sampling theorem considerations apply, i.e. aliassing takes place if the maximum Doppler frequency f_{max} exceeds the Nyquist limit $f_t/2$.

It follows that the maximum velocity that can unambiguously be observed is given by

$$\left|V_{max}\right| < \left|\frac{f_t \lambda}{4}\right|.$$

Range ambiguity results from the inability to distinguish between the return from a given pulse and returns from earlier pulses scattered from greater ranges. Maximum unambiguous range is given by

$$R_{max} = \frac{c}{2f_t}.$$

The combination of unambiguous range and velocity intervals is thus

$$V_{max}.R_{max} = c\lambda/8,$$

which is independent of pulse repetition frequency. For a 300 kHz sonar, for example, this restricts unambiguous velocity and range resolution to ±10 cm/s and 10 metres.

The enhanced temporal and spatial resolution available from coherent techniques offers possibilities for determining the parameters of small scale turbulence, and it is in this context in particular that much pioneering work was done (Lhermitte, 1985; Lhermitte and Serafin (1984)). The major effect of turbulence is to increase the spectral variance of the Doppler signal: measurement of the spectral width - or second moment - as well as the mean is therefore required. Interpretation may, however, be complicated by other contributions to spectral broadening from current shear and by any limitation in target residence time in the acoustic beam. Coherent processing techniques are discussed in Pinkel (1980) and Rowe et al. (1986).

3.5 Broadband processing

The use of coded transmissions and application of broadband signal processing techniques provides a compromise between coherent and the simple incoherent systems. In comparison with the incoherent system improved spatial resolution and reduced velocity variance results, while the range performance is retained. Two such sonars have been implemented. Brumley et al. (1991) use correlated pulse pairs, while the method adopted by Pinkel and Smith (1992) involves the transmission, within a pulse, of a number of repeats of a broadband subcode. Doppler shift is estimated from the complex autocovariance of the return at a lag equivalent to the subcode length. The transmission of multitone and of frequency shift keying (FSK) waveforms has been investigated by Andreucci et al. (1992).

4.0 ELECTROMAGNETIC SENSING USING THE GEOMAGNETIC FIELD

It was originally predicted by Faraday (1832) that electric fields would be induced in streams as a consequence of the motion of electrically conducting water in the Earth's magnetic field. Faraday's own experiments, conducted in the River Thames in London, were unsuccessful owing to the masking of the effect by electrode polarization potentials, but confirmation of his prediction was later achieved by Young, Gerrard and Jevons (1920).

Early theoretical studies of the electric field induced in the sea were made by Longuet-Higgins (1949) and Longuet-Higgins et al. (1954) and were concerned essentially with two dimensional steady flow involving particular velocity distributions. These analyses were subsequently extended by Sanford (1971) to a more general three dimensional horizontally unbounded model which included non uniform water depth and the effects of an electrically conducting sedimentary layer. The basic relationship determining induced e.m.f. is, as in the case of the flowmeter discussed in Section 2.4, $\nabla\phi = \underline{V} \times \underline{B} - \underline{J}\sigma^{-1}$ (Ohm's Law). A simple two dimensional model serves to illustrate the physics involved. We suppose that the sea is divided into a large number of thin horizontal layers within each of which the velocity is constant (Fig. 4.1). The vertical component of Earth's field will induce in each layer an e.m.f.

$$E_i = V(z)\, B_z D$$

where D is the width of the flow and axes and vectors are as defined in the figure. With the assumption that D >> h an equivalent circuit can be envisaged, consisting of a series of voltage generators, E_i in series with resistances $R_i = D/\sigma dx$. Currents flow horizontally, returning through the seabed, of resistance R. Denoting the potential difference across the flow by $\Delta\phi$ we have:

$$\Delta\phi + i_i R_i = E_i$$

$$= V(z) B_z D$$

$$i_i = -\frac{1}{R_i}(\Delta\phi - V(z) B_z D)$$

$$\text{Hence } I = -\frac{\sigma}{D}\int_0^h (\Delta\phi - V(z) B_z D)\, dz$$

$$= -\frac{1}{R_i}(\Delta\phi - \overline{V}\, B_z D) = \frac{\overline{V}\, B_z D}{R + R_i}$$

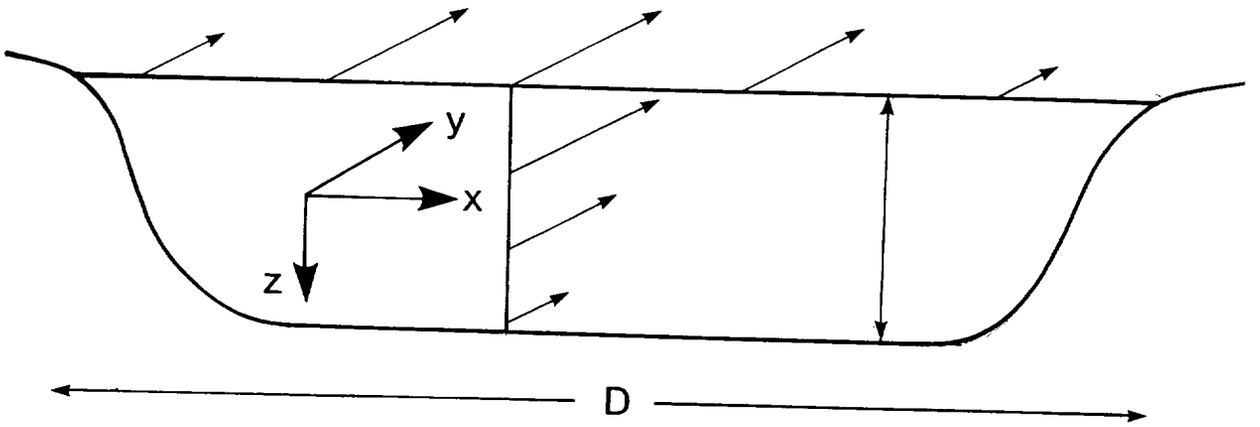

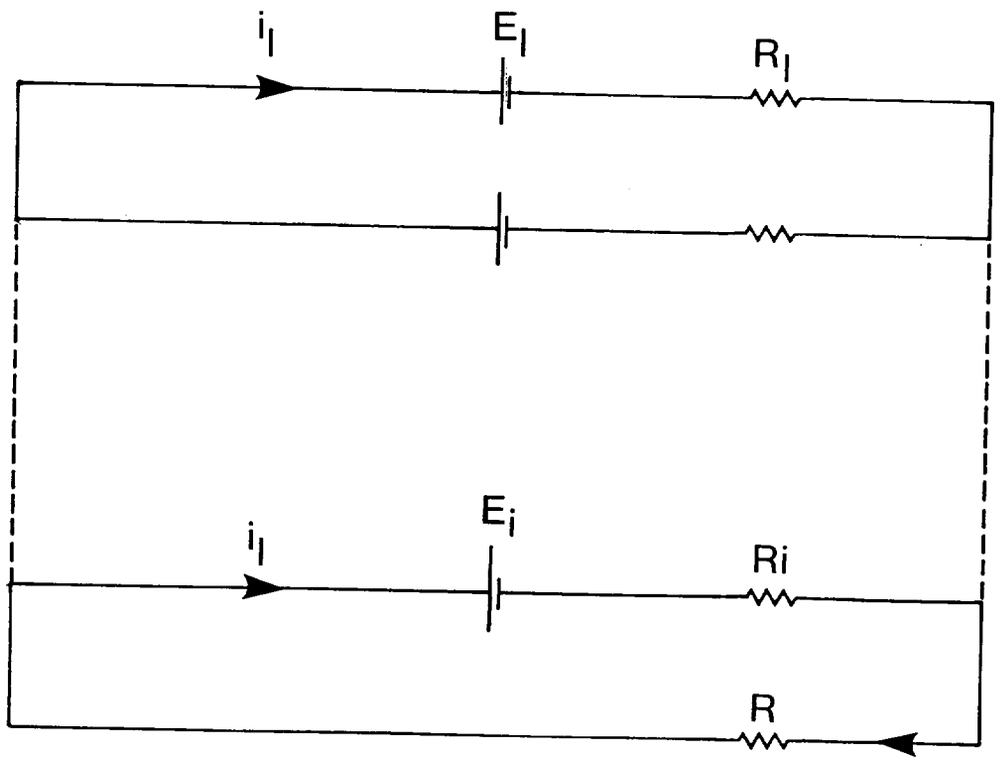

Fig. 4.1 Simplified equivalent circuit for oceanic flow

Thus the individual generators and resistances can be replaced by a single e.m.f. related to the vertically averaged flow and a single resistance. The potential difference across the flow is then $\Delta\phi = \frac{\overline{V}\, B_z D}{1 + (R_{i/R})}$ and this is the potential difference detected by a pair of fixed electrodes. A pair of electrodes moving with the flow, on the other hand, will not detect $\Delta\phi$, only $i_i R_i$, i.e. the circulating current density created by the induced e.m.f. The electrodes can be thought of as being connected to the arms of a potentiometer, also moving with the flow and cutting the geomagnetic flux. Across these also is induced an e.m.f. equal to $\overline{V}\, B_z D$ which balances out the e.m.f. induced in the moving fluid.

The moving electrodes will therefore detect a potential difference $B_z D\left(V(z) - \frac{\overline{V}}{1 + (R_{i/R})}\right)$, which is caused by the component of the flow at right angles to the line joining the electrodes. Expressed more formally (Sanford, 1971), these results can be summarised as

(1) the electric field induced in the ocean as a consequence of its bulk motion in Earth's field may be written as $\underline{B} \times \overline{\underline{V}}^*$, where $\overline{\underline{V}}^*$ is the vertically averaged flow, weighted according to conductivity. It is given by:

$$\overline{\underline{V}}^* = \frac{\int_{-h}^{o} \sigma(z) - \underline{V}(z)dz}{(1+\lambda)\int_{-h}^{o} \sigma(z)dz} \equiv \frac{\sigma\,\overline{\underline{V}}}{\bar{\sigma}(1+\lambda)}$$

where λ is the ratio of the electrical conductivity of the seabed to that of seawater. To a first approximation this ambient field can be considered to result from the vertically averaged, or barotropic flow component in the ocean.

(2) A pair of electrodes moving in the sea with absolute velocity $\underline{V}$ will detect a local potential difference $\underline{B} \times (\underline{V} - \overline{\underline{V}}^*)$.

These results provide the basis for 3 forms of current measurement, which are considered below.

4.1 Towed Electrodes (GEK)

The method of towed electrodes - or the geomagnetic electro-kinetograph (GEK) - provides a means of measuring near-surface currents V(0) from a ship underway (von Arx, 1950; Longuet-

Higgins et al., 1954). Two electrodes are towed in line at some distance behind the ship and the potential between them is recorded.

$$\nabla\phi = \underset{\sim}{B} \times (\underset{\sim}{V} - \overline{\underset{\sim}{V}}^{*}).\underset{\sim}{n}$$
$$= \underset{\sim}{B} \times (V_s + \underset{\sim}{V}(0) - \overline{\underset{\sim}{V}}^{*}).\underset{\sim}{n}$$

where V_s is the velocity of the ship relative to the water and n is a unit vector directed along the line of the electrodes

$$= \underset{\sim}{B} \times \underset{\sim}{V}(0) - \overline{\underset{\sim}{V}}^{*}.\underset{\sim}{n}$$

i.e. the electrode velocity relative to the water does not appear in the measurement since n is colinear with the ship's velocity. The measurement provides the flow component at right angles to the line joining the electrodes. Measurement of the full vector requires the ship to steam along two orthogonal courses.

Hitherto we have discussed only the effects of the vertical component of Earth's field. The horizontal component B_x (assuming $\underset{\sim}{B}$ to lie solely in the xz plane) gives rise to a vertical potential gradient $B_x V_y$. This contributes to the measured horizontal gradient only if a horizontal velocity gradient exists: the error is $\sim hB_x d\overline{V}/dx$.

From the discussion above it can be seen that towed electrodes do not measure currents absolutely and it is necessary to find alternative ways to determine $\overline{\underset{\sim}{V}}^{*}$. In terms of potential gradient measured across the electrodes, the method is most sensitive in deep water, where the largest velocities may be confined to a shallow surface layer and in consequence $V(0) >> \overline{\underset{\sim}{V}}^{*}$. This is usually not the case in shallow waters, where strong tidal streams may occupy much of the water column. If, in addition, the seabed conductivity is relatively low then the towed electrodes may record near-zero signals. Hughes (1962) concluded that although the method can yield good results in deep water it is not appropriate for routine shallow water application partly for the reasons outlined above and partly due to the horizontal variability of currents. In some coastal areas, also, Earth currents unrelated to local water movement may be present. However, good results were obtained by Nagata et al. (1981) in a comparison between towed electrodes and current meters moored in shallow water. This was attributed to the existence of a thick sedimentary layer of high conductivity.

4.2 Profiling Instruments

Various methods have been used to determine the vertical profile of horizontal current $\underline{V}(z)$, including for example direct-reading and recording current meters lowered from ships (Düing and Johnson, 1972); buoyancy driven sensors on unattended moorings (van Leer et al., 1974); and free-falling probes horizontally advected by currents, tracked acoustically using seabed transponders (Spain et al., 1981).

The electromagnetic profiler developed by Sanford et al. (1978), also, is allowed to free fall and is advected horizontally by the local velocity V(z) at depth z. It thus records a potential difference $\Delta\phi = \underline{B} \times (\underline{V}(z) - \overline{\underline{V}}^*)$. The instrument has a cylindrical form and is equipped with angled fins so as to induce steady rotation at 0.15 Hz about the vertical axis throughout its descent, thereby modulating the potential difference detected at the electrodes. This rotation enables the direction of the flow vector to be established. It also permits the wanted signal - typically in the range 1-100μV - to be extracted from much larger offset d.c. potentials (up to millivolts in magnitude) arising from electro-chemical effects, and temperature differences.

The potential gradients in horizontal x and y directions resulting from the probe velocity $\underline{V}(z) = \hat{i}V_x + \hat{j}V_y + \hat{k}V_z$ are $\frac{\partial\phi}{\partial x} = B_zV_y - B_yV_z$; $\frac{\partial\phi}{\partial y} = B_xV_z - B_zV_x$. In addition to the terms involving B_z, V_z combines with the horizontal components of Earth's field B_x, B_y to produce unwanted horizontal potential gradients which must be corrected for or, as in the original instrument, reduced at source. The instrument has undergone substantial refinement since its introduction, particularly in the resiting of its electrode ports for improved sensitivity. A further development (Sanford et al., 1985) included a measurement of $\overline{\underline{V}}^*$, the barotropic, largely depth independent contribution to the current. This has been achieved by mounting a downward looking doppler sonar in the nose of the instrument (Fig. 4.2). The transducers are arranged in a Janus configuration so as to determine vertical and horizontal components of the velocity relative to the sea floor over the last 60-300 metres of the downward excursion. Subtraction of the electromagnetically derived velocities from those obtained using the doppler sonar yields $\overline{V}^*$, which can then be added to the e.m. profile to provide the absolute current profile V(z). Use of the absolute velocity profiler has shown that it can provide measurements to within 1 cm/s and that the conversion of $\overline{V}^*$ to $\overline{V}$ can be achieved with similar accuracy.

Electromagnetic profiling measurements clearly show promise. Duda et al. (1988) have extended the technique to an instrument which can conduct multiple profiles. Amongst other recent and planned developments are an expendable current profiler (XCP) and a 3 axis towed profiler which, used in conjunction with accurate ship's navigation, could provide measurements of $\overline{V}^*$ and vertical profiles of absolute velocity (Sanford, 1986).

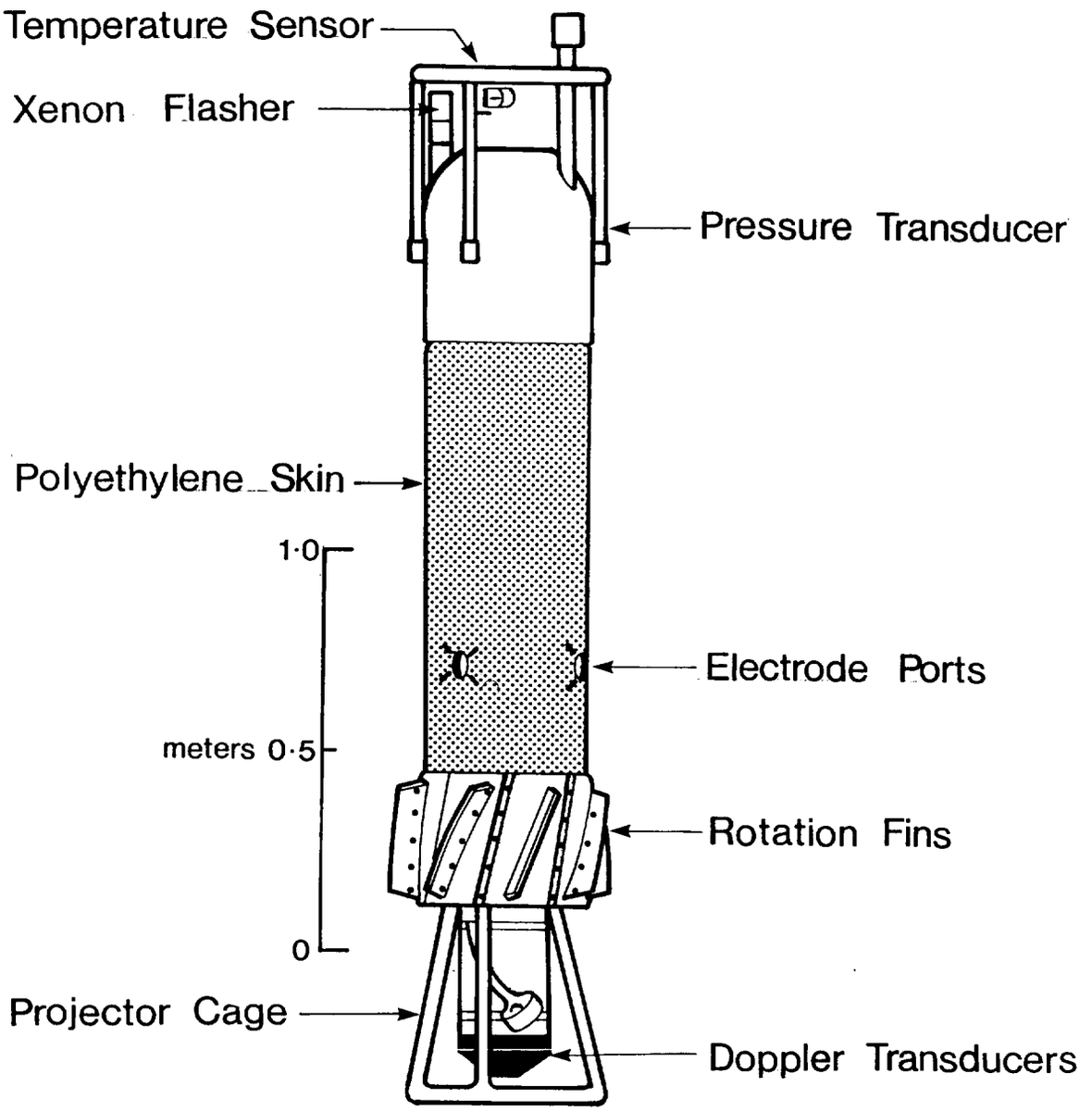

Fig. 4.2 The Absolute Velocity Profiler (AVP) as built for profile work in the 1978 Local Dynamics Experiment of POLYMODE (Sanford et al., 1985)

4.3 Fixed Arrays and Submarine Cables

Fixed point measurements of the horizontal electric field in the deep ocean, which yield $\overline{V}^*$, seem to be a promising though presently underutilised method of obtaining the barotropic component of the transport. Chave et al. (1990) report a series of measurements made in the central North Pacific using free-fall recording electrometers. These ocean floor instruments had a span of 6 metres and employed a salt bridge electrode arrangement. The time series of velocity $\overline{V}^*$, thus obtained was compared with the conductivity weighted, vertically integrated transport derived from a current meter string moored nearby between surface and bottom. The similarity of the two data sets was found to be limited only by noise introduced into the records by current meter rotor stalling in weak currents and by inadequate vertical resolution of large wavenumber components of the velocity field.

The fixed electrode method can also be applied in the determination of flow through a channel wherever the existence of a submarine telephone cable across the channel provides access to electrodes on each side. Around the UK cable measurements have been made across the Dover Straits (Bowden, 1956; Cartwright and Crease, 1963) and in the Irish Sea (Bowden and Hughes, 1961; Hughes, 1969). Elsewhere Larsen and Sanford (1985) have determined the volume transport of the Florida Current by measuring the voltage difference between Florida and Grand Bahama Island; Spain and Sanford (1987) used a combination of profiler and cable observations to achieve accurate measurement.

Although the cable method is very useful in providing estimates of transport it is in no sense absolute for the reasons outlined earlier in Section 4.0. It is customary for a cable system to be calibrated by making direct observations of currents, for knowledge of the conductivity of underlying sea bed and other factors is insufficient for a prediction of the sensitivity to be made on a theoretical basis alone. Methods adopted have included profilers, recording current meters moored at selected points in the channel, and drifting drogued floats. This may not always be sufficient, however - particularly if measurements of currents are required over a period which differs from the calibration interval. Reasons why the sensitivity may vary with time include the variability in flow regimes as a result of complex topography or varying conductivity; and the fact that unless the sea bed is an insulator the sensitivity will vary with water depth if the tidal range is a significant fraction of the mean depth. Robinson (1976) has modelled the response of cables in the Irish Sea, applying the substantial advance in electromagnetic flowmeter theory made by Bevir (1970) in developing the concept of a vector weighting function. Thus the potential difference between two electrodes in a fluid moving with velocity $\underline{V}$ through a magnetic field $\underline{B}$ can be expressed as

$$\Delta\phi = \int \underset{\sim}{V} \cdot \underset{\sim}{W} \, d\tau$$

where the vector weighting function $\underset{\sim}{W}$ can be expressed as $\underset{\sim}{W} = \underset{\sim}{B} \times \nabla\underset{\sim}{G}$ $\nabla\underset{\sim}{G}$ depends only upon the physical characteristics of the flowmeter, the electrical conditions at the boundaries of the chosen topographic model and the electrical conductivity. It is equivalent at any point in the model to the electric current density that would result were unit 'virtual' current to be injected into the sea at one electrode, and recovered at another. The merit of this purely mathematical concept is that it enables potential flow theory to be applied in determining $\nabla\underset{\sim}{G}$, and hence $\underset{\sim}{W}$. The problem thus reduces to a series of relatively straightforward numerical computations at each point of the model grid prior to summing the scalar product of $\underset{\sim}{V}$ and $\underset{\sim}{W}$ over the entire model so as to determine u. The grid of the Irish Sea cable models developed by Robinson is shown in Fig. 4.3, together with the virtual current distribution for the Nevyn-Howth cable. It was found that whilst the theoretically determined cable sensitivity agreed quite well with the empirical calibration for flows at the dominant M_2 semi diurnal tidal frequency, long period residual and mean flows were not measured accurately by the cable. This suggested the presence of non linear effects - for example rectification of tidal flows, irregular flow regimes, modulation of the signal by tidal rise and fall - and it points to the need for theoretical modelling of cable response so as to help understand fully the sources of all contributions to the output voltage and consequent limitations in the accuracy of measurement.

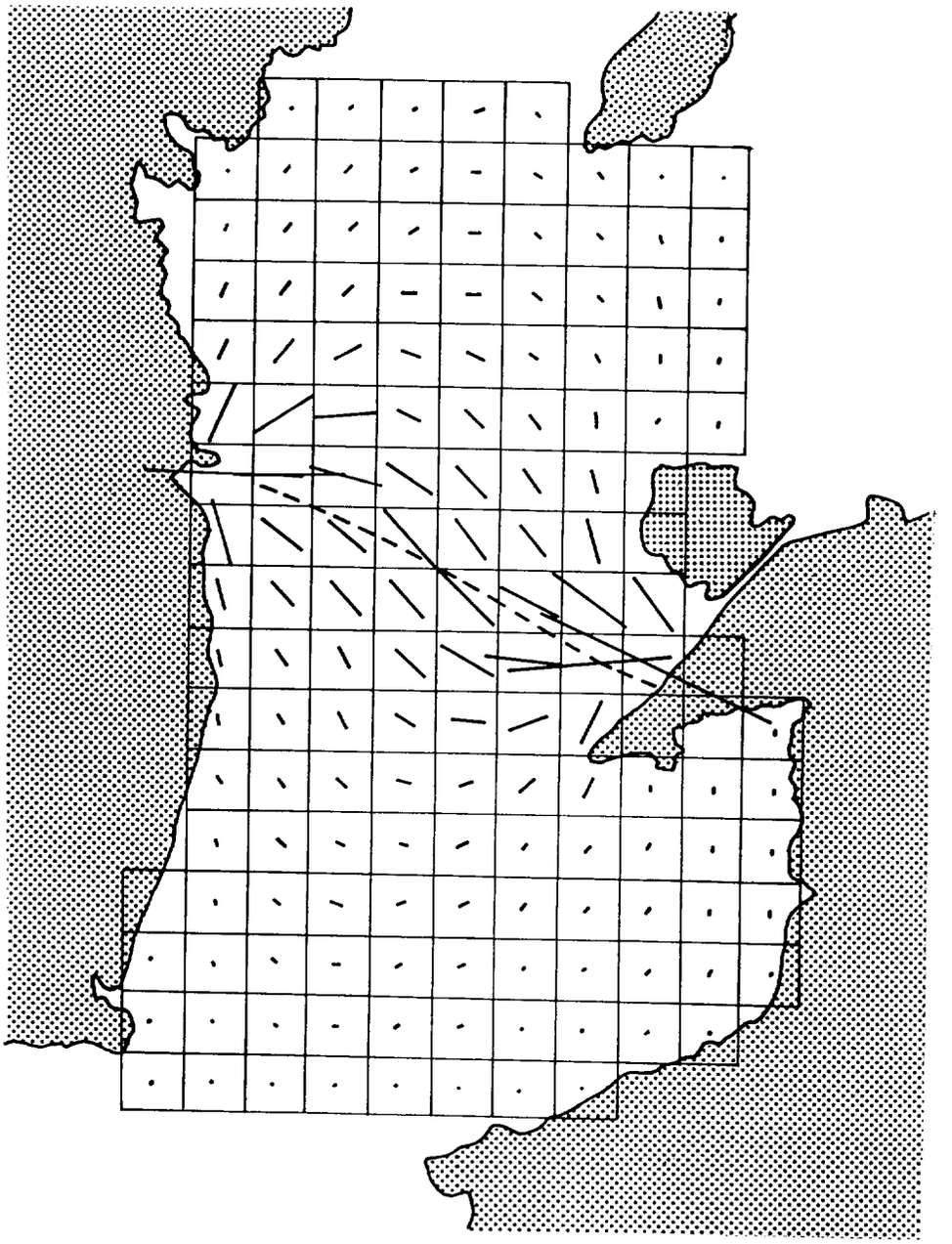

Fig. 4.3 Virtual current distribution for the Nevyn-Howth submarine cable (Robinson, 1976)

5.0 RADAR BACKSCATTER TECHNIQUES

Radar backscatter techniques have their origin in work by Crombie (1955) who, in transmitting 13.5 MHz radio waves out over the sea, observed a marked Doppler shift in signals which were backscattered from the sea surface. Detailed discussion of electromagnetic wave interactions with the sea surface lies outside the scope of this review though Barrick (1972), Barrick et al. (1974) and the review by Shearman (1986) are helpful in this respect. For present purposes it suffices to assume that the scattering mechanism responsible for Crombie's observations, which provides means of measuring surface currents, is Bragg resonance. Conceptually, Bragg resonance can be described as the constructive reinforcement of radio waves reflected back selectively from those sea waves having half the radio wavelength (Fig. 5.1), in a manner analogous to X-ray diffraction from atoms in a crystal lattice. This selective reinforcement produces two Bragg lines in the frequency spectrum (Fig. 5.2), symmetrically disposed about the transmitted carrier frequency in the absence of a current, whose displacement from the carrier is related to the phase velocity of advancing and receding waves, i.e. $f = \pm\sqrt{\frac{g}{\pi\lambda}}$ where λ is the electromagnetic wavelength. The presence of an underlying current displaces the spectra unidirectionally from their symmetrical positions, and it is from this displacement that an estimate of any radial current component is made, making the assumption that waves and currents are linearly superimposed. A second order spectrum is also generated but this is of more interest in the remote measurement of surface gravity waves and will not be considered further here.

Radar returns are range-gated, thus providing estimates of radial current component at intervals along the beam, while averaging over a number of pulses improves signal to noise ratio and hence measurement precision. The aerial design usually provides for radial observations at a number of azimuth angles. In order to define the current vector a second transmitting and receiving system is employed, surveying the same area from a different angle, ideally orthogonally.

The attraction of the coastally based HF ground wave radar method lies in its ability to produce, rapidly, maps of surface currents (Fig. 5.3) in a way that would be difficult and prohibitively expensive using either moored current meters or drifters. It is thus especially useful in establishing flow patterns and characteristics (Prandle, 1987; Gurgel et al., 1986) wherever these are dominated by coastal boundaries or topography, e.g. around headlands, islands or in estuaries. Most systems are built to operate between 25 and 30 MHz, a choice of frequency that provides best resolution of Doppler shift within a limited integration time and reduces the probability of interference from unwanted skywave transmissions. It does, however, reduce the maximum ground wave range attainable to ~50 km or less. Lower frequency systems have been used successfully to

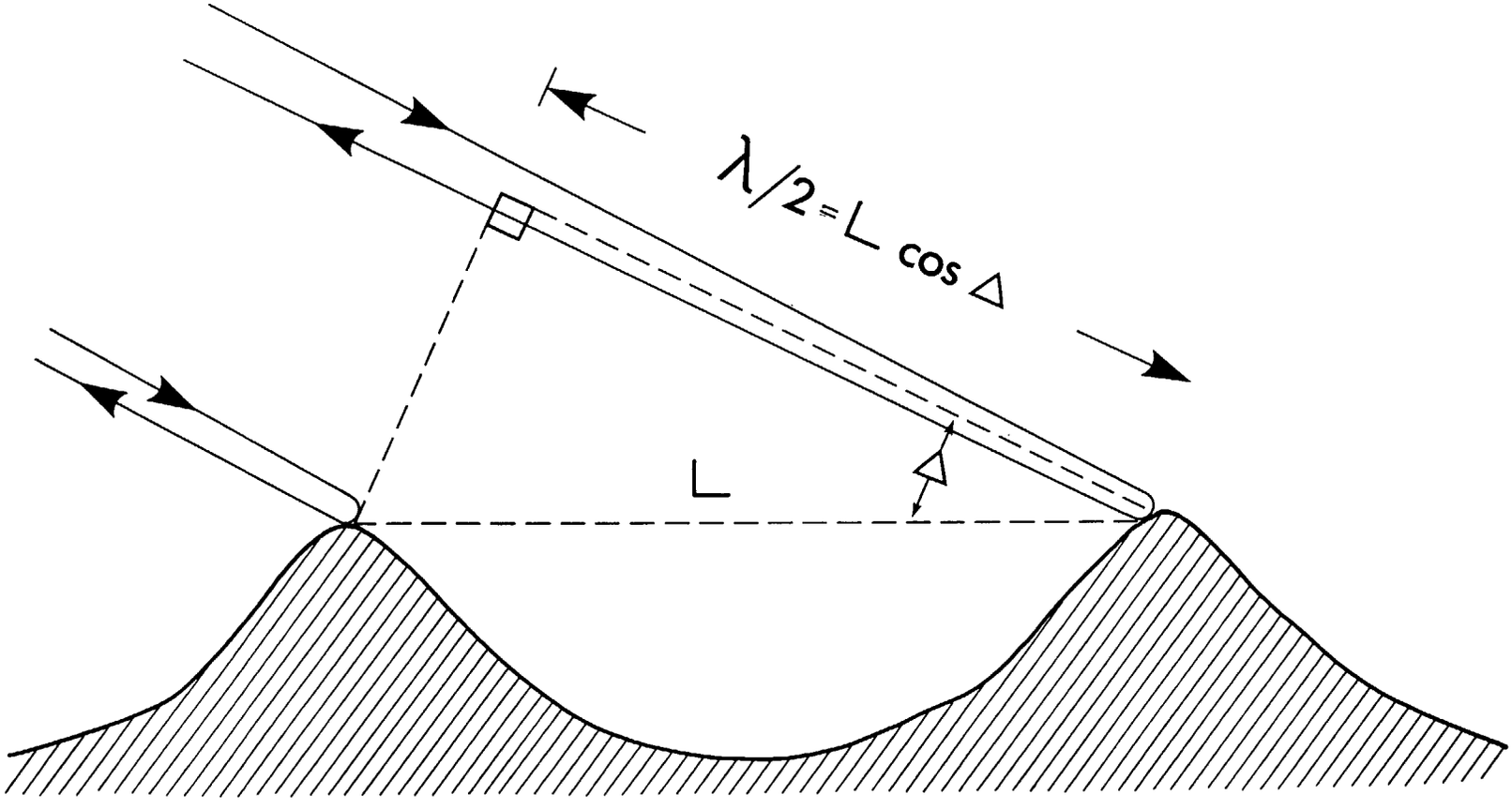

Bragg Resonant Diffraction Condition.

Fig. 5.1 Conceptual view of resonant Bragg backscatter

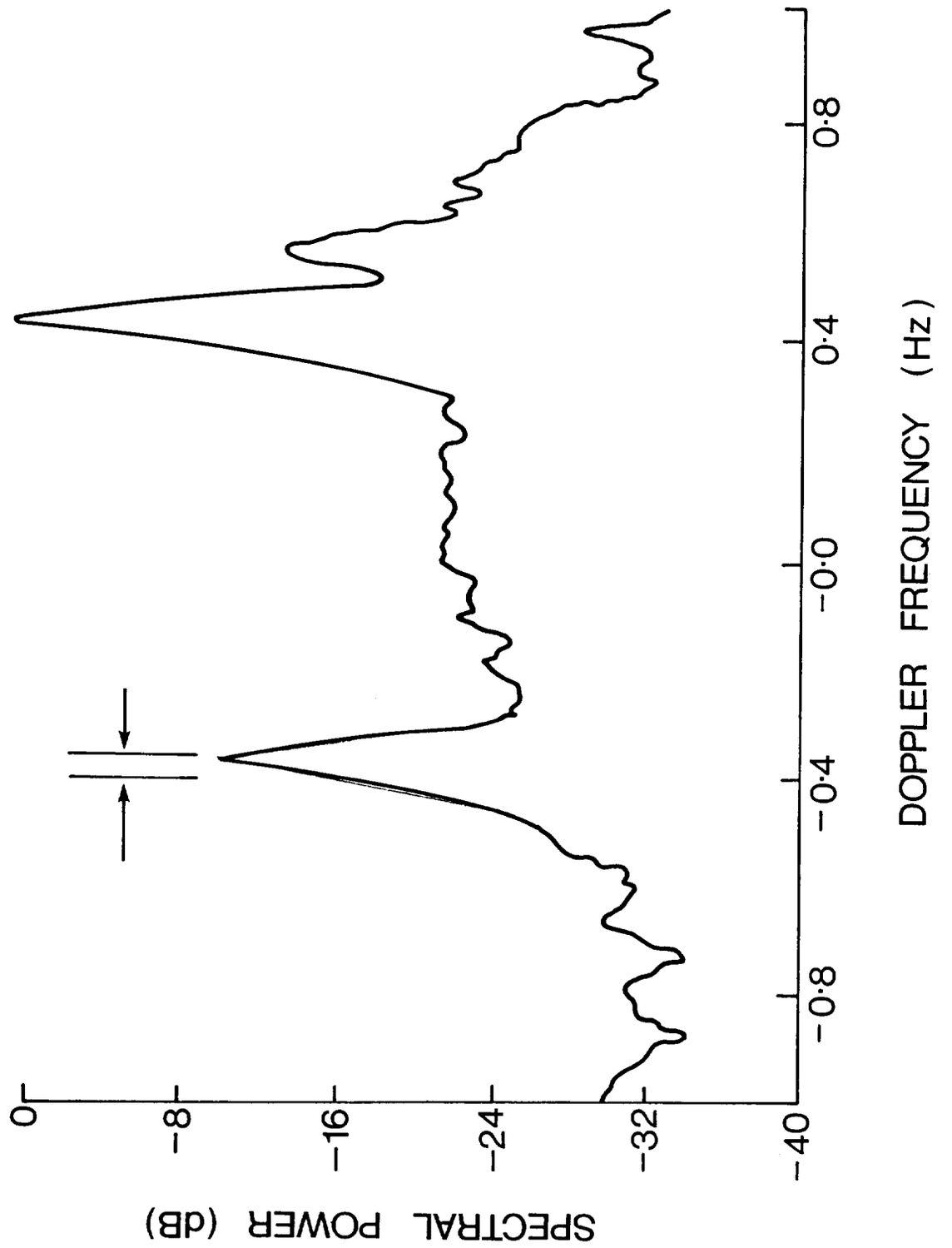

Fig. 5.2 Spectrum of backscattered e.m. radiation showing first order Bragg lines. Asymmetrical distribution of the lines about zero results from a mean current superimposed on the phase velocity of the waves.

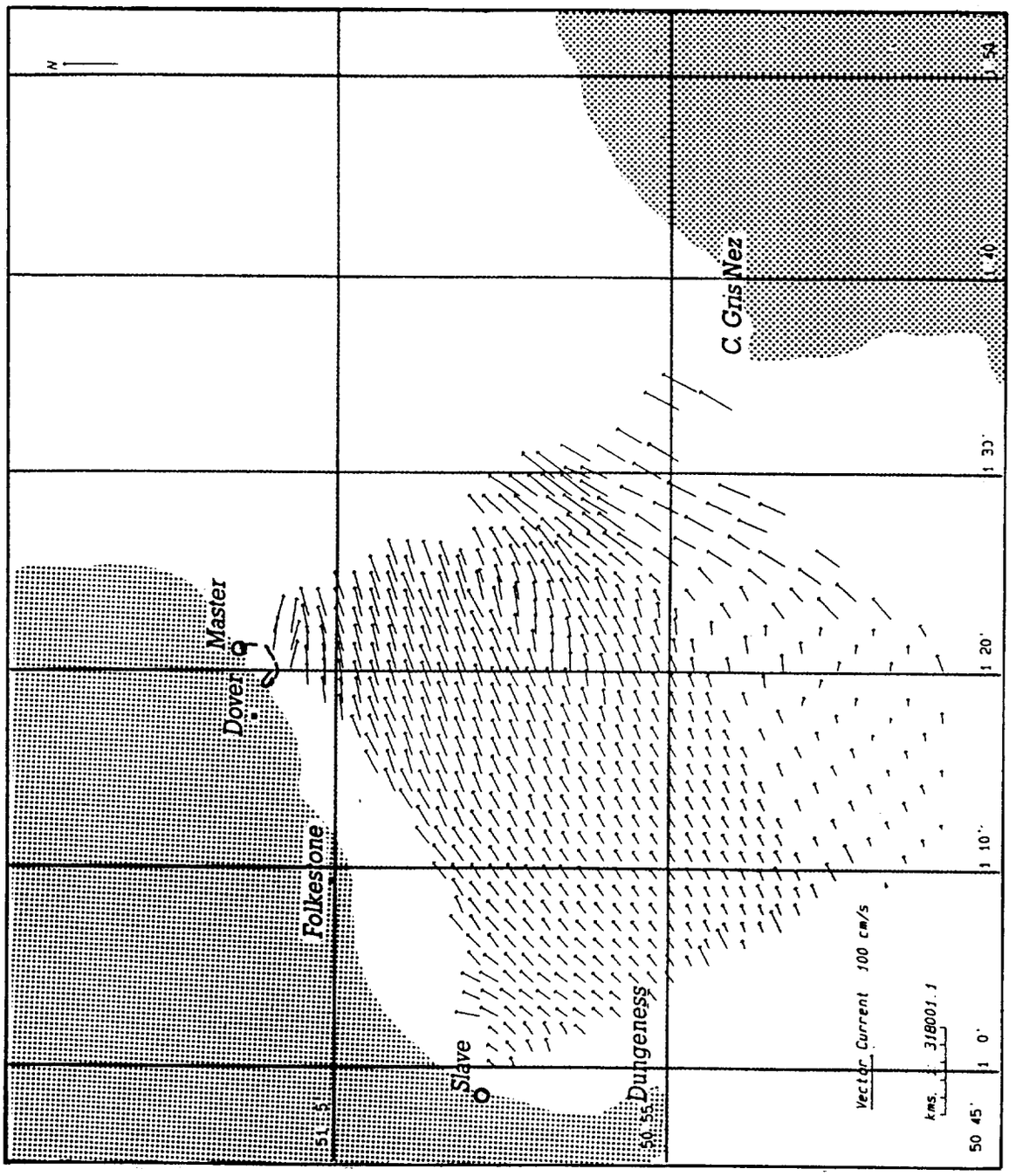

Fig. 5.3 Map of surface currents in the straits of Dover produced by OSCR system

provide ranges to ~200 km; higher frequency systems are being developed for measurement of currents in more localised areas such as estuaries.

The depth of measurement associated with the hf radar technique is determined by hydrodynamic considerations - in simple conceptual terms it can be regarded as the depth at which gravity waves 'sense' the underlying current structure. It is not related to the penetration depth of incident electromagnetic radiation. Stewart and Joy (1974) derived a first order one dimensional expression (subsequently extended to second order by Ha, 1979) for the phase velocity of a wave superimposed on a current. The phase velocity c is given by

$$c = c_o \pm 2k \int_o^\infty V(z) \exp(-2kz)\, dz$$

where c_o is the velocity in still water, k is the wavenumber and V(z) is the vertical current profile. Thus the unidirectional displacement of the Bragg spectra due to current is the current component averaged over depth with exp(-2kz) as a weighting function.

Evaluation of this integral equation - and hence estimation of the effective radar sampling depth - is hampered by lack of knowledge of the near-surface current structure. There are three possibilities which might be considered:

(i) An exponential profile of the form $V(z) = V(0) \exp(-az)$. The current modifies the phase velocity of the wave by an amount:

$$\Delta = c - c_o = \pm \frac{2kV(0)}{2k+a}$$

(ii) A linear profile yields $\Delta = c - c_o = \pm V(z)_{z=(2k)^{-1}}$,
i.e. the mean sampling depth is $\sim(\lambda/4\pi)$ where λ is the wavelength of the scattering gravity wave. Consideration of the equation above suggests that the Stokes drift current associated with the scattering wave which decays with depth as exp(-2kz) would be sampled at a depth $\sim 0.7(\lambda/4\pi)$.

(iii) A logarithmic profile of the form:

$$V(z) = V(0) - \frac{u^*}{K} \ln\left(\frac{z}{z_o}\right)$$

where u^* is the friction velocity, z_o is the characteristic roughness scale and $K \sim 0.4$ is von Karman's constant. For this case, Ha (1979) infers a sensing depth $\sim 0.022\lambda$.

These three examples suggest that whatever form the current profile takes, the sampling depth associated with a radar operating at ~27 MHz, for example, is less than 1 metre. But it is probably an order greater than the penetration depth, δ, of the incident electromagnetic wave, which is given by:

$$\delta = \sqrt{\frac{2}{\omega\mu\sigma}}$$

For an angular frequency $\omega = 2.7 \times 10^7$ rad/sec,
Permeability $\mu = 4\pi \times 10^{-7}$,
Conductivity $\sigma = 4.3$ Siemens/metre,

$\delta = 0.047$ m.

The dependence of the mean sampling depth on the wavelength of the incident electromagnetic wave can provide a means of investigating the vertical structure of currents, if multifrequency transmissions are made. As yet this technique does not appear to have been used widely, though Teague (1986) in making simultaneous observations at 6.8, 13.3, 21.7 and 29.75 MHz reports results consistent with a logarithmic shear in the uppermost metre.

HF radar systems differ somewhat in detailed implementation and performance. Nearly all have been landbased at coastal sites, though Teague has described an experiment based on a ship mounted system. The earliest system in operational use was the 25.6 MHz Coastal Oceans Dynamics Atmospheric Radar (CODAR) developed by Barrick et al. (1977), which transmits within a wide beam and employs a small direction finding receiving aerial consisting of four monopoles. Processing involves the application of FFT routines to resolve equirange echoes within the beam, and signals from the individual aerials are compared in order to determine direction (Leise, 1984). An example of present use of the system is given in Schlick et al. (1990).

A number of different systems are operational in various countries. These include the 27 MHz Ocean Surface Current Radar (OSCR) which originated at the Rutherford-Appleton Laboratory in the UK and has been further developed by MAREX Ltd. This also transmits a wide beam, but differs from the CODAR approach in using a switched delay line matrix to form a steerable narrow (8°) receiver beam, using a 16 element 85 m array of monopoles. With a beam dwell time of ~2 minutes, current resolution is ~$\pm$1 cm/s within cells of typically 1.2 x Rθ km where R is range and $\theta \sim \pm 0.1$ rad. The maximum range of the system is ~50 km in calm conditions, rather less in storm conditions. The system has no ambiguities and offers rather better resolution than does the CODAR, although the shore station requires greater space, and is less portable.

The Mk II version of the OSCR system incorporates a number of improvements. In this form by application of digital beam forming techniques, vector measurements can be made of up to 700 predetermined points which may be either on an orthogonal grid or as defined by the user. Simultaneous data collection is carried out over the whole area illuminated by the transmitting antenna within a five minute period. An account of the use of the system is given in Osborne (1991).

5.1 Intercomparisons

A number of comparisons have been made between hf radar and current meter data; also between integrated radar measurements and Lagrangian drifter tracks. Examples include the work of Holbrook and Frisch (1981) who compared the output of the CODAR system with records from VACMs moored at 4, 10 and 20 metres depth; Janopaul et al (1982) who intercompared three different radar systems with instruments at 7 and 10 metres depth. Fig. 5.4 shows some results from Collar and Howarth (1987) who compared data from surface current buoys measuring at 1 m depth with corresponding observations made by the OSCR system. Such comparisons have limitations, in part because the radar and current meters are responsive to different horizontal scales of motion, though use of a small current meter array distributed through a radar cell can improve matters. More fundamentally the radar senses a depth integrated current, whereas the current meter samples at a point. Furthermore, in virtually all experiments reported to date the moored instruments have sampled well below the effective mean depth of the radar and cannot therefore be expected to record the same current when the current structure is strongly sheared with depth under the influence of wind stress.

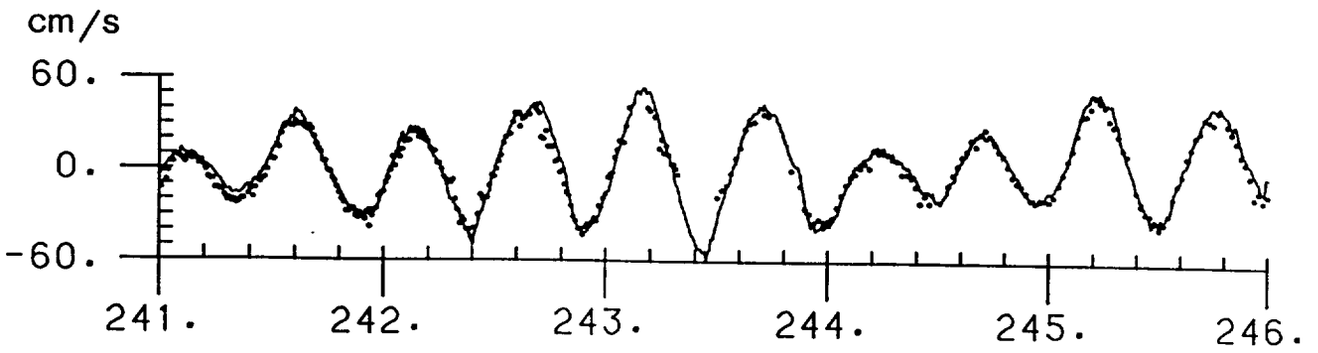

Fig. 5.4 Comparison of data obtained from surface slope following buoys measuring at 1 m depth with data derived from h.f. Ocean Surface Current Radar (OSCR) (from Collar et al., 1988)

The weight of evidence from recent studies conducted by IOS has confirmed that the mean depth of response for radars operating at 27 MHz lies within 1 m of the surface. There is also support for the view that the radar includes a contribution from Stokes Drift in its measurement, as suggested by Barrick (1986). Finally the point should be made that in making comparisons in coastal waters it may be necessary to make allowance for the current shear in the bottom boundary layer.

A number of simultaneous observations have also been made using radar and surface drifters (Barrick et al., 1977; Ha, 1979; Collar and Howarth, 1987). Drifters can be drogued so as to follow the local water mass at depths commensurate with the radar averaging depth though care is required in drogue design (section 7.2).

Agreement between the two techniques to within a few cm/s has been reported in several of the studies, though mostly in relatively calm conditions, in which variability within the radar footprint almost certainly provides the ultimate limitation.

5.2 Microwave backscatter

Electromagnetic backscatter techniques have also been developed for use at centimetric wavelengths, where capillary waves provide the primary scatterers for the resonant Bragg process. In the pulsed dual frequency method two microwave frequencies f_1, f_2 are transmitted simultaneously; f_1 and f_2 are chosen such that $f_1 - f_2 = 2\lambda_w$, where λ_w is a readily observed water wavelength. The Bragg condition $\lambda = 2\lambda_w \cos\theta$ again applies, where θ is the angle of incidence at the water surface. The system is essentially short range, well suited to platform mounting. In the Norwegian MIROS 5.8 GHz system, $f_1 - f_2$ = 10 MHz, transmitted pulses are of 500 nS duration, illuminating a patch 75 m in range at a distance of between 0.5 and 1 km from the sensor. The beam is 30° in azimuth and a sequence of 6 observations is made within an arc of 180°; the evaluation of the current vector relies upon measurement in two orthogonal directions and on making the assumption of spatial homogeneity in the currents. Processing is similar to that applied at hf frequencies except that prior to converting the Fourier transform of the received signal the component at $f_1 - f_2$ is isolated from the product $r(f_1, t)\, r^*(f_2, t)$ (where * denotes the complex conjugate). The selection of a range of values of $f_1 - f_2$ again provides means for investigating the vertical structure of near-surface currents (Schuler et al., 1981).

6.0 ACOUSTIC TOMOGRAPHY

The resolution of physical features at large scales in the ocean requires an approach which does not rely wholly on an array of point measurements; the logistics of implementation become increasingly difficult as the array size increases. The application of acoustic tomography was originally proposed by Munk and Wunsch (1979) as a possible way forward in dealing with the problem and has received a considerable amount of attention in recent years.

6.1 Acoustic propagation characteristics

The technique is made possible by the acoustic propagation characteristics of the ocean. A detailed review of the many aspects of acoustic propagation is not possible here: the reader is advised to consult the extensive literature, including the text by Urick (1982). For present purposes the major constraints can be said to be those of refraction (or, equivalently, temporal and spatial changes in sound velocity), of spatial spreading of the wavefront with increasing range, and of losses arising from absorption, which increase rapidly with increasing frequency.

A direct consequence of the temperature, pressure and, to a lesser extent, salinity dependence of the sound propagation speed is the creation of sound ducts or channels, which provide the means by which sound propagation can take place over much longer distances than would otherwise be achieved. The main example of channelling is the Deep Sound, or SOFAR (Sound Fixing and Ranging) channel, though seasonal surface ducting is another case.

The first order coefficients of sound speed (c) dependence on temperature, salinity and pressure (at P ~1 bar, S 35‰, T ~10°) are:

$$\left(\frac{\partial c}{\partial T}\right)_{P,S} \sim 3.5 \text{ m/s/°C}$$

$$\left(\frac{\partial c}{\partial S}\right)_{P,T} \sim 1.2 \text{ m/s/‰}$$

$$\left(\frac{\partial c}{\partial P}\right)_{T,S} \sim 0.016 \text{ m/s/dbar}$$

c therefore diminishes quite rapidly at first during the transition from relatively warm surface waters down through the thermocline but thereafter reduces more slowly. At some depth typically between 1000 and 1500 metres the pressure dependence predominates and a minimum therefore occurs in the sound speed. The effect is thus akin to that of a waveguide, or duct, in which sound rays

radiated within certain angles of the horizontal are refracted back toward this axis and so propagate about the axis of the duct. The consequence is that beyond a certain distance cylindrical spreading obtains, in which attenuation is proportional to $(\text{range})^{-1}$, rather than the more commonly experienced spherical spreading for which attenuation is proportional to $(\text{range})^{-2}$. The form of typical acoustic propagation paths for a fairly typical sound velocity profile with depth is shown in Fig. 6.1.

6.2 Deep ocean tomography

The measurement technique consists of measuring the one-way travel times of acoustic signals between a number of sources and receivers moored in the deep sound channel. The possibility of making such measurements using a movable ship-based receiver has also been studied (Cornuelle et al., 1989). The refractive properties of the medium are - as outlined above - such that for each source-receiver pair a multiplicity of ray paths exists in the vertical plane. Each has its own characteristic upper and lower turning depths and each has a characteristic propagation time determined by the variability of the temperature field through which it passes. Early arrivals at a receiver are associated with sound paths which oscillate through the entire water column; later arrivals are associated with near axial propagation. By resolving individual arrival times and by then applying linear inverse theory to the data sets it is possible to determine the three-dimensional sound speed field and hence to infer the temperature and density fields. From this geostrophic current can in principle be computed. If the source-receiver pairs are so configured that travel time differences can be derived from measurements along reciprocal paths, in a manner analogous to the acoustic travel time current meter, then direct measurement of the spatially-averaged current is possible.

In order to provide reasonably optimum mesoscale sampling tomography experiments have been carried out with source-receiver separations of typically a few hundred kilometres, yielding temperature-induced spreads in arrival times of up to 200 msec. This immediately constrains the system design in that the pulse needs to be sufficiently narrow (wide bandwidth) to enable multiple arrivals to be resolved, yet needs to contain enough energy to meet signal to noise detection thresholds. Pulse compression techniques have been applied to suit this purpose. Worcester et al. (1985) have described the application of a periodically repeated phase-encoded linear maximal shift register sequence, following earlier work (Spindel 1979; Spindel et al., 1982) along similar lines. The transmission signal consisted of 24 sequences of 511 digits, each digit occupying 4 cycles of a 400 Hz carrier. Coherent averaging of the received sequences and cross correlation processing of each sequence with a replica of the transmitted sequence together provide a processing gain of 40 db. Propagation losses (spherical spreading and attenuation) amounted to 115 db. Hence for an acoustic source level of 186 db relative to 1 μPa at 1 m, and an estimated noise level within a 100 Hz

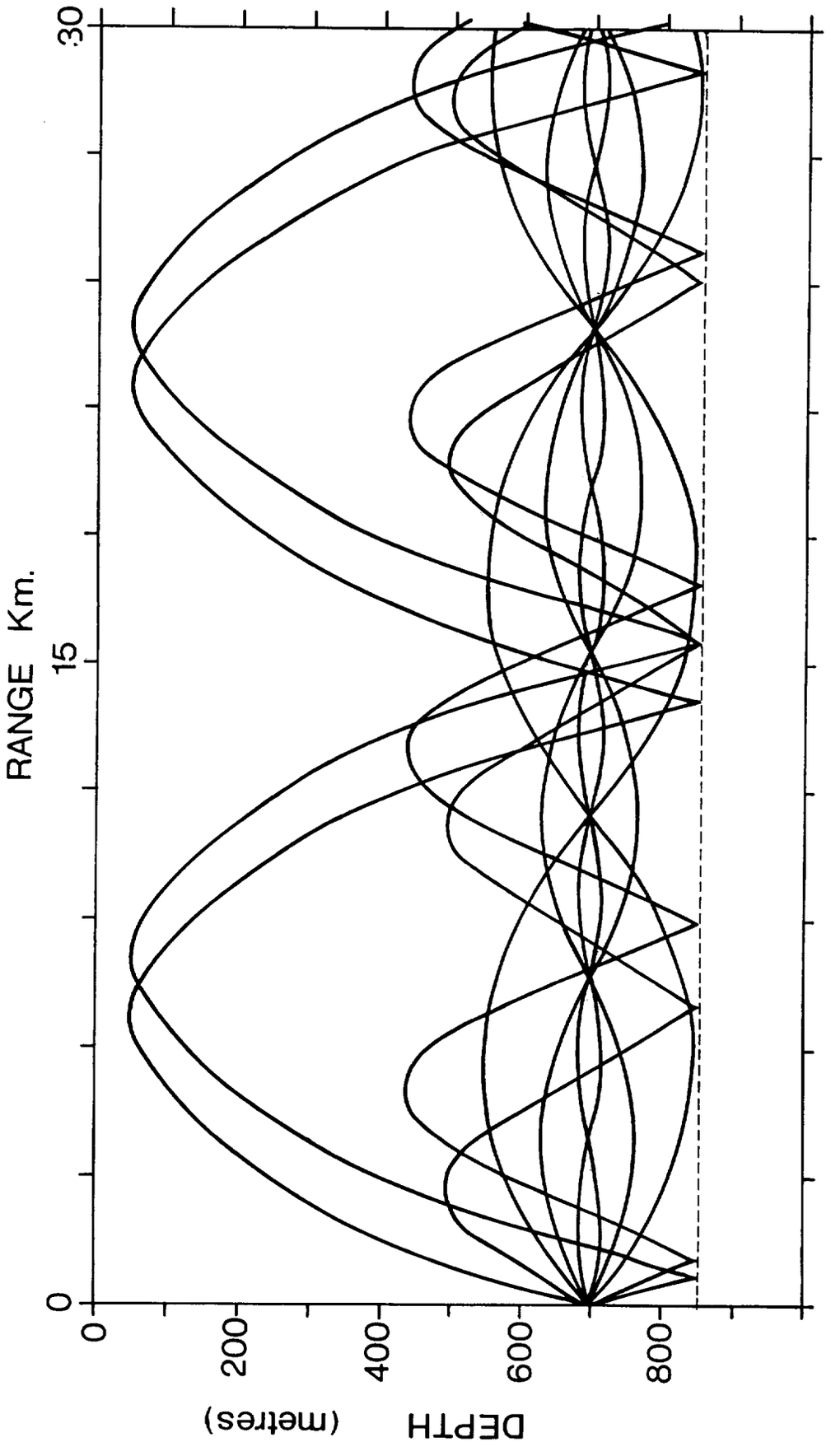

Fig. 6.1 Acoustic propagation paths for a sound source located at 700 m depth

detection bandwidth of 87 db, the available post-processing signal to noise ratio was approximately 25 db.

Reciprocal path time differences are at least an order of magnitude smaller than the spreads in the one-way travel times. A mean current of 5 cm/s, for example, over a 300 km path produces a time difference of only 13 msec. The resolution of arrival times to within about 1 msec is therefore required. The minimum signal to noise ratio, S, needed is contained in the expression:

$$\sigma_t = (2\pi B\sqrt{2S})^{-1}$$

which relates the rms travel time error, σ_t, in a matched filter to the rms bandwidth, B. Worcester et al. (1985) quote an overall system bandwidth of 33.5 Hz, yielding σ_t = 0.3 ms for 25 db signal to noise ratio.

The long term stability of timing throughout the network of sources and receiver is crucial: over a four month deployment period 1 ms accuracy in timing requires a stability of order 1 in 10^{10}. This was achieved using a two-clock system in which the phase of the output from a continuously running low power (10 mw) crystal oscillator was compared at regular intervals with that of a rubidium standard. Continuous operation of the standard was not possible owing to relatively high (13 watts) power consumption. A high order of stability is required, also, in the physical dimensions of the network if the one-way travel times are of primary interest. The response of a mooring to the barotropic tides, internal tides or currents associated with the mesoscale activity can produce instrument excursions of 100 m or more; these result in changes in travel times which are indistinguishable from the wanted signal arising from fluctuations in sound speed along the transmission path. Mooring motion is not a problem for two-way measurements since to first order the errors subtract. In practice perturbations in instrument position caused by mooring motion can be monitored to an estimated accuracy of a few metres: the technique adopted was to attach an interrogator to the mooring, adjacent to the source-receiver pair. This measured continuously the ranges to three transponders arranged equilaterally around the base of the mooring.

The results of a gyre-scale experiment conducted over a triangular path with ~1000 km legs in the central North Pacific in 1987 are amongst the first to be compared with data derived by other means (Worcester et al., 1990). Tidal currents obtained from differential travel time measurements agreed well with data derived from a numerical tidal model and with values registered by a current meter mooring. Good correlation was also obtained at low frequencies with the barotropic currents computed from electric field measurements made by bottom moored electrometers (Chave et al., 1990).

6.3 Shallow water applications

Tomographic techniques involving reciprocal transmissions are potentially of great value in areas of shallower water. This is especially true for applications involving the monitoring of transport across sills and through straits, where a single measurement averaged two-dimensionally is needed rather than a series of point observations.

The propagation characteristics of sound in shallow water, however, differ markedly from transmission in deep water, where sound paths may be wholly associated with refraction; and pulse arrivals are well spread in time and are identifiable with specific paths. In shallow waters, in the absence of a mid-water sound channel, rays make multiple interactions with the sea surface and sea bed. The attenuation of sound with distance is correspondingly much greater, especially for paths associated with both surface and bottom reflections. The greatest propagation distances, typically of a few tens of kilometres, are obtained in the case of those paths which involve a combination of refraction and bottom reflection. Shallow water measurement is further complicated by the fact that in shallow water the spread in arrival times is generally less than in deep water. Multipath arrivals overlap and form groups, with the consequence that resolution becomes very difficult (De Ferrari and Nguyen, 1985). In making reciprocal transmission observations in the Florida straits (Ko et al., 1989) found it impossible to make individual pulse-to-pulse comparisons as a result of the variability arising from the effects of multipath interference. Instead, received signals were smoothed, taking averages over a number of pulses, and the resulting signal envelope was taken as the basis of the measurement. Both the experimentally measured envelopes and those derived from the application of predictive ray models showed similar qualitative features, including a characteristic strong late peak followed by a sharp cut-off. These were used as a basis for travel-time estimation. The precision of measurement was estimated as 0.2 ms, corresponding to 2 cm/s in the depth-averaged current.

Results obtained thus far in shallow water reciprocal path acoustic measurements appear promising when compared with measurements made with discrete moored instruments. The technique is currently being applied by IOS in order to estimate the mass transport through the Faroe - Shetland channel in the NE Atlantic.

7.0 LAGRANGIAN TECHNIQUES

Lagrangian methods, in which a parcel of water is labelled by a floating body whose drift rate is measured, probably represent the earliest means of determining currents. In its simplest form a Lagrangian drifter is a small passive tracer which, when used in sufficiently large numbers with means of retrieval, has in the past provided useful, though limited information on current statistics (see Monahan et al., 1974 for a review of methods).

With the development of various remote methods for the periodic location of drifter position Lagrangian techniques now provide powerful investigative methods for a wide range of scales of motion, extending from ~10^2 m in some coastal applications to >10^3 km in ocean circulation studies (see, for example, Davis, 1991). Two main categories of Lagrangian sensors can be said to exist: surface-floating drifters for surface or near-surface current measurements and neutrally buoyant, acoustically tracked floats for deep ocean circulation studies. The technologies and problems of implementation are very different and so are considered separately below.

7.1 Surface Drifters

Whatever the scales of motion under investigation the Lagrangian arrangement usually adopted takes the form of a surface float supporting a tethered drogue which is coupled to the water mass at the depth of interest. In this system, in steady state conditions, drag forces, $\underline{F}_S$, $\underline{F}_D$ alone are assumed to act on the drogue and surface float combination due to the local water velocities at the surface and at the depth of measurement. At the surface the float will also be subjected to some degree of wind forcing, $\underline{F}_A$, though good design will minimize this. Provided that forces on the tether itself are negligible,

$$\underline{F}_A + \underline{F}_S + \underline{F}_D = 0$$

$$\text{and } \underline{F}_i = \frac{1}{2} \rho A_i C_i (\underline{V}_i - \underline{V}) \left| \underline{V}_i - \underline{V} \right|$$

$$i = A,S,D$$

where A_i is the surface area of the component body

C_i is the drag coefficient and ρ the water density

$\underline{V}$ is the vector velocity of the float/drogue combination over the seabed;

$\underline{V}_i$ is the true water velocity over the seabed at the depth of the component.

From these two equations an expression for V_D can be obtained in terms of the fixed parameters A_A, A_S, A_D, C_A, C_S, C_D, and velocities $\underline{V}_A$ $\underline{V}_S$. Note that $\underline{V}_D$ cannot be explicitly determined without knowledge of $\underline{V}_S$, and either direct slippage measurement ($\underline{V}_D$ - $\underline{V}$) or knowledge a priori of vertical current shear. The slippage velocity at the drogue is of major importance. A non-zero value means that the drifting float/drogue combination cannot be truly Lagrangian: and if this occurs in an extreme situation in which large horizontal current shears exist the drifter trajectory can be quite unrepresentative of the flow pattern. Good drifter design thus seeks to reduce slippage at the drogue to a minimum, for example by maintaining the ratios of $C_D A_D / C_S A_S$ and $C_D A_D / C_A A_A$ as large as possible.

The simple static balance, however, provides an inadequate basis for calculating forces, due to the effects of the oscillatory flows associated with surface gravity waves. The dynamic forces are frequently two orders of magnitude greater than those associated with the mean component of the motion, and, in a manner analogous to the situation discussed for Eulerian sensors, rectification can ensue and provide unwanted slippage. Niiler et al. (1987) point out that the specific reasons for rectification are difficult to identify but suggest that these may include:

- presentation of a different surface area to the motion at different phases of the wave cycle,
- wave breaking over the float,
- planing of the surface float when the tether lines become slack during part of the wave cycle,
- snatch loading of the tether line at certain times in the wave cycle, leading to irregular motion,
- production of horizontal lift forces by relative vertical flow.

Wave forces may also include those due to Stokes drift velocities. In this context, the wave propulsion of free floating buoys can readily be demonstrated in regular waves in a wavetank (e.g. Nath, 1978; McClimans, 1980). In the case of spar buoys judicious choice of natural heave and pitch frequencies can produce a range of propagation velocities and backward as well as forward motion can be generated.

Wind forces, though generally much smaller for well designed drogued drifters, are similarly difficult to estimate with much precision due to the fluctuating nature and uncertain profile of the wind field very close to the sea surface, and to the interaction of the buoy motion with this.

These uncertainties in the dynamic behaviour of the drifter-drogue combination - heightened by the fact that the wind and wave conditions experienced in situ are frequently

unknown - makes the estimation of errors in buoy trajectories very difficult. Discussion of the effects of wind forcing on buoy trajectories can be found in Kirwan et al. (1975, 1978); the effect of waves is considered in Booth (1981). More recent discussions of the interpretational problem can be found in Krauss et al. (1989), Poulain and Niiler (1990) and Krauss et al. (1990).

Substantial efforts have been devoted both to numerical modelling studies (Nath, 1977a; Chhabra, 1985; Chereskin et al., 1989) and to experimental studies of the system dynamics, using scaled models in wave tanks and wind tunnels (Nath, 1977b), also full scale tests at sea (Vachon, 1975; Saunders, 1976; Geyer, 1989; Mackas et al., 1989). The results of such studies aid the design process and subsequently permit systematic assessment of Lagrangian capability in a range of conditions. In effect it represents the Lagrangian equivalent to Eulerian instrument calibration. The recent development of the low-cost drifter (Dahlen, 1986; Chhabra et al., 1987) provides an example of this approach.

In assessing the extent to which truly Lagrangian measurement can be attained, the possible influence of wind driven Langmuir circulations should also be noted. The effect has received little attention, but it has been suggested that the vortices may attract drifters to the convergence zones in which forward velocities are slightly higher than in surrounding water, and thereby cause some slight upward bias in Lagrangian statistics.

7.2 Hull and Drogue Forms

A variety of hull and drogue forms has been either tried or proposed, and in these it is possible to recognize two generations of designs. Early designs were fashioned to a significant extent by the advent of satellite-based location systems. Many drifters were equipped with barometric pressure, and temperature sensors in order to satisfy primarily meteorological objectives: these were generally undrogued, for Lagrangian current measurement was of secondary interest. Surface floats tended to be of a spar form and were provided with a flotation collar so as to increase buoyancy. Materials were usually PVC, glass reinforced plastic, or aluminium. More recently the evolution of drifters more suited to current measurement has placed emphasis on reducing the size of the surface element and hence its drag; also on the use of shapes which are less likely to incur rectification of the oscillatory forces. The spherical (Niiler et al., 1987), pear shaped (Booth and Ritchie, 1983) and very short cylindrical (Dahlen, 1986) hull forms now in use should assist in reducing such problems.

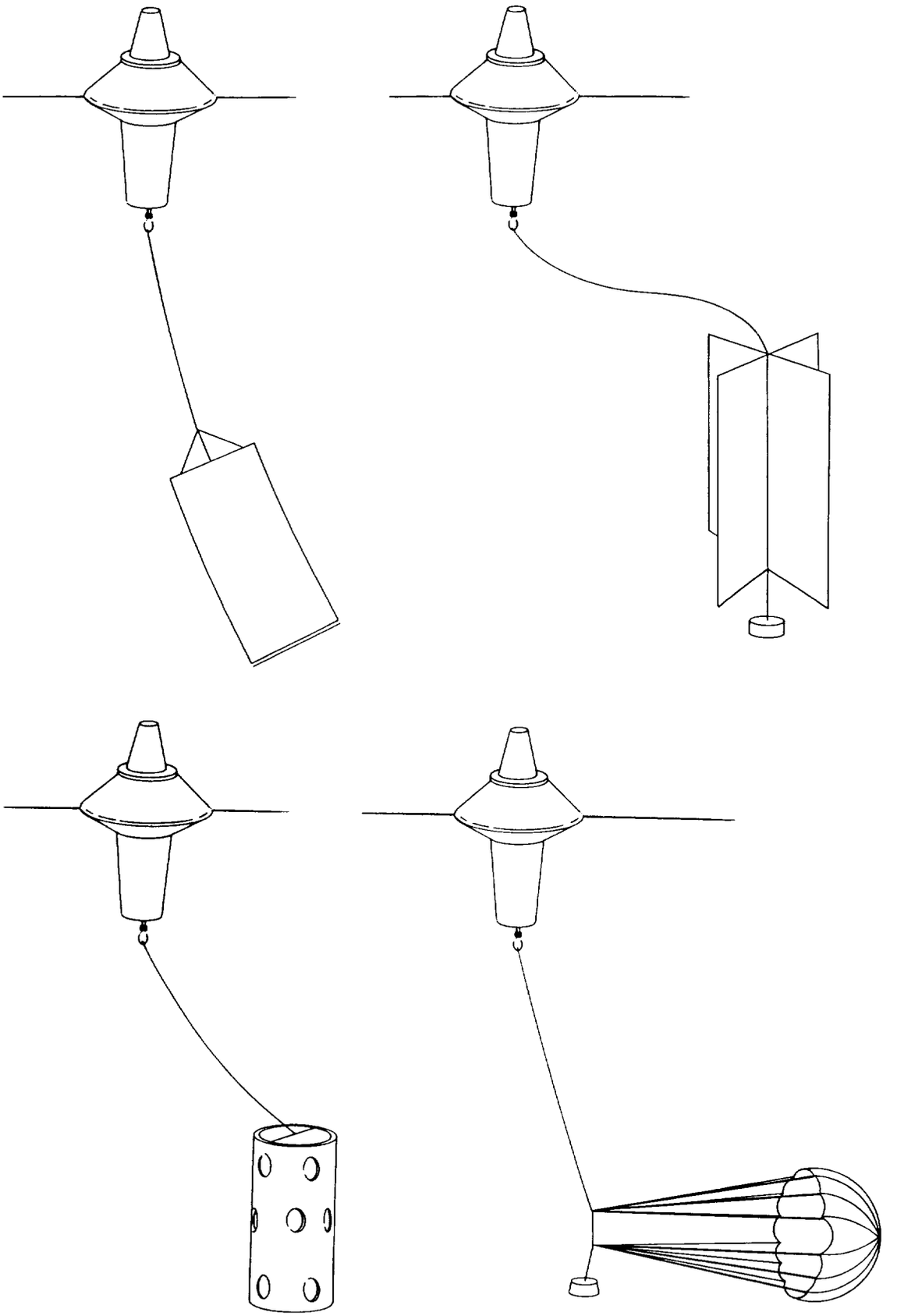

Fig. 7.1 Principal drogue types

The principal drogue types used (Fig. 7.1) include the parachute, window blind, cruciform (crossed vanes) and 'holey-sock', which is essentially a vertical fabric cylinder containing a number of perforations.

Parachutes seem to be relatively less favoured than other types of drogue; proper deployment and operation depends upon the existence of a slippage velocity - unless the considerable additional complexities of spreader bars and additional canopy buoyancy are incorporated - and this, as discussed earlier, represents a fundamental disadvantage for a Lagrangian tracer. There is also evidence for instability, tangling of shrouds at low velocities, and a dependence of properties on material porosity (Vachon, 1974). In contrast the window blind drogue has found widespread application. It stows conveniently, is easily deployed and in steady conditions aligns readily at right angles to the flow. However, sufficient ballast weight is required at the bottom of the drogue to prevent it streaming upward in the flow, and this in turn implies a need for adequate reserve buoyancy in the surface element and compliance in the tether so as to minimize snatch loadings. There remains some uncertainty concerning the behaviour of the window blind drogue in dynamic conditions and this has led to the introduction of the 'holey sock' and crossed vane forms which provide greater uniformity of properties with respect to direction.

Ensuring a long drogue lifetime - and devising a reliable indicator of drogue failure - have presented major difficulties when designing drifting buoy systems. Drogue loss indicators of various types have been tried but until recently have not proved to be sufficiently reliable. Greatest reliability is probably achieved if the sensing unit can be contained entirely within the buoy hull, as for example in the Draper LCD (Dahlen, 1986). In this instance a strain gauge bonded inside the bottom of the buoy hull is used to detect a change in the mean tension in the tether line when the drogue is lost.

Drogue design calculations require a knowledge of the drag coefficient, C_i, appropriate for the drogue form. A number of empirical determinations of drag coefficient have been made for commonly used drogue types. Some (Vachon, 1973, 1980) were conducted mostly in steady state conditions; others have been made in conditions which included regular oscillatory forcing (Nath et al., 1979).

The present development of drifters is influenced by a number of requirements, including those for

- minimum cost, in order to maximize the numbers of buoys available for deployment
- ease of stowage and deployment: drifters are nowadays used worldwide and both ships of opportunity and aircraft are employed for deployment

- ruggedness and longevity
- a calibrated performance, approximating as closely as possible to true Lagrangian behaviour.

These requirements have together enhanced the tendency towards smaller surface elements and lighter drogues.

Examples of recent developments include the Low Cost Drifter (Dahlen, 1986) which uses a pillbox surface element/nylon holey sock combination; also the design (Niiler et al., 1987) which adopts a 38 cm dia. fibreglass surface sphere and a triaxial-vaned, semi-rigid drogue.

7.3 Surface Measurement

Lagrangian measurement in the uppermost metre or two is simplified in one sense because drifter and drogue can be combined to form an integral assembly. On the other hand potential errors resulting from wave orbital rectification and uncertainties in the response to the strongly sheared Stokes drift assume greater importance. Effective design minimizes effects due to inertia, achieves a high degree of damping of residual pitch and heave oscillations, maintains symmetry in drag forces over a wave cycle and avoids as far as possible the forces associated with breaking waves. The objective should be to achieve good wave slope following by the float and its integral drogue, while reducing surface penetration to the minimum required for identification or to allow radio telemetry where this is used for position location. Otherwise substantial wind forcing can result. The dynamics of practical drogue types in very near surface conditions in general does not appear to have been given the attention received by Eulerian instruments. Davis (1982) reported the results of laboratory examinations of three surface buoy configurations, in which large mean drifts were found in one case: satisfactory performance was achieved in the case of a cruciform drogue closely coupled to the instantaneous surface by means of four small flotation elements attached by flexible lines to the outer corners of the drogue. The integral cruciform drogue has also been employed in surface current measurement programmes at IOS, using acoustic location techniques. In other investigations very close to the surface, Churchill and Csanady (1983) used free floating slabs of densely entwined rubberized strands (synthetic horsehair); at slightly greater depths the separated float-drogue combination was used, again, using a thick disc of horsehair material as the drogue.

7.4 Position Location Systems

7.4.1 Short Range

The usefulness of Lagrangian methods depends largely on the availability of suitable methods of determining position. Of methods presently available radio tracking is perhaps the most commonly used for the resolution of small to medium scales of motion although the need for floats to remain within radio range of fixed stations - typically tens of kilometres - tends to confine application to coastal areas. In the Coastal Ocean Dynamics Experiment, for example, in which 164 buoys were deployed (Davis, 1985) transmission ranges up to 75 km were achieved: buoys were located using mobile direction finding triangulation with a bearing accuracy of ±2°. Radio navigation systems can also be used in conjunction with telemetry to provide drifter location to within a few tens of metres - as for example in the system developed by Roberts et al. (1991) in which Decca Navigator signals received by surface drifters were converted and retransmitted ashore. Loran C has also been used for this purpose (Crawford, 1988).

Acoustic tracking of transponding surface floats has also been used (Collar, 1978; Churchill & Csanady, 1983), though this method is weather-dependent and the presence of a ship is required for float retrieval and redeployment because in most circumstances acoustic ranges are limited to perhaps 10 km or so. The technique is therefore expensive but does have an advantage in that it is not limited to coastal waters. The precision of the position location is dependent on the detection of transponder pulse arrivals: resolution of position to 10 m or so is feasible, though as in all range triangulation methods the accuracy deteriorates if the baseline geometry is unfavourable. Fig. 7.2 illustrates the method adopted at IOS for surface measurements in shelf seas, in which use is made of the transponder/receiver systems designed for deep float tracking (Section 7.6). In deep water fixed bottom transponders and a remotely triggered interrogator are initially surveyed in by making range and bearing measurements from the ship while steaming a series of courses at various fixed headings. In coastal waters transit bearings are taken on surface markers; alternatively transponder positions may be derived at the instant of deployment by taking visual bearings on prominent landmarks. In either case ship position is thereafter determined from direct range measurements from transponders. During the interrogation sequence, repeated at intervals between 10 and 30 minutes dependent on current speed, the ship interrogates floats, bottom transponders and the remote interrogator at 5.1 kHz, each unit replying at a unique frequency within the interval 5.7-6.7 kHz. The remote interrogator then repeats the sequence, being triggered by a signal at 7.1 kHz from the ship. Simple geometry shows that each float position can be derived from the ship-float and remote interrogator-float ranges. For favourable fixing geometry, mean surface current over 30 minutes can be obtained in this way to within ~±2 cm/s.

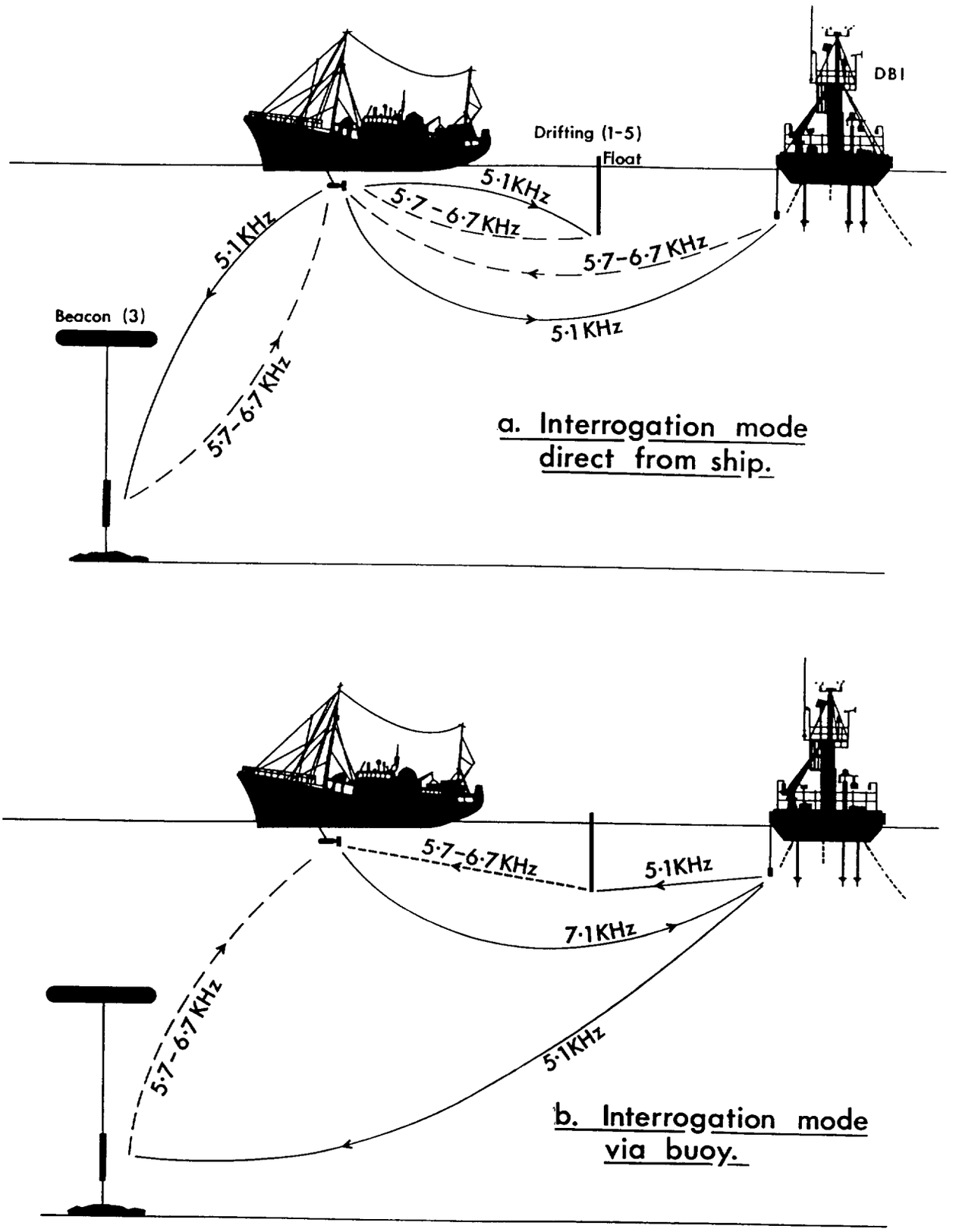

Fig. 7.2 IOS float tracking system (surface floats)
(a) Interrogation mode direct from ship
(b) Interrogation mode via buoy

7.4.2 Long Range

At larger scales the emergence of the Argos data telemetry and location system carried on the NOAA series of polar orbiting satellites has enabled Lagrangian measurements to be made worldwide with a positioning accuracy of a few hundred metres. The satellite receivers operate on a random access basis, low power buoy transmitters (Platform Transmit Terminal-PTT) being pulsed continuously at preset intervals between 50 and 200 seconds with a pulse code modulated signal of approximately 1 second duration, containing up to 256 bits of data. From the measurement of carrier frequency, at each of several uplinks during a pass (a minimum of 5 is required to achieve standard accuracy) the rate of change of Doppler shift enables the position of the transmitter to be determined at the ground based computer facilities. The frequency with which fixes can be obtained is latitude dependent ranging from 3 or 4 times daily at the Equator to a theoretical maximum of 27 at the Poles.

PTT transmissions are simultaneously rebroadcast by the satellite and are also stored for downloading to the principal ground stations in North America and France. Data amd PTT position are available to the user at the system computers at Toulouse, France and Landover, USA within three or four hours of reception at the satellite - and within perhaps as little as 75 minutes if a local User Terminal is available and can receive the echoed PTT transmission. Apart from its use in large scale drifting buoy networks during the Global Weather Experiment and currently in the Tropical Ocean Global Atmosphere experiment the Argos system has seen much use in circulation studies in each of the major oceans. Fig. 7.3 shows the circumnavigation of the North Atlantic over a period of 42 months by a surface buoy deployed in January 1979 east of Newfoundland. The track shows clearly the existence of mesoscale eddies of more than 100 km diameter in addition to the large scale classical circulation pattern.

The accuracy with which velocity can be inferred from Argos-tracked drifters has been analyzed by D'Asaro (1992).

7.5 Deep Ocean Floats

7.5.1 Isobaric floats

Deep Lagrangian float techniques, pioneered by Swallow (1955, 1957), are based on the principle that a body whose compressibility is less than that of sea water will gain buoyancy as it sinks. By careful adjustment of the excess weight at the surface, therefore, the float can be arranged to gain enough buoyancy to become neutrally buoyant at a predetermined depth, whereupon no

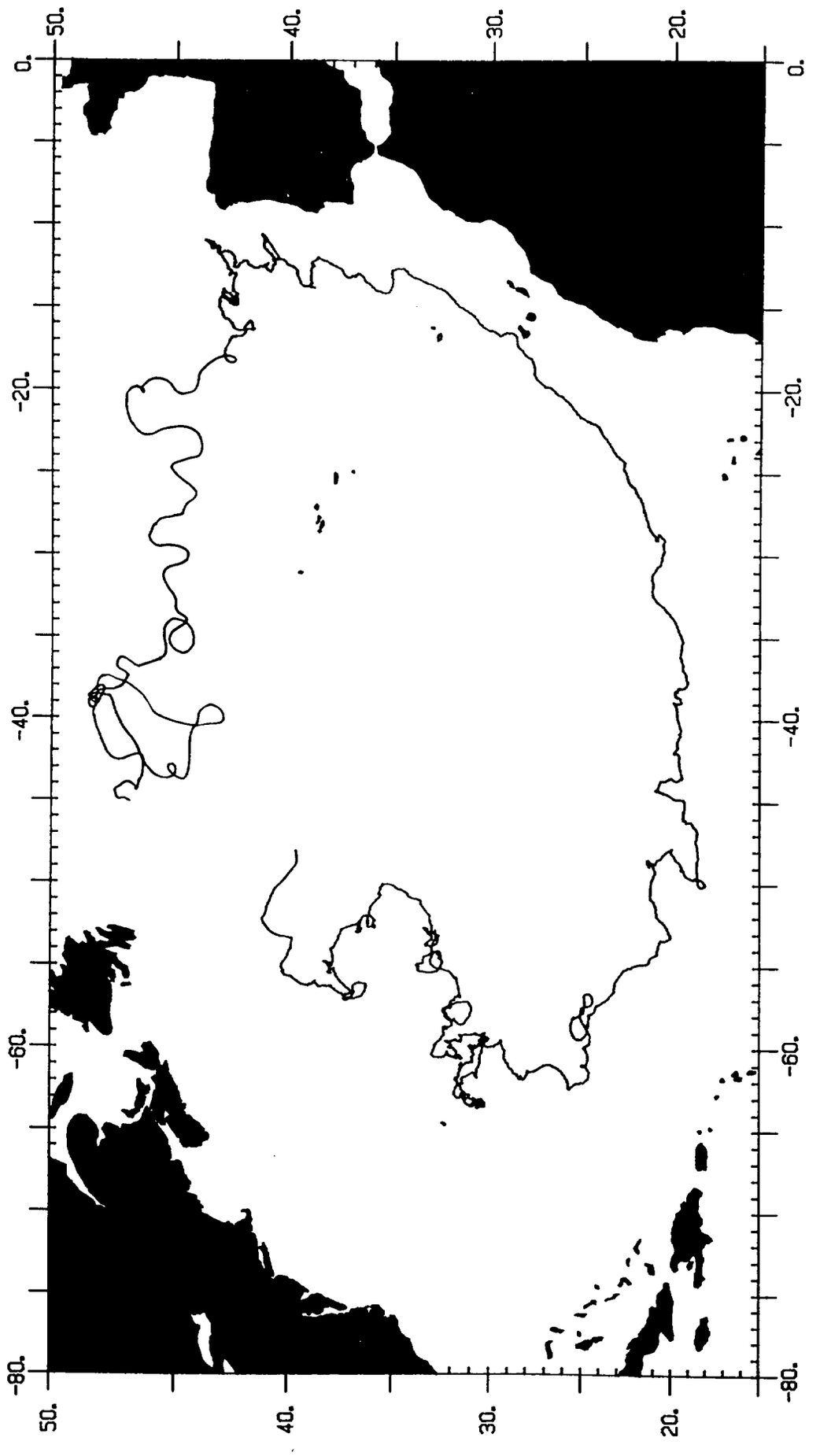

Fig. 7.3 The classical clockwise surface circulation pattern of the N.E. Atlantic revealed by a drifting buoy tracked via the Argos system over 42 months.

further sinking will occur. This is essentially isobaric balancing. The horizontal movement of the float then gives a direct measurement of the Lagrangian current at that depth.

Acoustic tracking represents the only practicable way of locating floats in view of the severe attenuation suffered by electromagnetic waves in sea water, and acoustic propagation characteristics (Section 6.1) essentially determine the way in which deep ocean float techniques can be applied to current measurement. Floats can be tracked over long ranges by using low acoustic frequencies and by making use of the deep sound channel.

With a choice of float transponder frequency below 1 kHz so as to minimize absorption losses, ranges exceeding 1000 km are readily attained. In the absence of the ducted propagation modes - or at higher frequencies - maximum ranges at which acoustic floats may be located are generally less than 100 km, a fact which really implies the need for an attendant ship throughout an experiment in order to retrieve and redeploy floats or receiving stations.

7.5.2 Isobaric balancing

The relationship between the incremental load $\delta\mu$ required for neutral buoyancy at an in-situ density ρ, once a float of mass M has been adjusted so as to have neutral buoyancy in a laboratory tank, can be derived simply as follows. Suppose the float is neutrally buoyant in water of density ρ_o and temperature T_o. Then at the desired depth h the float density would be

$$\rho_f = \rho_o (1 + C_f) - \alpha(T - T_o))$$

where C_f is the bulk compressibility* of the float per unit change in depth and α is the temperature coefficient of volume expansion of the float. The incremental mass required to make the float sink to the desired depth will therefore be given by

$$\delta M = M\left(\frac{\rho - \rho_f}{\rho_f}\right)$$

$$= M\left(\frac{\rho}{\rho_o(1 + C_f - \alpha(T - T_o))} - 1\right)$$

Float balancing is carried out in a tank of well mixed water whose density should be determined to about 5 ppm and temperature to 0.1°C. Entrainment of air bubbles in the weighing

*For standard shapes (e.g. long tubes or spheres) compressibility may be readily calculated using standard formulae with a knowledge of the elastic constants of the material and internal and external dimension.

operations must be avoided. Subsequently, when applying the equation above corrections may be needed for the effects of temperature and pressure on external steel ballast weights.

The following are representative values obtained in balancing a Minimode float for operation at 4000 metres depth:

Temperature	2.5°C	At working depth
Salinity	34.92‰	
Depth	4000 m	
Temperature	12.7°C	Laboratory tank
Salinity	32.04‰	
Coefficient of compressibility C_f		$= 1.62 \times 10^{-6}$/metre
Coefficient of thermal expansion		$= 60 \times 10^{-6}$/°C
Mass of float		= 49.500 kgm
At 4000 m $C_f = 1.62 \times 10^{-6} \times 4000$		= 0.00648
$\alpha(T - T_o) = 60.10^{-6}$ (2.5 - 12.7)		= 0.000612

Recourse to oceanographic tables shows that for seawater of temperature 12.7° and 32.04‰ salinity, $\sigma_T = 24.181$.

Hence with the float adjusted for neutral buoyancy in the laboratory tank $\rho_o = 1.024181$.

From the expression above, $\rho_f = 1.031444$.

Again from oceanographic tables, for T = 2.5°, S = 34.92‰, $\rho = 1.045907$. Hence the mass to be added to achieve neutral buoyancy at 4000 m depth, $\delta M = \left(\frac{1.045907}{1.031444} - 1\right) . 49500 = 694$ gm.

Experience at IOS shows that floats made from aluminium tube may initially be positioned to within about ±100 m of the chosen depth, later improving to ±50 m as the float history develops with successive deployments: a float consisting of a single glass sphere can be positioned with a precision of about 250 m improving to about 100 m.

Once it has achieved its working depth a float sinks at a rate of somewhat less than 1 m/day due to creep in the housing. In SOFAR floats (Webb, 1977) this was compensated by the inclusion of a circuit, controlled by the pressure transducer, which connects a zinc anode to the aluminium housing, thereby forming a Zn Al seawater battery. With the circuit complete zinc goes into solution producing a gradual gain in buoyancy.

7.5.3 Isopycnal floats

Better representation of Lagrangian motion may be achieved if the float is designed to follow surfaces of constant density (isopycnal) rather than constant pressure (isobaric). Isopycnal surface following requires that the compressibility of the float should be matched closely to that of sea water and, in addition, that the coefficient of thermal expansion of the float should be significantly smaller than that of sea water. Rossby et al. (1985) have successfully developed a technique for doing this, using a cylindrical float of borosilicate glass. The matching of the compressibility of the float to that of sea water (~-4.4 x 10^{-6} m^{-1}) was achieved by attaching a spring-loaded piston open to the ambient pressure and free to move in an aluminium cylinder. The piston diameter and spring constant were selected to provide the required reduction in volume with increasing pressure.

For an isopycnal float the thermal expansion coefficient is important, since it may determine whether isopycnal operation can be sustained in conditions in which the effects of temperature and salinity gradients run counter to each other. For an isopycnal float the restoring force is:

$$F_{isopycnal} = \rho g\left[(\alpha_w - \alpha_f)\frac{\partial T}{\partial Z} + \frac{1}{V}\frac{\partial V}{\partial S}\cdot\frac{\partial S}{\partial Z}\right]$$

(where suffix w refers to water properties and S is salinity).

Rossby et al. estimate the restoring force for a glass float (of volume $10^4 cm^3$) operating in the western North Atlantic to be ~17 dynes/m: an aluminium float is closer to marginal operation at ~6 dynes/m. In isobaric operation a substantially larger restoring force $\rho g(C_w - C_f)\frac{\partial p}{\partial Z}$ is contributed: for the example of the IOS float given above this is ~140 dynes/m.

7.6 Float Designs

Early float designs (Swallow, 1955) made use of aluminium alloy scaffold tubing, an optimum ratio of wall thickness to tube diameter for the required change in volume being achieved by solution in caustic soda. The floats carried simple 10 kHz acoustic pingers and were tracked a few at a time from an attendant ship equipped with hydrophone pairs so as to provide direction finding capability. An improved method of ship-based tracking developed by Swallow et al. (1974) at IOS enabled up to 18 floats to be tracked simultaneously and yet permitted the ship to carry out a concurrent CTD observation programme. The work was undertaken in support of the Mid Ocean Dynamics Experiment (MODE) and had as its objective the resolution of fluctuations in current at scales considerably smaller than the mesoscale eddy activity (~300-400 km in wavelength) and at depths between 500 and 4000 m. Floats were to be recoverable, using an independent acoustic command system to drop an external ballast weight, so that tactical redeployment could be

arranged as required. Each float was a transponder, thus providing a direct measure of the range of the float from the ship, whose position was determined by Loran C. Float positions were then obtained by combining ranges from different ship positions at different times. The interrogation pulse length was 30 msec, transmitted at a frequency of 5.1 kHz at intervals of 8 seconds over a period of several minutes. Each individual float responded at a unique frequency within the range 5.56 to 6.60 kHz. Acoustic ranges obtained using this system were dependent on ray propagation but sometimes reached 70 km. The accuracy with which float position could be determined from the most frequently occupied interrogator depths of 500 m and 3000 m was limited by a combination of errors in range measurement and errors in estimating the position of the interrogator array. Range measurement errors resulted from timing delays in the transmitting and receiving equipment, and from uncertainties in the sound velocity appropriate to the particular propagation path achieved from among the multiplicity of paths possible. Fixing errors were generally within ±0.5 km.

A further development of the system introduced an additional interrogation mode in which a complementary series of interrogation pulses from an interrogator moored remotely at a known position could be triggered from the ship. This enabled the range of each float to be determined consecutively, firstly from the ship, then from the remote interrogator. During the initial ship interrogation sequence the remote interrogator transponded as a float, thus providing a direct measurement of the baseline length for the range-range measurement.

7.7 SOFAR Floats

The earliest experiments with neutrally buoyant floats in the deep sound channel took place towards the end of the 1960s (Rossby and Webb, 1970, 1971) using existing hydrophone stations on Bermuda, Eleuthera (Bahamas) and Puerto Rico. The 300W float output signal was a low frequency, 1.2 second c.w. pulse. In the initial experiments a set of 90 pulses was transmitted, 1 minute apart, every 6 hours. In the later experiments a lower frequency was used, 380 Hz, and transmissions were made every 2 mins. Additional pulses transmitted in between the primary pulses in a time-delay mode afforded a means of monitoring water temperature, and hence float depth. The timing in each float was controlled by a highly stable clock synchronized to the shore station receivers. Thus reception of float signals at two stations provided range-range determination of float position, ambiguity being resolved from a knowledge of previous or initial position. In the event of a float clock losing synchronisation position could still be determined provided that signals were received by a third station. The hyperbolic or phase difference method then yielded float position.

The impetus for further development of long range long term drifters came from the Mid Ocean Dynamics Experiment (MODE) and, subsequently from the POLYMODE. For MODE twenty floats were constructed (Rossby et al., 1975), designed for operation at 1500 metres depth and for an endurance of 1 year. Three carrier frequencies in the vicinity of 270 Hz were used, together with selection from 7 pulse repetition frequencies to provide twenty one signal channels. Overall position fixing accuracy was estimated as 2-3 km. Floats were 5.2 metre 30.5 cm diameter aluminium cylinders, which carried two shorter organ pipe acoustic resonators. In addition to the timing and acoustic transmission circuits, some floats contained subsystems for recording temperature, depth (pressure) and vertical flows past the float, sensed by float rotation induced by the attachment of paddles around the float. An auxiliary acoustic command system permitted ultimate retrieval of the float by releasing a ballast weight.

Floats designed for POLYMODE represented another step in the evolutionary development of deep float techniques (Webb, 1977). Provision was made for simultaneous tracking of 200 or more floats, including time delay modulation telemetry of in situ measurements, while signalling performance related to energy expenditure was optimized so as to achieve lifetimes of 2-5 years. The basic location signal was now an 80 second linearly swept frequency transmission once every 8 hours and the float ensemble employed both time division and frequency division multiplexing, using ten frequency channels between 230 and 270 Hz, and 10 minute time slots. The development of synchronous autonomous listening stations, set on deep sea moorings also, permitted a much wider geographical application of long range SOFAR tracking techniques.

7.8 RAFOS System

The RAFOS system - as is implied by the reversal of the SOFAR acronym - is a more recent development (Rossby et al., 1986; 1993), in which transmissions are made from sound sources moored within the deep sound channel. Following the techniques established for the SOFAR float system, the acoustic signal consists of an 80 second linearly swept c.w. pulse centred at 260 Hz but in this case it is received synchronously by the drifting floats. At each float, signal detection is achieved - after dual stage conversion - filtering and limiting, by sampling the signal at a 10 Hz rate and performing an 800 bit complex correlation. The RAFOS arrangement has advantages in that just a few sound sources can provide means of location for an arbitrary number of floats. Furthermore float power requirements can be reduced significantly, so enabling floats to be made smaller, lighter and more cheaply. The floats are designed for isopycnal operation and consist of small borosilicate glass cylinders 1.5 m long x 8.6 cm in diameter, closed at one end and sealed at the other by an aluminium cap. Retrieval of the data from a float at the end of the mission affords an example of the way in which satellite and oceanographic technologies can be very effectively

combined: the float simply sheds a ballast weight after a preprogrammed time interval and ascends to the surface. Under float clock control data are transmitted repeatedly via the Argos system, several days' operation ensuring transfer of the 2835 bytes generated by a mission of typically 6 weeks duration.

7.9 ALACE Floats

The latest stage in the evolution of subsurface float design is represented by the Autonomous Lagrangian Circulation Explorer (ALACE) (Davis et al., 1992). This is a float of variable buoyancy which permits the exploration of large scale low frequency currents and provides, also, for the periodic measurement of vertical profiles of physical parameters in the upper ocean. The float is arranged to be neutrally buoyant at depth but changes its buoyancy periodically by pumping hydraulic fluid from an internal reservoir to an external bladder, so increasing total volume and hence buoyancy. On reaching the surface, communication and position determination are achieved through use of the Argos system. Return to depth is effected simply by releasing the fluid in the bladder back into the internal reservoir. The system is designed for long-term deployment: the predicted life for a float equipped with Lithium batteries exceeds 100 cycles to 1000 m over a period of 8 years.

8.0 EMERGING CORRELATION TECHNIQUES

The availability of increasingly powerful microprocessors, coupled with higher density memory arrays, has, in the past few years, encouraged the development of more sophisticated data processing techniques for self-contained instruments. In this report the application of cross correlation techniques to acoustic signals in scintillation methods and in correlation sonars appears to show considerable promise. Spatial correlation techniques are also being applied to images of the sea surface derived from earth observation satellites.

8.1 Scintillation Methods

The scintillation method relies on the fact that a signal passing through a medium whose propagation characteristics have a randomly varying element will itself acquire random fluctuations in amplitude and phase. In the sea such fluctuations in acoustic signals result from temperature, salinity fine structure and turbulent motion along the acoustic path. Mean flow can then be deduced from the spatial movement with time of the acoustic signals characteristic of a particular acoustic path.

Farmer and Clifford (1986), Farmer et al. (1987) and Lemon and Farmer (1990) have applied the technique to the measurement of flow in a tidal channel and a river estuary using two adjacent but independent sound paths transverse to the flow. With the assumption that the turbulent structure changes more slowly than the rate of advection, the computed cross correlation between signals transmitted along the two paths yields a maximum correlation at the delay, τ, associated with the mean flow transverse to the sound paths. For a path separation of D the mean flow is given by $V = D/\tau$, the mean flow being the transport in a cross-section determined by the vertical scale of the irregularities which contribute most strongly to the scintillations.

8.2 Correlation Sonar

Acoustic correlation sonar was developed for use as a ship's log some years ago and is now being applied to current measurement. Unlike doppler systems, which require narrow beams at oblique angles, correlation sonars use wide beams and measure the velocity of scatterers in a plane orthogonal to the boresight. For a given array size this permits the use of lower frequencies than in a doppler system; hence the range attainable by a correlation sonar may be substantially greater. An additional advantage of this system is that the measurement is independent of sound speed.

The basic principle of correlation sonar may be explained in the following manner (Fig. 8.1): a pulse is transmitted from T at time t_o. It is backscattered from a scatterer at point A and is received at receiver R_1. A second pulse delayed by τ with respect to the first is transmitted from T.

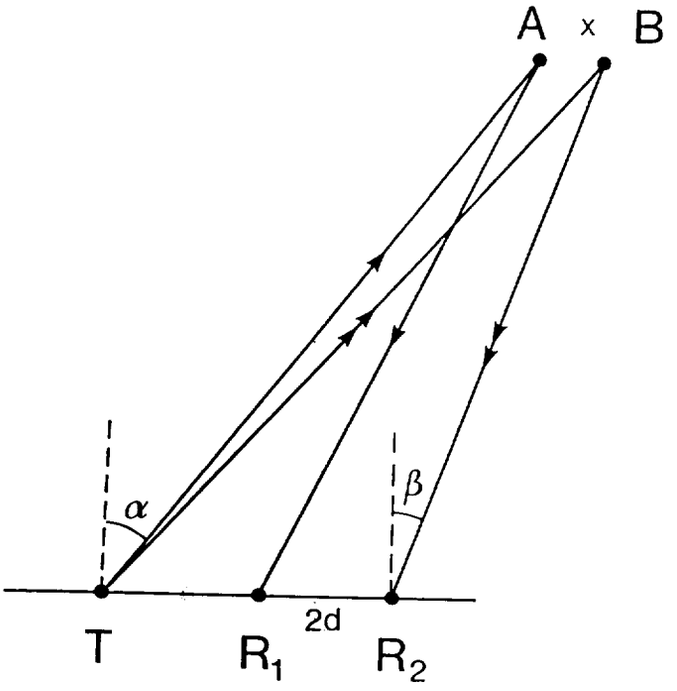

Fig. 8.1

The scatterer A has been advected a distance x to B and the pulse is now received at receiver R_2 separated from R_1 by distance 2d. Defining the angles as shown, the path differences at t_o and $t_o + \tau$ are ~x sin α for the upward path, and -(2d - x) sin β' for the downward path after scattering has taken place. Summing these, the path lengths overall will approach equality for distant scatterers if x = d. In that case the wavefront scattered from the particle at B and received at R_2 will be closely correlated with the wavefront scattered from the earlier position at A and received at R_1. The speed of the scatterers V = d/τ. In practice either d or τ may be fixed and the other parameter measured from correlations in the received signals. In the spatial correlation system the time between pulses is fixed and cross correlations are made between the reference signal and each transducer in a two dimensional receiving array positioned around the transmitting element. The correlation over a series of N pulses is given by

$$K = \frac{\sum_{i=1}^{N} (x_{i-1} - \bar{x})(y_i - \bar{y})}{\left(\sum_{i=1}^{N} (x_{i-1} - \bar{x})^2 \left(\sum_{i=1}^{N} (y_i - \bar{y})^2 \right) \right)^{1/2}}$$

where x_i is the i^{th} echo sample on the reference receiver delayed by one interpulse period, y_i is the simultaneous echo sample from the receiver which is being correlated with the reference.

The position of maximum cross correlation is then found by interpolation, the inter-pulse period being chosen to be sufficiently small that at maximum velocities the peak cross correlation occurs within the array and not outside it. As yet current profiling using range gated correlation sonar is in its infancy: relatively few publications on the topic have appeared in the literature. Rather more information is available on the application of the technique to the measurement of ship or vehicle speed using bottom echo (Atkins and Smith, 1987; Denbigh, 1984; Dickey et al., 1983; Hole et al., 1992). Recent results relating to current profiling, reported by Bradley et al. (1990) and Bradley and Kuo (1992) appear very encouraging.

8.3 Correlation Methods in Remote Sensing

The presence of large scale currents in the ocean is manifest in changes in the dynamic height of the ocean surface. Estimates of the magnitude of the flow can in principle be inferred from satellite altimetry measurements. For smaller scales the measurement of flow by the cross correlation of sequential satellite derived images of the sea surface shows promise. The techniques have been applied to images produced by the infra red radiometer (advanced very high resolution radiometer - AVHRR) carried on the NOAA weather satellites and the coastal zone colour scanner (CZCS) operating at visible wavelengths. The basic requirement is for the existence over a period of time of suitable thermally distinct or visible features in the image sequence. Surface flow rates are then deduced from feature displacements derived from spatial cross correlation between successive images. Selected features are typically a few km in size. A number of recent studies have included comparisons with field data. Garcia and Robinson (1989) used images derived from the CZCS to compute advective velocities in the English Channel and found consistency with previous studies in the area. Tokmakian et al. (1990) tested the technique in two ways. In the first method a quasi-geostrophic numerical model was used to advect the surface temperature field obtained from the AVHRR and so produce a set of synthetic images. The maximum cross correlation method was then applied to the images and a comparison made between the predictions of the correlation technique with the velocity field of the model. The second method applied data derived from acoustic doppler current profiler transects. The tests showed that best results obtain when sequential images are available at closely spaced intervals. Errors were of the order of 0.14 ms^{-1} for images separated by 6 hours, increasing to 0.25 ms^{-1} or more when the separation increased to 18 hours. Currents inferred from CZCS images, which are separated by at least 24 hours, had associated errors comparable with those of the AVHRR images with similar separation. These findings contrast with those of Svejkovsky (1988) who applied a subjective visual analysis to sequential satellite images and compared displacements with those of concurrently

deployed surface drogued drifters. Overall levels of agreement to within 6 cm/s were found. Sources of error in the technique, modelled by Wahl and Simpson (1990), are largely associated with the changes that take place in the images with time and thereby lead to decorrelation. These include rotation and distortion by large scale currents, and mixing. AVHRR images are particularly affected by surface heating and cooling. Wahl and Simpson found the most rapid decorrelation to be associated with variability in heating, caused by broken stratus clouds, which may provide an upper limit for time separations between sequential images of 6-9 hours. Changes in CZCS images are brought about by biological growth, grazing and sinking.

In spite of some limitations, it seems likely that improvements in the technique will be sought since it offers potential advantages of comprehensive but relatively inexpensive synoptic flow field coverage over relatively large areas.

9.0 CONCLUDING REMARKS

Instruments and observational techniques for current measurement have evolved in response to a wide range of differing requirements. Some of these requirements are quite easily satisfied, others still offer considerable scope for ingenuity and may require the application of more than one measurement technique. Achievement of complete maturity of a technique - loosely defined as its widespread acceptance within the community - usually takes some years of painstaking application and involves comparison with alternative methods of measurement. In this respect the techniques outlined above are in varying stages of evolution.

A substantial fraction of this report has been devoted to measurement using discrete moored instruments. No apology is made for this balance since Eulerian measurement until now has represented the most widespread technique and will continue to be widely applied. It can, however, be regarded as mature since it seems unlikely that much fundamental advance will occur in this area in the future, although improvements in detail will undoubtedly be made. Lagrangian methods, also, have been long established and their limitations in representing the flow have been well documented. The advent of satellite-based position fixing and data telemetry systems has greatly enhanced the attractiveness of such methods for long term/large scale measurement. The way forward is represented by the profiling drifter, which periodically ascends to the surface, making observations as it does so, in order to fix position, and telemeter data.

Two trends have been apparent for some time now and seem likely to continue. The first is the increasing economic pressures which dictate the need to derive the maximum amount of information from a single instrument. This, for example, will undoubtedly fuel the further development of non-invasive acoustic techniques. Non coherent doppler sonar, into which considerable effort has been put in recent years, appears to be nearing maturity, though some sources of error in measurement remain to be fully identified - and measurements at depth are as yet limited by lack of adequate transducers. It seems probable that the current state of the art will be supplanted within a few years by pulse coherent doppler sonar and especially by the arrival of correlation sonar.

The second trend is the way in which many observations are now being made in connection with the parallel development of numerical modelling techniques - the data are being used to initialize and validate models. An example of this is to be found in coastal seas, for which the development of h.f. backscatter techniques able to provide data with an accuracy to within 10 cm/s over a wide area has proved a major asset. This technique is now well established, through the manner in which underlying current is inferred from the displacement of the first order doppler spectra might still be considered to provide scope for some research.

The same trend is particularly evident in oceanic measurement. Here the focus on climate-related objectives has in turn emphasized the requirement for data gathering over large spatial and temporal scales. The scope of the measurement task is so vast that all of the armoury of methods currently available will be needed. It seems likely, also, that indirect measurement of current - by mapping vertical density structure and inferring flow via geostrophy will provide a major contribution.

Acoustic tomography, providing the three-dimensional temperature structure could provide one element of this, but it seems likely that development of robotic techniques for data gathering - for example profiling drifters and autonomous vehicles - represent the way forward.

10. REFERENCES

AANDERAA, I. 1964
A recording and telemetering instrument.
Nato Subcommittee on Oceanographic Research, Technical Report No. 16, 46 pp.

ANDREUCCI, F., CAMPOREALE, C. & FOGLIUZZI, F. 1992
Acoustic Wideband Techniques for the Remote Estimation of the Sea Current Velocity.
pp. 614-619 in 'Oceans '92', Proceedings of the IEEE Conference.
New York: Institute of Electrical & Electronic Engineers.

APPELL, G.F. 1978
A review of the performance of an acoustic current meter.
University of Delaware, College of Marine Studies, Technical Report DEL-SG-3-78, 35-58.

APPELL, G.F. 1979
Performance assessment of advanced ocean current sensors.
IEEE Journal of Oceanic Engineering, OE-4, 1-4.

APPELL, G.F., MOONEY, K.A. & WOODWARD, W.E. 1983
A framework for the laboratory testing of Eulerian current measuring devices.
IEEE Journal of Oceanic Engineering, OE-8, 2-8.

APPELL, G.F., MERO, T.N., SPRENKE, J.J. & SCHMIDT, D.R. 1985
An intercomparison of two acoustic doppler current profilers.
pp. 723-730 in Proceedings of the IEEE Conference on Ocean Engineering and the Environment, November 1985, San Diego, California, USA.
New York: Institute of Electrical & Electronic Engineers.

ATKINS, P. & SMITH, B.V. 1987
High accuracy two axis velocity measuring device.
pp. 77-82 in Proceedings of the IERE 5th International Conference on Electronics for Ocean Technology, March 1987, Edinburgh.
London: Institution of Electronic & Radio Engineers.

AUBREY, D.G., SPENCER, W.D. & TROWBRIDGE, J.H. 1984
Dynamic responses of electromagnetic current meters.
Woods Hole Oceanographic Institution Technical Report WHOI-84-20, 150 pp.

AUBREY, D.G. & TROWBRIDGE, J.H. 1985
Kinematic and dynamic estimates from electromagnetic current meter data.
Journal of Geophysical Research, 90, 9137-9146.

BARBER, T.R. 1971
Steady displacements of moorings produced by ocean currents.
National Institute of Oceanography Report, A54, 13 pp. & figs.

BARRICK, D.E. 1972
First order theory and analysis of MF/HF/UHF scatter from the sea.
IEEE Transactions on Antennas and Propagation, AP20, 2-10.

BARRICK, D.E. 1986
The role of the gravity-wave dispersion relation in H.F. radar measurements of the sea surface.
IEEE Journal of Oceanic Engineering, OE-11, 286-292.

BARRICK, D.E., HEADRICK, J.M., BOGLE, R.W. & CROMBIE, D.D. 1974
Sea backscatter at H.F.: interpretation and utilization of the echo.
Proceedings of the Institute of Electrical & Electronic Engineers, 62, 673-680.

BARRICK, D.E., EVANS, M.W. & WEBER, B.L. 1977
Ocean Surface Currents mapped by radar.
Science, 198, 138-144.

BEARDSLEY, R.C. 1987
A comparison of the vector-averaging current meter and New Edgerton, Germeshausen and Grier Inc. Vector-Measuring Current Meter on a surface mooring in Coastal Ocean Dynamics Experiment I.
Journal of Geophysical Research, 92, 1845-1859.

BERTEAUX, H.O. 1976
Buoy Engineering.
New York: John Wiley & Sons, 314 pp.

BERTEAUX, H.O. & WALDEN, R.G. 1969
Analysis and experimental evaluation of single point moored buoy systems.
Woods Hole Oceanographic Institution Technical Report No. 69-36, 71 pp.

BEVIR, M.K. 1970
The theory of induced voltage: electro-magnetic flowmeters.
Journal of Fluid Mechanics, 43, 577-590.

BIVINS, L.E. 1975
Turbulence effects on current measurement.
University of Miami, Coral Gables, Florida, USA: MS Thesis, 104 pp.

BOOTH, D.A. 1981
On the use of drogues for measuring subsurface ocean currents.
Deutsche Hydrographische Zeitschrift, 34, 284-294.

BOOTH, D.A. & RITCHIE, D. 1983
SMBA satellite tracked buoy and drogue.
Scottish Marine Biological Association, Dunstaffnage Marine Research Laboratory, Marine Physics Group Report No. 22, 9 pp. & figs.

BOWDEN, K.F. 1956
The flow of water through the Straits of Dover related to wind and differences in sea level.
Philosophical Transactions of the Royal Society, A 248, 517-551.

BOWDEN, K.F. & HUGHES, P. 1961
The flow of water through the Irish Sea and its relation to wind.
Geophysical Journal of Royal Astronomical Society, 5, 265-291.

BRADLEY, S.E., DEINES, K.L. & ROWE, F.D. 1990
Acoustic Correlation Current Profiler.
pp. 306-313 in Proceedings of the IEEE Fourth Working Conference on Current Measurement, 3-5 April 1990, Maryland (eds. G.F. Appell & T.B. Curtin).
New York: Institute of Electrical & Electronic Engineers.

BRADLEY, S.E. & KUO, S.Y. 1992
Long range acoustic correlation current profiler
pp. 648-653 in 'Oceans '92', Proceedings of the IEEE Conference.
New York: Institute of Electrical & Electronic Engineers.

BRISCOE, M.G. 1982
How good are current meter data?
pp. 19-27 in Proceedings of the IEEE Second Working Conference on Current Measurement.
New York: Institute of Electrical & Electronic Engineers.

BRISCOE, M.G., SIGNELL, R. & LONGWORTH, S. 1986
A VMCM-S4 current meter intercomparison on a surface mooring in shallow water.
pp. 7-11 in Proceedings of the IEEE Third Working Conference on Current Measurement, 22-24 January 1986, Airlie, Virginia (eds. G.F. Appell & W.E. Woodward).
New York: Institute of Electrical & Electronic Engineers.

BROWN, N.L. & LAWSON, K.D. 1980
A high precision acoustic current sensor.
pp. 57-74 in Proceedings of the Near Surface Experimental Technology Workshop, Norda, USA.

BRUMLEY, B.H., CABRERA, R.G., DEINES, K.L. & TERRAY, E.A. 1991
Performance of a broad-band Acoustic Doppler Current Profiler.
IEEE Journal of Oceanic Engineering, 16, 402-407.

CARTWRIGHT, D.E. & CREASE, J. 1963
A comparison of the geodetic reference levels of England and France by means of the sea surface.
Proceedings of the Royal Society, A 1355, 558-580.

CHAVE, A.D., LUTHER, D.S. & FILLOUX, J.H. 1990
Spatially averaged velocity from the sea floor horizontal electric field.
pp. 46-53 in Proceedings of the IEEE Fourth Working Conference on Current Measurement, 3-5 April 1990, Maryland (eds. G.F. Appell & T.B. Curtin).
New York: Institute of Electrical & Electronic Engineers.

CHERESKIN, T.K., HALPERN, D. & REGIER, L.A. 1987
Comparison of shipboard acoustic Doppler current profiler and moored current measurements in the equatorial Pacific.
Journal of Atmospheric and Oceanic Technology, 4, 742-747.

CHERESKIN, T.K., NILLER, P.P. & POULAIN, P.M. 1989
A numerical study of the effect of upper ocean shear on flexible drogued drifters.
Journal of Atmospheric and Oceanic Technology, 6, 243-253.

CHERESKIN, T.K., FIRING, E. & GAST, J.A. 1989
Identifying and screening filter skew and noise bias in ADCP current profiler measurements.
Journal of Atmospheric and Oceanic Technology, 6, 1040-1054.

CHERESKIN, T.K. & HARDING, A.J. 1993
Modelling the performance of an acoustic Doppler current profiler.
Journal of Atmospheric and Oceanic Technology, 10, 41-63.

CHHABRA, N.K. 1977
Correction of vector averaging current meter records from the MODE-1 central mooring for the effects of low-frequency mooring motion.
Deep-Sea Research, 24, 279-287.

CHHABRA, N.K. 1985
Computation of errors in current meters attached to near-surface moorings.
Journal of Geophysical Research, 90, 4995-4999.

CHHABRA, N.K., DAHLEN, J.M. & SCHOLTEN, J.R. 1987
Calibration of the Draper Laboratory Low Cost Drifter (LCD).
Charles Stark Draper Laboratory Inc., Cambridge, Massachusetts, USA, Report CSDL-R-1906, 137 pp.

CHURCHILL, J.H. & CSANADY, G.T. 1983
Near-surface measurements of quasi-Lagrangian velocities in open water.
Journal of Physical Oceanography, 13, 1669-1679.

CLAY, P.R. & LONGWORTH, S.P. 1986
A performance of the InterOcean S4 electromagnetic current meter.
Woods Hole Oceanographic Institution Technical Report WHOI-86-42, 26 pp.

CLAYSON, C.H. 1983
A vector averaging electromagnetic current meter for near-surface measurement.
pp. 81-87 in Proceedings of the IEEE Third Working Symposium on Oceanographic Data Systems, IEEE Computer Society.
New York: Institute of Electrical & Electronic Engineers.

COLLAR, P.G. 1978
Near-surface current measurement from a surface-following data buoy, DB1. Pt. I.
Ocean Engineering, 5, 181-196.

COLLAR, P.G. & GWILLIAM, T.J.P. 1977
Some laboratory measurements on an acoustic current meter developed at Christian Michelsen Institute, Norway.
Institute of Oceanographic Sciences Report, No. 47, 15 pp. & figs. (unpublished manuscript).

COLLAR, P.G., CARSON, R.M. & GRIFFITHS, G. 1983
Measurement of near-surface current from a moored wave-slope follower.
Deep-Sea Research, 30, 63-75.

COLLAR, P.G. & HOWARTH, M.J. 1987
A comparison of three methods of measuring surface currents in the sea: radar, current meters and surface drifters.
Department of Energy Offshore Technology Report No. OTH 87272, 46 pp.

COLLAR, P.G., HUNTER, C.A., PERRETT, J.R. & BRAITHWAITE, A.C. 1988
Measurement of near-surface currents using a satellite-telemetering buoy.
Journal of the Institution of Electronic & Radio Engineers, 58, 258-265.

CORNUELLE, B., MUNK, W. & WORCESTER, P. 1989
Ocean acoustic tomography from ships.
Journal of Geophysical Research, 94, 6232-6250.

CRAWFORD, W.R. 1988
The use of Loran-C drifters to locate eddies on the continental shelf.
Journal of Atmospheric and Oceanic Technology, 5, 671-676.

CROCKER, T.R. 1983
Near-surface Doppler sonar measurements in the Indian Ocean.
Deep-Sea Research, 30, 449-467.

CROMBIE, D.D. 1955
Doppler Spectrum of Sea Echo at 13.56 Mc/s.
Nature, 175, 681-682.

CUSHING, V. 1976
Electromagnetic water current meter.
Paper 25C in 'Oceans 76', Proceedings of the MTS-IEEE Conference , September 1976, Washington D.C., USA.
New York: Institute of Electrical & Electronic Engineers.

CUTCHIN, D., CHRISTENSEN, J., KNOOP, R., STILLMAN, J., WOODWARD, W. 1986
Acoustic Doppler current profiling from a volunteer commercial ship.
pp. 98-105 in Proceedings of the IEEE Third Working Conference on Current Measurement, 22-24 January 1986, Airlie, Virginia (eds. G.F. Appell & W.E. Woodward).
New York: Institute of Electrical & Electronic Engineers.

DAHLEN, J. 1986
The Draper LCD: A calibrated, low cost, Lagrangian Drifter.
Charles Stark Draper Laboratory Inc., Cambridge, Massachusetts, USA, Report CSDL-P-2670.

D'ASARO, E.A. 1992
Estimation of velocity from Argos-tracked surface drifters during OCEAN STORMS.
Journal of Atmospheric and Oceanic Technology, 9, 680-686.

DAVIS, R.E. 1982
On relating Eulerian and Lagrangian velocity statistics: single particles in homogeneous flows.
Journal of Fluid Mechanics, 114, 1-26.

DAVIS, R.E. 1985
Drifter observations of coastal surface currents during CODE: The method and descriptive view.
Journal of Geophysical Research, 90, 4741-4755.

DAVIS, R.E. 1991
Lagrangian ocean studies.
Annual Review of Fluid Mechanics, 23, 43-64.

DAVIS, R.E. & WELLER, R.A. 1980
Propeller current sensors.
pp. 141-153 in Air-Sea Interaction: Instruments and Methods (eds. F. Dobson, L. Hasse & R. Davis).
New York: Plenum Press.

DAVIS, R.E., WEBB, D.C., REGIER, L.A. & DUFOUR, J. 1992
The Autonomous Lagrangian Circulation Explorer (ALACE).
Journal of Atmospheric and Oceanic Technology, 9, 264-285.

DE FERRARI, H.A. & NGUYEN, H. 1985
Acoustic Reciprocal Transmission Experiments, Florida Straits.
Journal of the Acoustical Society of America, 79, 299-315.

DELCROIX, T., MASIA, F. & ELDIN, G. 1992
Comparison of Profiling Current Meter and Shipboard ADCP measurements in the Western Equatorial Pacific.
Journal of Atmospheric and Oceanic Technology, 9, 867-871.

DENBIGH, P.N. 1984
Ship velocity determination by Doppler and correlation techniques.
IEE Proceedings, 131, 315-326.

DICKEY, F.R., BOOKHEIMER, W.C. & RHOADES, K.W. 1983
Implementation and testing of a deepwater correlation velocity sonar.
pp. 437-446 in the Proceedings of the Offshore Technology Conference, 1983, Vol. 3.
Houston, Texas: OTC.

DIDDEN, N. 1987
Performance evaluation of a shipboard 115 kHz acoustic Doppler current profiler.
Continental Shelf Research, 7, 1231-1243.

DILLON, D.B. 1973
An inventory of current mathematical models of scientific data gathering moors.
Hydrospace-Challenger Inc. Technical Report No. TR44500001, 53 pp.

DUDA, T.F., COX, C.S. & DEATON, T.K. 1988
The Cartesian Diver: A self profiling Lagrangian velocity recorder.
Journal of Atmospheric and Oceanic Technology, 5, 16-33.

DÜING, W. & JOHNSON, D. 1972
High resolution current profiling in the Straits of Florida.
Deep-Sea Research, 19, 259-274.

DUNCAN, C.P. & SCHADLOW, S.G. 1981
World surface currents from ships' drift observations.
International Hydrographic Review, LVIII, 101-111.

EAMES, M.C. 1968
Steady state theory of towing cables.
Quarterly Transactions of the Royal Institute of Naval Architecture, 110, 185-206.

FARADAY, M. 1832
Experimental researches in electricity.
Philosophical Transactions of the Royal Society, 122, 163-194.

FARMER, D.M. & CLIFFORD, S.F. 1986
Space-Time Acoustic Scintillation Analysis: A New Technique for Probing Ocean Flows.
IEEE Journal of Oceanic Engineering, OE-11, 42-50.

FARMER, D.M., CLIFFORD, S.F. & VERRALL, J.A. 1987
Scintillation structure of a turbulent tidal flow.
Journal of Geophysical Research, 92, 5369-5382.

FINKE, M. & SIEDLER, G. 1986
Drag coefficients of oceanographic mooring components.
Journal of Atmospheric and Oceanic Technology, 3, 255-264.

FLATT, D.F., GRIFFITHS, G. & HOWARTH, M.J. 1988
Measurement of current profiles.
Proceedings of the Conference, 'Oceanology International '88', 8-11 March 1988, Brighton, UK.
London, UK: Graham & Trotman Ltd.

FOFONOFF, N.P. & ERCAN, Y. 1967
Response characteristics of a Savonius rotor current meter.
Woods Hole Oceanographic Institution Technical Report WHOI-67-33, 36 pp.

FREITAG, H.P., McPHADEN, M.J. & PULLEN, P.E. 1992
Fish-induced bias in acoustic Doppler current profiler data.
pp. 712-717 in Proceedings of the IEEE Conference, 'Oceans '92'.
New York: Institute of Electrical & Electronic Engineers.

GARCIA, C.A.E. & ROBINSON, I.S. 1989
Sea surface velocities in shallow seas extracted from sequential coastal zone colour scanner satellite data.
Journal of Geophysical Research, 94, 12681-12691.

GAUNT, D.I. 1975
Design and development of moored buoy systems.
pp. 1-11 in Technology of Buoy Mooring Systems.
London: Society for Underwater Technology.

GAUNT, D.I. & HUNTER, C.A. 1975
The design of long term submerged equipment associated with the UK Data Buoy.
pp. 31-41 in Technology of Buoy Mooring Systems.
London: Society for Underwater Technology.

GEYER, W.R. 1989
Field calibration of mixed-layer drifters.
Journal of Atmospheric and Oceanic Technology, 6, 333-342.

GORDON, R.L. 1990
A review of interesting results obtained with acoustic doppler current profilers.
pp. 180-191 in Proceedings of the IEEE Fourth Working Conference on Current Measurement, 3-5 April 1990, Maryland (eds. G.F. Appell & T.B. Curtin).
New York: Institute of Electrical & Electronic Engineers.

GOULD, W.J. 1973
Effects of nonlinearities of current meter compasses.
Deep-Sea Research, 20, 423-427.

GOULD, W.J. 1977
Measurements of currents in the open sea.
Institute of Oceanographic Sciences Report, No. 54, 38 pp. & figs. (unpublished manuscript).

GOULD, W.J. & SAMBUCO, E. 1975
The effect of mooring type on measured values of ocean currents.
Deep-Sea Research, 22, 55-62.

GRIFFIN, D.A. 1988
Mooring design to minimize Savonius rotor overspeeding due to wave action.
Continental Shelf Research, 8, 153-158.

GRIFFIN, O.M., VANDIVER, J.K. & SKOP, R.A. 1982
The strumming vibrations of marine cables.
Ocean Science and Engineering, 7, 461-498.

GRIFFITHS, G. 1979
The effect of turbulence on the calibration of electromagnetic current sensors and an approximation of their spatial response.
Institute of Oceanographic Sciences Report, No. 68, 14 pp. & figs. (unpublished manuscript).

GRIFFITHS, G. 1986
Intercomparison of an acoustic doppler current profiler with conventional instruments and a tidal flow model.
pp. 169-176 in Proceedings of the IEEE Third Working Conference on Current Measurement, 22-24 January 1986, Airlie, Virginia (eds. G.F. Appell & W.E. Woodward).
New York: Institute of Electrical & Electronic Engineers.

GRIFFITHS, G. 1990
Near-surface current shear in the open sea.
Department of Energy Offshore Technology Report No. OT0-90-024, 19 pp. & Annex (47 pp.).

GRIFFITHS, G., COLLAR, P.G. & BRAITHWAITE, A.C. 1978
Some characteristics of electromagnetic current sensors in laminar flow conditions.
Institute of Oceanographic Sciences Report, No. 56, 14 pp., Appendix & figs. (unpublished manuscript).

GRIFFITHS, G. & FLATT, D. 1987
A self-contained acoustic doppler current profiler - design and operation.
pp. 41-47 in Proceedings of the IERE 5th International Conference on Electronics for Ocean Technology, March 1987, Edinburgh.
London: Institution of Electronic & Radio Engineers.

GURGEL, K-W, ESSEN, H-H & SCHIRMER, F. 1986
CODAR in Germany - a status report valid November 1985.
IEEE Journal of Oceanic Engineering, OE-11, 251-257.

GYTRE, T. 1976
The use of a high sensitivity ultrasonic current meter in an oceanographic data acquisition system.
Radio and Electronic Engineer, 46, 617-623.

GYTRE, T. 1980
Acoustic Travel Time Current Meters.
pp. 155-170 in Air-Sea Interaction: Instruments and Methods (eds. F. Dobson, L. Hasse & R. Davis).
New York: Plenum Press.

HA, E.C. 1979
Remote sensing of ocean surface current and current shear by HF backscatter radar.
Stanford University, Ph.D. Dissertation, 134 pp.

HALPERN, D. 1987
Comparison of upper ocean VACM and VMCM observations in the equatorial Pacific.
Journal of Atmospheric and Oceanic Technology, 4, 84-93.

HALPERN, D. 1980
Moored current measurements in the upper ocean.
pp. 127-140 in Air-Sea Interaction: Instruments and Methods (eds. F. Dobson, L. Hasse & R. Davis).
New York: Plenum Press.

HALPERN, D., WELLER, R.A., BRISCOE, M.G., DAVIS, R.E. & McCULLOUGH, J.R. 1981
Intercomparison tests of moored current measurements in the upper ocean.
Journal of Geophysical Research, 86, 419-428.

HAMMOND, T.M. & COLLINS, M.B. 1979
Flume studies of the response of various current meter rotor/propellers to combinations of unidirectional and oscillatory flow.
Deutsche Hydrographische Zeitschrift, 32, 39-58.

HAMMOND, T.M., PATTIARATCHI, C.B., OSBORNE, M.J. & COLLINS, M.B. 1986
Field and flume comparisons of the modified and standard (Savonius-rotor) Aanderaa self-recording current meters.
Deutsche Hydrographische Zeitschrift, 39, 41-63.

HANSEN, D.S. 1985
Asymptotic performance of a pulse to pulse incoherent Doppler sonar in an oceanic environment.
IEEE Journal of Oceanic Engineering, OE-10, 144-158.

HANSEN, D.S. 1986
Design and calibration issues for current profiling systems: high frequency volumetric backscattering in an oceanic environment.
pp. 191-202 in Proceedings of the IEEE Third Working Conference on Current Measurement, 22-24 January 1986, Airlie, Virginia (eds. G.F. Appell & W.E. Woodward).
New York: Institute of Electrical & Electronic Engineers.

HENDRY, R.M. & HARTLING, A.J. 1979
A pressure induced direction error in nickel-coated Aanderaa current meters.
Deep-Sea Research, 26A, 327-355.

HERON, M.L., DEXTER, P.E. & McGANN, B.T. 1985
Parameters of the air-sea interface by high frequency ground-wave Doppler radar.
Australian Journal of Marine and Freshwater Research, 36, 655-670.

HINE, A. 1968
Magnetic compasses and magnetometers.
London: Adam Hilger Ltd., 385 pp.

HOERNER, S.F. 1965
Fluid dynamic drag (2nd edition).
Midland Park, New Jersey: S.F. Hoerner.

HOLBROOK, J.R. & FRISCH, A.S. 1981
A comparison of near-surface CODAR and VACM measurements in the Strait of Juan de Fuca, August 1978.
Journal of Geophysical Research, 86, 10908-10912.

HOLE, S.K., WOODWARD, B. & FORSYTHE, W. 1992
Design Constraints and Error Analysis of the Temporal Correlation Log.
IEEE Journal of Oceanic Engineering, 17, 269-279.

HOWARTH, M.J. 1981
Intercomparison of AMF VACM and Aanderaa current meters moored in fast tidal currents.
Deep-Sea Research, 28A, 601-607.

HUGHES, P. 1962
Towed electrodes in shallow water.
Geophysical Journal, 7, 111-124.

HUGHES, P. 1969
Submarine cable measurements of tidal currents in the Irish Sea.
Limnology and Oceanography, 14, 269-278.

JANOPAUL, M.M., BROCHE, P., DE MAISTRE, J.C., ESSEN, H.H., BLANCHET, C., GRAU, G. & MITTELSTAEDT, E. 1982
Comparison of measurements of sea currents by hf radar and by conventional means.
International Journal of Remote Sensing, 3, 409-422.

JOHNS, W.E. 1988
Near-surface current measurements in the Gulf Stream using an Upward Looking Acoustic Doppler Current Profiler.
Journal of Atmospheric and Oceanic Technology, 5, 602-613.

JOHNSON, W.R. & ROYER, T.C. 1986
A comparison of two current meters on a surface mooring.
Deep-Sea Research, 33, 1127-1138.

JOYCE, T.M., BITTERMAN, D.S. & PRADA, K.E. 1982
Shipboard acoustic profiling of upper ocean currents.
Deep-Sea Research, 29, 903-913.

JOYCE, T.M. 1989
On in-situ 'calibration' of shipboard ADCPs.
Journal of Atmospheric and Oceanic Technology, 6, 169-172.

KENNEY, B.C. 1977
Response characteristics affecting the design and use of current direction vanes.
Deep-Sea Research, 24, 289-300.

KIRWAN, A.D., McNALLY, G., CHANG, M-S. & MOLINARI 1975
The effect of wind and surface current on drifters.
Journal of Physical Oceanography, 5, 361-368.

KIRWAN, A.D., McNALLY, G. & PAZAN, S. 1978
Wind drag and relative separations of undrogued drifters.
Journal of Physical Oceanography, 8, 1146-1150.

KOSRO, P.M., REGIER, L. & DAVIS, R.E. 1986
Accuracy of shipboard Doppler current profiling during CODE.
p. 97 in Proceedings of the IEEE Third Working Conference on Current Measurement, 22-24 January 1986, Airlie, Virginia (eds. G.F. Appell & W.E. Woodward).
New York: Institute of Electrical & Electronic Engineers.

KOSRO, P.M. 1985
Shipboard acoustic current profiling during the Coastal Ocean Dynamics Experiment.
Scripps Institution of Oceanography Ref. 85-8, 119 pp.

KO, D.S., DE FERRARI, H.A. & MALANOTTE-RIZZOLI, P. 1989
Acoustic Tomography in the Florida Strait: Temperature, Current and Vorticity Measurements.
Journal of Geophysical Research, 94, 6197-6211.

KRAUSS, W., DENGG, J. & HINRICHSEN, H-H. 1989
The response of drifting buoys to currents and wind.
Journal of Geophysical Research, 94, 3201-3210.

KRAUSS, W., DENGG, J. & HINRICHSEN, H-H. 1990
Reply (to Poulain and Niiler, 1990).
Journal of Geophysical Research, 95, 801-803.

LARSEN, J.C. & SANFORD, T.B. 1985
Florida Current Volume Transports from voltage measurements.
Science, 227, 302-303.

LAWSON, K.D., BROWN, N.L., JOHNSON, D.H. & MATTEY, R.A. 1976
A three-axis acoustic current meter for small scale turbulence.
Instrument Society of America, ASI No. 76269, 501-508.

LAWSON, K.D., LESSIEUX, B.J., LUCK, J.M. & WOODY, D.C. 1983
The development of a spherical electromagnetic current meter.
pp. 187-193 in Proceedings of the IEEE Conference, 'Oceans 83'.
New York: Institute of Electrical & Electronic Engineers.

LEER, J. van, DÜING, W., ERATH, R., KENNELLY, E. & SPEIDEL, A. 1974
The Cyclosonde: an unattended vertical profiler for scalar and vector quantities in the upper ocean.
Deep-Sea Research, 21, 385-400.

LEISE, J.A. 1984
The analysis and digital signal processing of NOAA's surface current mapping system.
IEEE Journal of Oceanic Engineering, OE-9, 106-112.

LEMON, D. & FARMER, D. 1990
Experience with a multi-depth scintillation flowmeter in the Fraser Estuary.
pp. 306-314 in Proceedings of the IEEE Fourth Working Conference on Current Measurement, 3-5 April 1990, Maryland (eds. G.F. Appell & T.B. Curtin).
New York: Institute of Electrical & Electronic Engineers.

LHERMITTE, R.M. 1985
Water velocity and turbulence measurements by pulse coherent doppler sonar.
pp. 1159-1164 in Proceedings of the IEEE Conference 'Oceans 85' - Ocean Engineering and the Environment.
New York: Institute of Electrical & Electronic Engineers.

LHERMITTE, R.M. & SERAFIN, R. 1984
Pulse-to-pulse coherent Doppler sonar signal techniques.
Journal of Atmospheric and Oceanic Technology, 1, 293-308.

LODER, J.W. & HAMILTON, J.M. 1990
Degradation of paddle-wheel Aanderaa current measurements by mooring vibration in a strong tidal flow.
pp. 107-119 in Proceedings of the IEEE Fourth Working Conference on Current Measurement, 3-5 April 1990, Maryland (eds. G.F. Appell & T.B. Curtin).
New York: Institute of Electrical & Electronic Engineers.

LOHRMANN, A., HACKETT, B. & RØED, L.P. 1990
High resolution measurements of turbulence, velocity and stress using a pulse to pulse coherent sonar.
Journal of Atmospheric and Oceanic Technology, 7, 19-37.

LONGUET-HIGGINS, M.S. 1949
The electrical and magnetic effects of tidal streams.
Monthly Notices of the Royal Astronomical Society, Geophysical Supplement, 5, 285-307.

LONGUET-HIGGINS, M.S. 1972
On the interpretation of records of time varying currents.
Rapports et Procès-verbaux des Réunions, ICES, 162, 35-41.

LONGUET-HIGGINS, M.S., STERN, M.E. and STOMMEL, H. 1954
The electrical field induced by ocean currents and waves, with applications to the method of towed electrodes.
Papers in Physical Oceanography and Meteorology, 13, 37 pp.

MACKAS, D.L., CRAWFORD, W.R. & NIILER, P.P. 1989
A performance comparison for two Lagrangian drifter designs.
Atmosphere-Ocean, 27, 443-456.

MAGNELL, B.A. & SIGNORINI, S.R. 1986
Fall 1984 Delaware Bay Acoustic Doppler Profiler Intercomparison Experiment.
pp. 122-152 in Proceedings of the IEEE Third Working Conference on Current Measurement, 22-24 January 1986, Airlie, Virginia (eds. G.F. Appell & W.E. Woodward).
New York: Institute of Electrical & Electronic Engineers.

MAHAPATRA, P.R. & ZRNIC, D.S. 1983
Practical algorithms for mean velocity estimation in pulse doppler weather radars using a small number of samples.
IEEE Transactions on Geoscience and Remote Sensing, GE-21, 491-501.

MAHRT, K-H. 1980
Miniature acoustical sensor for fast in-situ measurements of currents and simultaneous density fluctuations in the same water sample.
pp. 198-203 in 'Oceans 80', Proceedings of the IEEE Conference, Seattle, USA.
New York: Institute of Electrical & Electronic Engineers.

McCLIMANS, T.A. 1980
Wave propulsion of spar buoys.
Proceedings of the American Society of Civil Engineers, 106, 410-414.

McCULLOUGH, J.R. 1975
Vector averaging current meter speed calibration and recording technique.
Woods Hole Oceanographic Institution Technical Report WHOI-75-44, 35 pp.

McCULLOUGH, J.R. 1980
Survey of techniques for measuring currents near the ocean surface.
pp. 105-126 in Air-Sea Interaction: Instruments and Methods (eds. F. Dobson, L. Hasse & R. Davis.
New York: Plenum Press.

McCULLOUGH, J.R. & GRÄPER, W. 1979
Moored acoustic travel time (ATT) current meters: evolution, performance and future design.
Woods Hole Oceanographic Institution Report No. WHOI-79-92, 117 pp. & Appendices.

MERO, T.N. 1982
Performance test results for the EG & G Vector Measuring Current Meter (VMCM) (1982) pp. 159-164 in Proceedings of the IEEE Second Working Conference on Current Measurement.
New York: Institute of Electrical & Electronic Engineers.

MERO, T.N., APPELL, G.F., McCULLOUGH, J.R. & MAGNELL, B. 1982
Laboratory verification of an Acoustic Current Meter Error Model.
IEEE Journal of Oceanic Engineering, OE-7, 161-165.

MONAHAN, E.C., HAWKINS, P.C. & MONAHAN, E.A. 1974
Surface current drifters: evolution and application.
University of Michigan, College of Engineering Sea Grant Program Report MICHU-SG-74-603, 46 pp.

MUNK, W.H. & WUNSCH, C. 1979
Ocean Acoustic Tomography: A Scheme for large-scale monitoring.
Deep-Sea Research, 26, 123-161.

MYERS, J.J., HOLM, C.H. & McALLISTER, R.F. 1969
Handbook of Ocean and Underwater Engineering.
New York: McGraw-Hill, 1094 pp.

NAGATA, Y., YONEMURA, K. & NISHIDA, H. 1981
GEK Measurements in a shallow water region.
Journal of the Oceanographical Society of Japan, 37, 21-30.

NATH, J.H. 1977a
Laboratory validation of numerical model drifting buoy-tether-drogue system.
Final Report to NOAA Data Buoy Office (Contract 03-6-038-128).

NATH, J.H. 1977b
Laboratory model tests of drifting buoy and drogue, Oregon State University.
Report to NOAA Data Buoy Office (Contract 03-6-038-711).

NATH, J.H. 1978
Drift speed of buoys in waves. (with an appendix by M.S. Longuet-Higgins)
pp. 859-877 in Proceedings of the Sixteenth Coastal Engineering Conference, Hamburg, Vol. I.
New York: American Society of Civil Engineers, 3060 pp. in 3 vols.

NATH, J.H., LIN CHENG-WEN, KERUT, E.G. & BROOKS, D.M. 1979
Hydrodynamic coefficients for flexible drogues.
pp. 595-610 in Proceedings of the Conference 'Civil Engineering in the Oceans IV', Vol. 2.
New York: American Society of Civil Engineers.

NIILER, P.P., DAVIS, R.C. & WHITE, H.J. 1987
Water-following characteristics of a mixed layer drifter.
Deep-Sea Research, 34, 1867-1881.

OSBORNE, M.J. 1991
OSCR and Interocean S4 current measurements in Poole Bay.
Underwater Technology, 17, 10-18.

OLSEN, J.R. 1972
Two component electromagnetic flowmeter.
Marine Technology Society Journal, 6, 19-24.

PATCH, S.K., BEARDSLEY, R.C. & LENTZ, S.J. 1990
A note on the response characteristics of the VACM compass.
pp. 129-133 in Proceedings of the IEEE Fourth Working Conference on Current Measurement, 3-5 April 1990, Maryland (eds. G.F. Appell & T.B. Curtin).
New York: Institute of Electrical & Electronic Engineers.

PATCH, S.K., DEVER, E.P., BEARDSLEY, R.C. & LENTZ, S.J. 1992
Response characteristics of the VACM compass and vane follower.
Journal of Atmospheric and Oceanic Technology, 9, 459-469.

PETTIGREW, N.R., BEARDSLEY, R.C. & IRISH, J.D. 1986
Field evaluations of a bottom mounted acoustic doppler profiler and conventional current meter moorings.
pp. 153-162 in Proceedings of the IEEE Third Working Conference on Current Measurement, 22-24 January 1986, Airlie, Virginia (eds. G.F. Appell & W.E. Woodward).
New York: Institute of Electrical & Electronic Engineers.

PINKEL, R. 1980
Acoustic Doppler techniques.
pp. 171-199 in Air-Sea Interaction: Instruments and Methods (eds. F. Dobson, L. Hasse & R. Davis).
New York: Plenum Press.

PINKEL, R. & SMITH, J. 1992
Repeat sequence codes for improved performance of Doppler sounders.
Journal of Atmospheric and Oceanic Technology, 9, 149-163.

POLLARD, R.T. 1973
Interpretation of near-surface current meter observations.
Deep-Sea Research, 20, 261-268.

POULAIN, P-M. & NILLER, P-P. 1990
Comment on "The response of drifting buoys to currents and wind".
Journal of Geophysical Research, 95, 797-799.

PRANDLE, D. 1987
The fine structure of nearshore tidal and residual circulations revealed by HF radar surface current measurements.
Journal of Physical Oceanography, 17, 231-245.

PULKKINEN, K. 1993
Comparison of different bin-mapping methods for a bottom-mounted acoustic profiler.
Journal of Atmospheric and Oceanic Technology, 10, 404-409.

PULLEN, P.E., McPHADEN, M.J., FREITAG, H.P. & GAST, J. 1992
Surface wave induced skew errors in Acoustic Doppler Current Profiler measurements from high shear regimes.
pp. 706-711 in 'Oceans '92', Proceedings of the IEEE Conference.
New York: Institute of Electrical & Electronic Engineers.

ROBERTS, G., LAST, J.D., ROBERTS, E.W. & HILL, A.E. 1991
Position-logging drifting buoys using Decca navigator and Argos for high-resolution spatial sampling.
Journal of Atmospheric and Oceanic Technology, 8, 718-728.

ROBINSON, I.S. 1976
A theoretical analysis of the use of submarine cables as electromagnetic oceanographic flowmeters.
Philosophical Transactions of the Royal Society, A 208, 355-396.

ROSSBY, T. & WEBB, D. 1970
Observing abyssal motions by tracking Swallow floats in the SOFAR channel.
Deep-Sea Research, 17, 359-365.

ROSSBY, T. & WEBB, D. 1971
The four month drift of a Swallow float.
Deep-Sea Research, 18, 1035-1039.

ROSSBY, T., VOORHIS, A.D. & WEBB, D. 1975
A Quasi-Lagrangian study of mid-ocean variability using long range SOFAR floats.
Journal of Marine Research, 33, 355-382.

ROSSBY, H.T., LEVINE, E.R. & CONNORS, D.N. 1985
The Isopycnal Swallow Float - A simple device for tracking water parcels in the ocean.
Progress in Oceanography, 14, 511-525.

ROSSBY, T., DORSON, D. AND FONTAINE, J. 1986
The RAFOS System.
Journal of Atmospheric and Oceanic Technology, 3, 672-679.

ROSSBY, T., ELLIS, J. & WEBB, D.C. 1993
An efficient sound source for wide-area RAFOS navigation.
Journal of Atmospheric and Oceanic Technology, 10, 397-403.

ROWE, F.D., DEINES, K.L. & GORDON, R.L. 1986
High resolution current profiler.
pp. 184-189 in Proceedings of the IEEE Third Working Conference on Current Measurement, 22-24 January 1986, Airlie, Virginia (eds. G.F. Appell & W.E. Woodward).
New York: Institute of Electrical & Electronic Engineers.

RUSBY, J.S.M., HUNTER, C.A., KELLEY, R.F., WALL, J. & BUTCHER, J. 1978
The construction and offshore testing of the UK Data Buoy (DB1 Project).
pp. 64-80 in Proceedings of the Conference 'Oceanology International 78', Technical Session J.
London: BPS Exhibitions.

SANFORD, T.B. 1971
Motionally induced electric and magnetic fields in the sea.
Journal of Geophysical Research, 76, 3476-3492.

SANFORD, T.B. 1986
Recent improvements in ocean current measurement from motional electric fields and currents.
pp. 65-77 in Proceedings of the IEEE Third Working Conference on Current Measurement, 22-24 January 1986, Airlie, Virginia (eds. G.F. Appell & W.E. Woodward).
New York: Institute of Electrical & Electronic Engineers.

SANFORD, T.B., DREVER, R.G. & DUNLAP, J.H. 1978
A velocity profiler based on the principles of geomagnetic induction.
Deep-Sea Research, 25, 183-210.

SANFORD, T.B., DREVER, R.G. & DUNLAP, J.H. 1985
An acoustic Doppler and Electromagnetic Profiler.
Journal of Atmospheric and Oceanic Technology, 2, 110-124.

SAUNDERS, P.M. 1976
Near-surface current measurements.
Deep-Sea Research, 23, 249-257.

SAUNDERS, P.M. 1980
Overspeeding of a Savonius rotor.
Deep-Sea Research, 27A, 755-759.

SAVONIUS, S.J. 1931
The S-rotor and its applications.
Mechanical Engineering, 53, 333-338.

SCHLICK, T., GURGEL, K-W., ESSEN, H-H. & SCHIRMER, F. 1990
pp. 15-21 in Proceedings of the IEEE Fourth Working Conference on Current Measurement, 3-5 April 1990, Maryland (eds. G.F. Appell & T.B. Curtin).
New York: Institute of Electrical & Electronic Engineers.

SCHOTT, F. 1986
Medium-range vertical acoustic Doppler current profiling from submerged buoys.
Deep-Sea Research, 33A, 1279-1292.

SCHOTT, F. & JOHNS, W. 1987
Half-year long measurements with a buoy mounted acoustic Doppler current profiler in the Somali Current.
Journal of Geophysical Research, 92, 5169-5176.

SCHULER, D.L., PLANT, W.J. & ENG, W.P. 1981
Remote sensing of the sea using one-and two-frequency microwave techniques.
pp. 617-623 in Oceanography from Space (ed. J.F.R. Gower).
New York: Plenum Press.

SCOR WORKING GROUP 21 1974
An intercomparison of some current meters.
UNESCO Technical Papers in Marine Sciences, No. 17, 116 pp.

SHEARMAN, E.D.R. 1986
A review of methods of remote sensing of sea-surface conditions by HF radar and design considerations for narrow beam systems.
IEEE Journal of Oceanic Engineering, OE-11, 150-157.

SHERCLIFF, J.A. 1962
The theory of electromagnetic flow measurement.
Cambridge: University Press, 146 pp.

SHERWIN, T.J. 1988
Measurements of current speed using an Aanderaa RCM4 current meter in the presence of surface waves.
Continental Shelf Research, 8, 131-144.

SIRMANS, D. & BUMGARNER, B. 1975
Numerical comparison of five mean frequency estimators.
Journal of Applied Meteorology, 14, 991-1003.

SKOP, R.A. & ROSENTHAL, F. 1979
Some new approximation techniques for mooring system design.
Marine Technology Society Journal, 13, 9-13.

SPAIN, P.F., DORSON, D.L. & ROSSBY, H.T. 1981
PEGASUS: A simple, acoustically tracked, velocity profiler.
Deep-Sea Research, 28, 1553-1567.

SPAIN, P. & SANFORD, T.B. 1987
Accurately monitoring the Florida Current with motionally induced voltages.
Journal of Marine Research, 45, 843-870.

SPINDEL, R.C. 1979
An underwater pulse compression system.
IEEE Transactions on Acoustics, Speech and Signal Processing, ASSP-27, 723-728.

SPINDEL, R.C., WORCESTER, P.F., WEBB, D.C., BOUTIN, P.R., PEAL, K.R., BRADLEY, A.M. 1982
Instrumentation for Ocean Acoustic Tomography.
pp. 92-99 in 'Oceans '82', Proceedings of the IEEE Conference.
New York: Institute of Electrical & Electronic Engineers.

STEWART, R.H. & JOY, J.W. 1974
HF radio measurements of surface currents.
Deep-Sea Research, 21, 1039-1049.

STOKES, G.G. 1847
On the theory of oscillatory waves.
Transactions of the Cambridge Philosophical Society, 8, 33, 441-445.

SVEJKOVSKY, J. 1988
Sea surface flow estimation from advanced very high resolution Radiometer and Coastal Zone Colour Scanner Satellite Imagery: a Verification Study.
Journal of Geophysical Research, 93, 6711-6743.

SWALLOW, J.C. 1955
A neutral-buoyancy float for measuring deep currents.
Deep-Sea Research, 3, 74-81.

SWALLOW, J.C. 1957
Some further deep current measurements using neutrally-buoyant floats.
Deep-Sea Research, 4, 93-104.

SWALLOW, J.C., McCARTNEY, B.S. & MILLARD, N.W. 1974
The Minimode float tracking system.
Deep-Sea Research, 21, 573-595.

TEAGUE, C.C. 1986
Multifrequency HF Radar Observations of Currents and Current Shears.
IEEE Journal of Oceanic Engineering, OE-11, 258-269.

THERIAULT, K.B. 1986a
Incoherent multibeam Doppler current profiler performance. Pt I - Estimate Variance.
IEEE Journal of Oceanic Engineering, OE-11, 7-15.

THERIAULT, K.B. 1986b
Incoherent multibeam Doppler current profiler performance. Pt II - Spatial Response.
IEEE Journal of Oceanic Engineering, OE-11, 16-25.

THORPE, S.A. 1986
Measurements with an automatically recording inverted echo sounder; ARIES and the bubble clouds.
Journal of Physical Oceanography, 16, 1462-1478.

THORPE, S.A., COLLINS, E.P. & GAUNT, D.I. 1973
An electromagnetic current meter for measuring turbulent flow near the ocean floor.
Deep-Sea Research, 20, 933-938.

TOKMAKIAN, R., STRUB, P.T., McLEAN-PADMAN, J. 1990
Evaluation of the maximum cross-correlation method of estimating sea-surface velocities from sequential satellite images.
Journal of Atmospheric and Oceanic Technology, 7, 852-865.

TREVORROW, M.V. & FARMER, D.M. 1992
The use of Barker codes in Doppler sonar measurements.
Journal of Atmospheric and Oceanic Technology, 9, 699-704.

TRUMP, C.L. 1986
Estimating absolute current velocities by merging shipboard Doppler current profiler data with Loran C data.
pp. 177-183 in Proceedings of the IEEE Third Working Conference on Current Measurement, 22-24 January 1986, Airlie, Virginia (eds. G.F. Appell & W.E. Woodward). New York: Institute of Electrical & Electronic Engineers..

TUCKER, M.J. 1972
Electromagnetic current meters: an assessment of their problems and potentialities.
Proceedings of the Society for Underwater Technology, 2, 53-58.

TUCKER, M.J., SMITH, N.D., PIERCE, F.E. & COLLINS, E.P. 1970
A two-component electromagnetic ship's log.
Journal of the Institute of Navigation, 23, 302-316.

URICK, R.J. 1982
Principles of Underwater Sound (3rd edition).
New York: McGraw-Hill, 384 pp.

VACHON, W.A. 1973
Scale model testing of drogues for free drifting buoys.
Charles Stark Draper Laboratory Inc., Cambridge, Massachusetts, USA, Report No. R769, 131 pp.

VACHON, W.A. 1974
Improved drifting buoy performance by scale model drogue testing.
Marine Technology Society Journal, 8, 58-62.

VACHON, W.A. 1975
Instrumented full scale tests of a drifting buoy and drogue.
Charles Stark Draper Laboratory Inc., Cambridge, Massachusetts, USA,
Report No. R947, 163 pp.

VACHON, W.A. 1980
Drifters.
pp. 201-218 in Air-Sea Interaction: Instruments and Methods (eds. F. Dobson, L. Hasse & R. Davis).
New York: Plenum Press.

VON ARX, W.S. 1950
An electromagnetic method for measuring the velocities of ocean currents from a ship underway.
Papers in Physical Oceanography and Meteorology, 11, 62 pp.

WAHL, D.D. & SIMPSON, J.J. 1990
Physical processes affecting the objective determination of near-surface velocity from satellite data.
Journal of Geophysical Research, 95, 13511-13528.

WEBB, D.C. 1977
SOFAR Floats for Polymode.
Paper 44B in 'Oceans 77', Proceedings of the MTS-IEEE Conference.
New York: Institute of Electrical & Electronic Engineers.

WELLER, R.A. & DAVIS, R.E. 1980
A vector measuring current meter.
Deep-Sea Research, 27A, 565-582.

WOODWARD, M.J. 1985
An evaluation of the Aanderaa RCM4 Current Meter in the Wave Zone.
pp. 755-762 in Proceedings of the IEEE Conference 'Ocean Engineering and the Environment', November 1985, San Diego, California, USA.
New York: Institute of Electrical & Electronic Engineers.

WOODWARD, W. & APPELL, G.F. 1973
Report on the evaluation of a vector averaging current meter.
NOAA Technical Memorandum, NOS NOIC-1, NSF, AG263, 64 pp.

WORCESTER, P.F., SPINDEL, R.C. & HOWE, B.M. 1985
Reciprocal acoustic transmission: Instrumentation for mesoscale monitoring of ocean current.
IEEE Journal of Oceanic Engineering, OE-10, 123-137.

YOUNG, F.B., GERRARD, H. & JEVONS, W. 1920
On electrical disturbances due to tides and waves.
Philosophical Magazine, Series 6, 40, 149-159.

ZEDEL, L.J. & CHURCH, J.A. 1987
Real time screening techniques for Doppler current profiler data.
Journal of Atmospheric and Oceanic Technology, 4, 572-581.